ELSEVIER

Coordination Chemistry Reviews
165 (1997) 163–237

COORDINATION CHEMISTRY REVIEWS

Lanthanides and actinides: annual survey of their organometallic chemistry covering the year 1995

Frank T. Edelmann *, Yurii K. Gun'ko

Chemisches Institut der Otto-von-Guericke-Universität Magdeburg, Magdeburg, Germany

Contents

---

* *Corresponding author.*

PII S0010-8545(97)00015-5

Keywords: Lanthanides; Actinides; Cyclopentadienyl complexes; Cyclooctatetraenyl complexes; Organometallic chemistry

---

1. Introduction

The review presents complexes of the lanthanides, actinides and also scandium and yttrium, which contain metal–carbon bonds as defined by section 29 of Chemical Abstracts. Abstracts of papers presented at conferences, dissertations and patents have mostly been excluded.

Several surveys of the organometallic compounds of f-elements have appeared in 1995. H. Schumann et al. [1] reviewed organometallic π-complexes of scandium, yttrium and the lanthanides in the oxidation state Ln^{+3} with aromatic ligands. The review is focused on the most successful methods for preparation of the compounds and their molecular structures. Organometallic complexes of rare earth metals with cyclopentadienyl, cyclooctatetraenyl, indenyl, fluorenyl and other aromatic π-ligands are considered in this comprehensive review (773 references).

W.J. Evans [2] described an approach to ancillary ligand sets via heterometallic stabilization as an alternative to the bis(pentamethylcyclopentadienyl) coordination in organometallic lanthanide chemistry. The purpose of the review article is to encourage development of new non-cyclopentadienyl ligand environments for yttrium and the lanthanides (53 references).

F.T. Edelmann [3] published a review on rare earth cyclooctatetraenyl complexes. Various types of mono- and bis(η^8-cyclooctatetraenyl)lanthanide complexes with metals in +2, +3 and +4 oxidation states were considered. Synthesis, reactivity and structural aspects of the compounds were discussed in detail (74 references).

2. Lanthanides

2.1. *Lanthanide complexes without supporting cyclopentadienyl and cyclopentadienyl-like ligands*

2.1.1. *Alkyl, alkynyl and arene complexes*

M.F. Lappert and coworkers [4] published the synthesis and characterization of a series of ytterbium(II) alkyl complexes. $[Yb(CHR_2)_2(OEt_2)_2]$ and $[Yb(CHR_2)_3Na]$ ($R = SiMe_3$) were synthesized by reactions of YbI_2 with two and tree equivalents of $NaCHR_2$:

$$YbI_2 + 2NaCHR_2 \xrightarrow{OEt_2} [Yb(CHR_2)_2(OEt_2)_2] + 2NaI$$

$$YbI_2 + 3NaCHR_2 \xrightarrow{hexane} [Yb(CHR_2)_3Na] + 2NaI$$

$R = SiMe_3$

Treatment of $[\mathrm{Yb(OR')_2(OEt_2)_2}]$ $(\mathrm{R'=C_6H_2Bu^t_2-2,6-Me-4})$ with two equivalents of $\mathrm{KCHR_2}$ led to a mixture of the products $[\mathrm{Yb(CHR_2)_2(OEt_2)_2}]$ and $[\mathrm{Yb(CHR_2)(OR')(OEt_2)_2}]$:

$$[\mathrm{Yb(OR')_2(OEt_2)_2}]+2\mathrm{KCHR_2}\xrightarrow{\mathrm{OEt_2}}[\mathrm{Yb(CHR)_2(OEt_2)_2}]$$
$$+[\mathrm{Yb(CHR_2)(OR')(OEt_2)_2}]+\mathrm{KOR'}$$

The complex $[\mathrm{Yb(CHR_2)_2(tmen)}]$ was obtained by reaction of $[\mathrm{Cp^*_2Yb(OEt_2)_2}]$ with $\mathrm{LiCHR_2}$ in the presence of tmen $(\mathrm{Me_2NCH_2CH_2NMe_2})$:

$$[\mathrm{Cp^*_2Yb(OEt_2)_2}]+2\mathrm{LiCHR_2}+\mathrm{tmen}\xrightarrow{\mathrm{OEt_2}}[\mathrm{Yb(CHR_2)_2(tmen)}]+2\mathrm{LiCp^*}$$

$[\mathrm{Yb(CHR_2)_2(OEt_2)_2}]$ reacted readily with 1,2-bis(dimethylphosphino)ethane (dmpe) or with $\mathrm{C_6H_4(NHR)_2}$-1,4:

$$[\mathrm{Yb(CHR_2)_2(OEt_2)_2}]+\mathrm{dmpe}\rightarrow[\mathrm{Yb(CHR_2)_2(dmpe)}]+2\mathrm{OEt_2}$$

$$[\mathrm{Yb(CHR_2)_2(OEt_2)_2}]+\mathrm{C_6H_4(NHR)_2}-1,4\xrightarrow{\mathrm{OEt_2}}$$
$$[\{\mathrm{Yb(CHR_2)(OEt_2)}\}_2\mathrm{C_6H_4(NR)_2}-1,4]+2\mathrm{CH_2R_2}$$

The complex $[\{\mathrm{Yb(CR_3)(\mu\text{-}OEt)(OEt_2)}\}_2]$ was synthesized by reaction of $\mathrm{YbI_2}$ with $\mathrm{KCR_3}$. The OEt ligand in the product could result from the cleavage of $\mathrm{OEt_2}$ by $\mathrm{KCR_3}$ or $[\mathrm{Yb(CR_3)_2}]$:

$$\mathrm{YbI_2}+2\mathrm{KCR_3}\rightarrow[\mathrm{Yb(CR_3)_2}]+2\mathrm{KI}$$

$$[\mathrm{Yb(CR_3)_2}]\xrightarrow{\mathrm{OEt_2}}1/2[\{\mathrm{Yb(CR_3)(\mu-OEt)(OEt_2)}\}_2]+\mathrm{CHR_3}+\mathrm{CH_2CH_2}$$

$$\mathrm{KCR_3}+\mathrm{OEt_2}\rightarrow\mathrm{CHR_3}+\mathrm{CH_2CH_2}+\mathrm{KOEt}$$

$$\mathrm{YbI_2}+2\mathrm{KCR_3}+\mathrm{KOEt}\xrightarrow{\mathrm{OEt_2}}1/2[\{\mathrm{Yb(CR_3)(\mu-OEt)(OEt_2)}\}_2]+2\mathrm{KI}$$

Lewis-base adducts of $[\{\mathrm{Yb(NR_2)(\mu\text{-}NR_2)}\}_2]$ were obtained by treatment with $\mathrm{NC_5H_4(CH_2R)}$-2 or $\mathrm{NC_5H_4(CHR_2)}$-2 in hexane:

$$[\{\mathrm{Yb(NR_2)(\mu-NR_2)}\}_2]+4\mathrm{NC_5H_4(CHXR)-2}$$
$$\rightarrow2[\{\mathrm{Yb(NR_2)_2}\{\mathrm{NC_5H_4(CHXR)-2}\}_2]\quad \mathrm{X=H\ or\ R}$$

The complexes $[\mathrm{Yb\{NC_5H_4(CHR)\text{-}2\}_2(dme)}]$ and $[\mathrm{K\{Yb[NC_5H_4(CHR)\text{-}2]_3\}(dme)_2}]$ were also synthesized by reactions of $\mathrm{YbI_2}$ with 2 and 3 equivalents of $[\mathrm{K\{NC_5H_4(CHR)\text{-}2\}(dme)\ (OEt_2)}]$, respectively. The compounds obtained in this work were characterized by ^{1}H and heteronuclear NMR-spectroscopy. The complex $[\{\mathrm{Yb(C(SiMe_3)_3)(\mu\text{-}OEt)(OEt_2)}\}_2]$ was characterized also by X-ray crystallography. The molecule consists of an ethoxo-bridged dimer, with each Yb atom in a distorted tetrahedral geometry (Fig. 1). The average Yb–C and Yb–OEt bond lengths are 2.573(13) and 2.27(1) Å, respectively.

W.J. Evans et al. [5] published the synthesis and structure of a homoleptic anionic

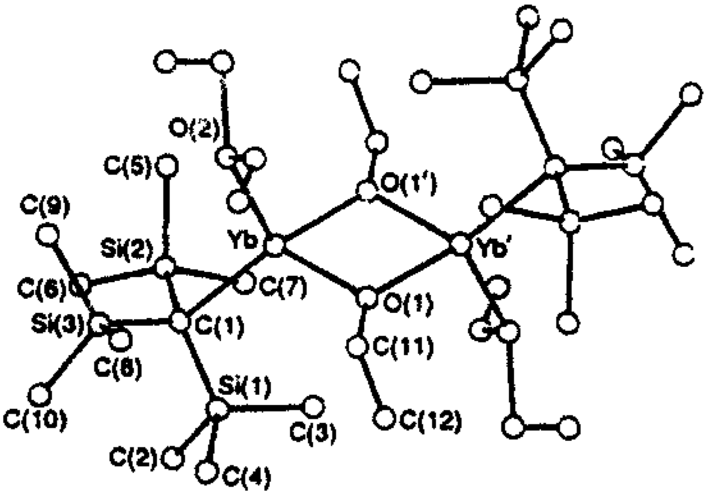

Fig. 1. Molecular structure of $[\{Yb(C(SiMe_3)_3)(\mu\text{-}OEt)(OEt_2)\}_2]$.

yttrium trimethylsilylmethyl complex, $\{(Me_3SiCH_2)_x(Me_3CO)_{1-x}Y(\mu\text{-}OCMe_3)_4[Li(THF)]_4(\mu_4\text{-}Cl)\}^+[Y(CH_2SiMe_3)_4]^-$. The complex was obtained by reaction of YCl_3 with 2 equivalents of $LiCH_2SiMe_3$ and 2 equivalents of $LiOCMe_3$. In the $[Y(CH_2SiMe_3)_4]^-$ anion (Fig. 2) the yttrium atom adopts a tetrahedral arrangement with C–Y–C angles ranging from 105.9(3) to 113.2(3)° and with an average Y–C bond distance of 2.42(2) Å. The geometry of the cation $\{(Me_3SiCH_2)_x(Me_3CO)_{1-x}Y(\mu\text{-}OCMe_3)_4[Li(THF)]_4(\mu_4\text{-}Cl)\}^+$ is a distorted bicapped square antiprism (Fig. 3) with the Y and Cl atoms in the capping positions, four Li atoms in one square face of the antiprism and four $OCMe_3$ groups in the other square face. The average Y–O(μ-OCMe$_3$) and Y–Cl distances in the cation are 2.270(5) and 3.263(2) Å, respectively.

M. Westerhausen et al. [6] reported the synthesis and structure of a

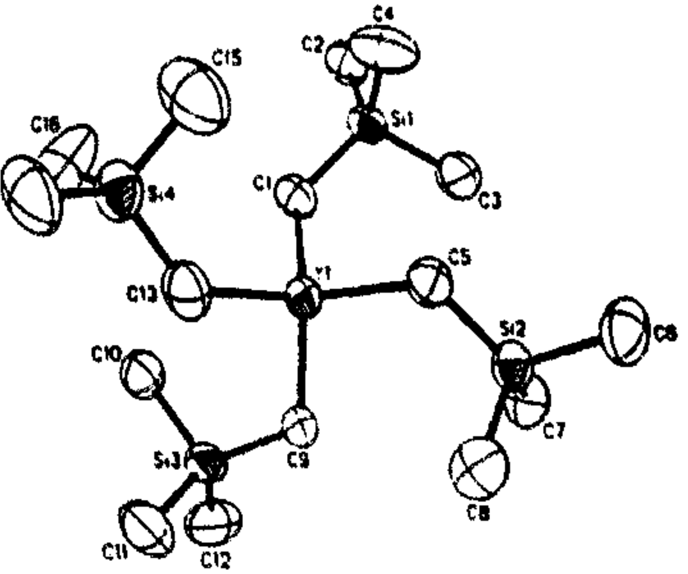

Fig. 2. Structure of the $[Y(CH_2SiMe_3)_4]^-$ anion.

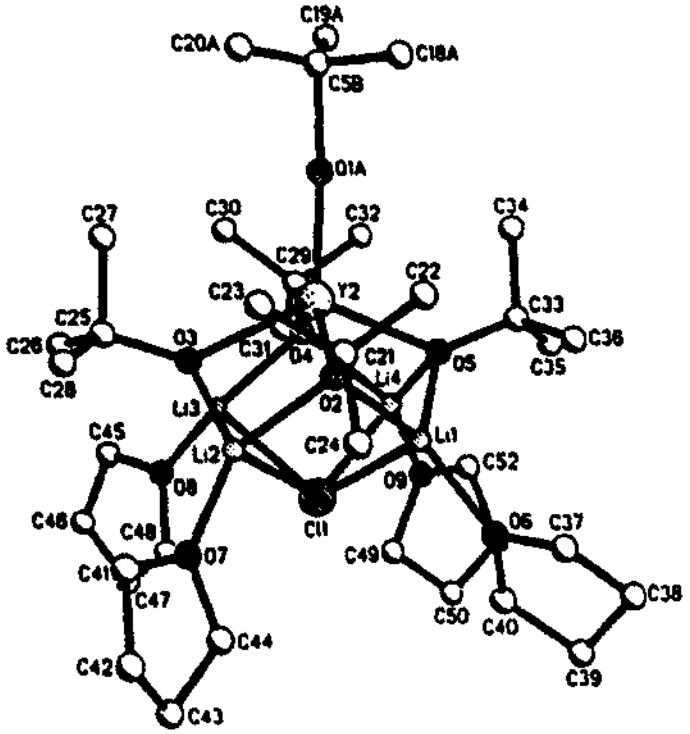

Fig. 3. Structure of the Me_3CO-containing component of the disordered $\{(Me_3SiCH_2)_x(Me_3CO)_{1-x}Y(\mu\text{-}OCMe_3)_4[Li(THF)]_4(\mu_4\text{-}Cl)\}^+$ cation.

$(Et_2O)_3LiCl$-adduct of $Y[CH(SiMe_3)_2]_3$:

$$YCl_3 + 3LiCH(SiMe_3)_2 \xrightarrow{OEt_2} (Et_2O)_3Li(\mu-Cl)Y[CH(SiMe_3)_2]_3 + 2LiCl$$

In the structure of $(Et_2O)_3Li(\mu\text{-}Cl)Y[CH(SiMe_3)_2]_3$ (Fig. 4) the Y and Li atoms are tetrahedrally coordinated and are connected via the μ_2 Cl-bridge. The Y Cl Li fragment is almost linear (175.9). The Y–C bond distances are ranging from 2.415(7) to 2.435(7) Å, while the Y–Cl distance is 2.598(2) Å.

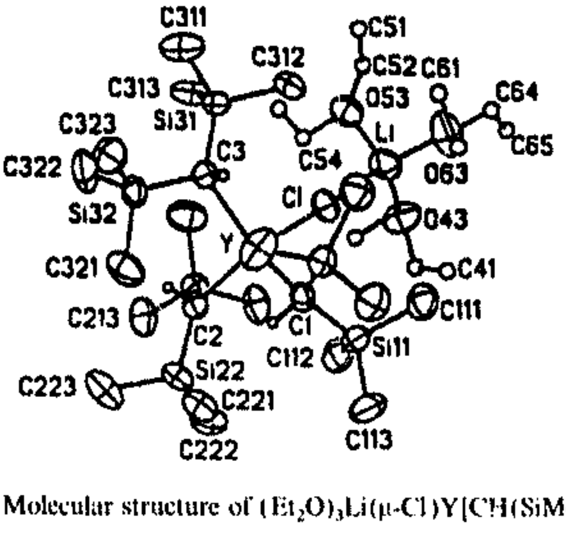

Fig. 4. Molecular structure of $(Et_2O)_3Li(\mu\text{-}Cl)Y[CH(SiMe_3)_2]_3$.

D.J. Berg et al. [7] prepared an yttrium alkyl adduct with deprotonated 4,13-diaza-18-crown-6 (DAC):

$$Y[CH_2SiMe_3]_3(THF)_2 + H_2DAC \rightarrow Y[DAC][CH_2SiMe_3] + 2SiMe_4 + 2THF$$

The complex Y[DAC][CH_2SiMe_3] was characterized by ^1H, ^{13}C and ^{89}Y NMR spectroscopy and by X-ray diffraction. In the monomeric structure (Fig. 5) the yttrium arrangement can be considered as consisting primarily of trigonal-planar coordination of alkyl- and two amido groups with secondary coordination of four ether oxygens. The Y–C and the two Y–N bond distances are 2.45(2), 2.27(2) and 2.26(2) Å, respectively. The analysis of the X-ray structure revealed that the yttrium atom in this compound has no agostic interactions with the alkyl group. The complex Y[DAC][CH_2SiMe_3] decomposes slowly in the solid state at room temperature and decomposes more rapidly in benzene solution thereby eliminating TMS.

H. Schwarz et al. [8] applied hybrid methods such as a mixing of Hartree–Fock exchange and density functional exchange to the cationic methyl complexes MCH_3^+ (M = Sc–Cu, La, Hf–Au). The methods were shown to be a promising alternative to rigorous high level ab initio theory for description of singly bonded open-shell transition metal complexes. According to these methods the bond dissociation energies for $ScCH_3^+$ and for $LaCH_3^+$ are in the range from 51.5 to 76.1 and from 52.7 to 59.3 kcal mol^{-1}, respectively.

K.-H. Thiele et al. [9] reported the synthesis and properties of some 1,4-diaryl-1,3-butadiene lanthanide complexes. The complexes Cp*La(1,4-$Ph_2C_4H_4$)·DME, Cp*La[1,4-{o-MeO-C_6H_4}$_2C_4H_4$]·2DME, [Li(THF)$_3$]

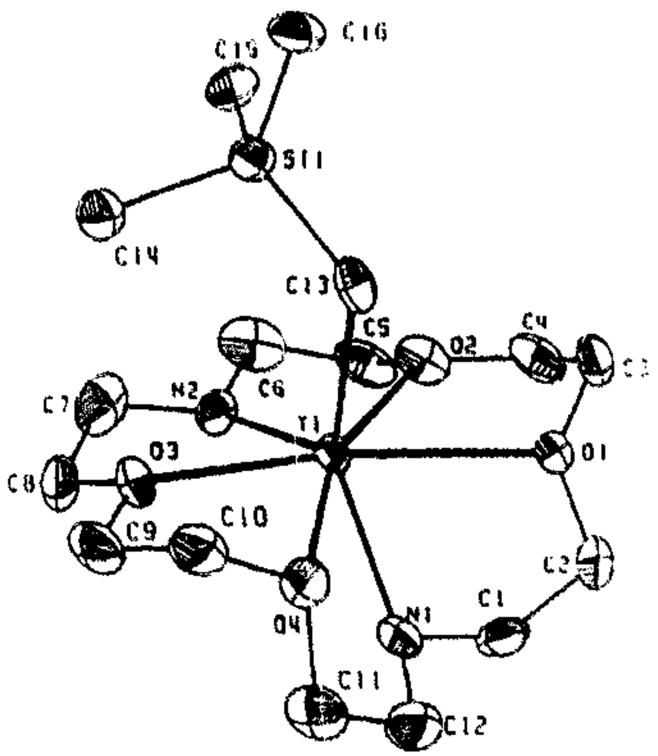

Fig. 5. Molecular structure of Y[DAC][CH_2SiMe_3] (DAC = deprotonated 4,13-diaza-18-crown-6).

$[Sm(1,4\text{-}Ph_2C_4H_4)_2]$, $[Li(DME)][\{1,4\text{-}(p\text{-}CH_3\text{-}C_6H_4)_2C_4H_4\}LuCl_2]$ and $[Li(DME)][\{1,4\text{-}(o\text{-}MeO\text{-}C_6H_4)_2C_4H_4\}LuCl_2]$ were prepared by reactions of the appropriate cyclopentadienyllanthanide halides with 1,4-diaryl-1,3-butadienes in the presence of alkali metals.

$$Cp^*LaI_2 + 2Li + RCH{=}CH-CH{=}CHR \xrightarrow{DME}$$
$$Cp^*La(RCH{=}CH-CH{=}CHR)\cdot nDME + 2LiI$$
$$(R = C_6H_5,\ n = 1;\ R = o-MeO-C_6H_4;\ n = 2)$$

$$Cp^*SmCl_2 + 2\ 1,4-Ph_2C_4H_4 + 2Li \xrightarrow{THF}$$
$$[Li(THF)_3][Sm(1,4-Ph_2C_4H_4)_2] + LiCl + \ldots$$

$$Cp^*LuCl_2 + 2\ 1,4-Ph_2C_4H_4 + 2Li \xrightarrow{DME}$$
$$[Li(DME)][1,4-R_2C_4H_4)LuCl_2] + Cp^*Li + \ldots$$
$$(R = p-Me-C_6H_4,\ o-MeO-C_6H_4)$$

Reaction of $SmCl_3(THF)_3$ with lithium and 1,4-diphenyl-1,3-butadiene led to the formation of $[Li(THF)_4][Sm(1,4\text{-}Ph_2C_4H_4)_2]$. One more samarium complex, $[1,4\text{-}(p\text{-}MeC_6H_4)_2C_4H_4]SmI\cdot 3THF$ was obtained by the reaction of metallic samarium with $1,4\text{-}(p\text{-}MeC_6H_4)_2C_4H_4$ in the presence of iodine.

$$SmCl_3(THF)_3 + 4Li + 2\ 1,4-Ph_2C_4H_4 \xrightarrow{THF}$$
$$[Li(THF)_4][Sm(1,4-Ph_2C_4H_4)_2] + 3LiCl$$

$$2Sm + I_2 + 1,4-(p-MeC_6H_4)_2C_4H_4 \xrightarrow{THF}$$
$$[1,4-(p-MeC_6H_4)C_4H_4]SmI\cdot 3THF$$

The complexes have been studied by elemental analysis, IR, NMR and EI-MS spectroscopy.

P. Biagini et al. [10] published the synthesis and catalytic activity of new $Ln(\eta^6\text{-arene})(AlX_3R)_3$ derivatives. The complexes $Ln(\eta^6\text{-}C_6H_5Me)(AlCl_3Me)_3$ ($Ln = Nd$, Sm or Y), $Ln(\eta^6\text{-}C_6H_5Me)(AlCl_3Et)_3$ ($Ln = Pr$ or Nd), $Gd(\eta^6\text{-}C_6H_5Me)(AlBr_3Me)_3$, $Nd(\eta^6\text{-}C_6H_5Me)(AlX_3Me)_3$ ($X = Br$ or I) and $Nd(\eta^6\text{-}C_6H_2Me_4)(AlCl_3R)_3$ ($R = Me$ or Et) were synthesized by treatment of the appropriate $Ln(\eta^6\text{-arene})(AlX_4)_3$ precursors with the corresponding AlR_3 in toluene solution.

$$Ln(\eta^6-arene)(AlX_4)_3 + 1.5AlR_3 \rightarrow Ln(\eta^6-arene)(AlX_3R)_3 + 1.5AlX_2R$$

The molecular structure of $Nd(\eta^6\text{-}C_6H_5Me)(AlCl_3Me)_3$ was studied by X-ray diffraction (Fig. 6). The Nd atom is located in the center of the basal plane formed by five Cl atoms and has a distorted pentagonal bipyramidal coordination arrange-

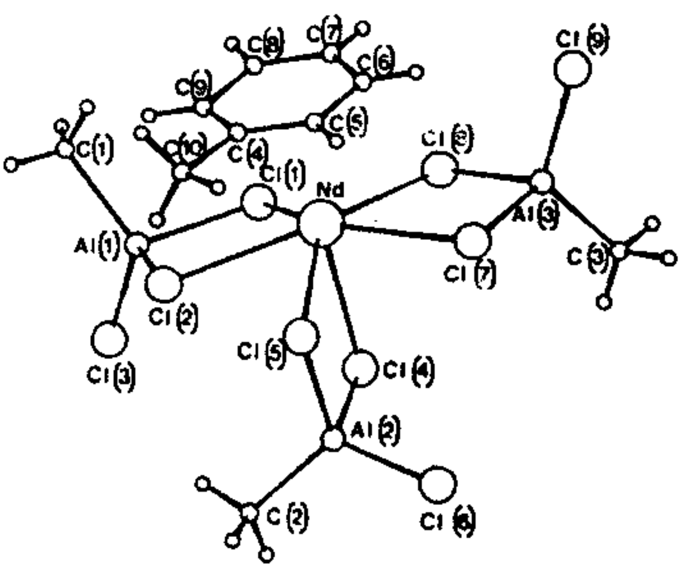

Fig. 6. Molecular structure of $Nd(\eta^6\text{-}C_6H_5Me)(AlCl_3Me)_3$.

ment. The Nd–Cl bond distances in the plane range from 2.848(4) to 2.884(4) Å, while the Nd–Cl(4) distance (out of the plane) is essentially shorter with 2.784(2) Å. The Nd–C bond distances are between 2.91(1) to 3.03(1) Å. Catalytic activity of the $Ln(\eta^6\text{-arene})(AlX_3R)_3$ derivatives in the polymerization of butadiene and ethylene has also been investigated in the course of this study.

2.1.2. *Endohedral metallofullerenes and lanthanide-filled carbon nanotubes*

K.B. Shelimov et al. investigated the La-containing carbon clusters LaC_n^+ [11,12] and $La_2C_n^+$ [12,13]. The cluster cations were generated by laser vaporization of a composite LaC_2/graphite rod, then the clusters were mass-selected and injected into a drift tube. Three families of ring isomers, La-containing graphite sheets and metallofullerenes were observed for the LaC_n^+ clusters. The suggested geometry for the ring isomers are a La atom inserted into a carbon ring, a La inside a carbon ring and various LaC_n and C_m rings fused together. LaC_{36}^+ and all LaC_n^+ fullerenes with $n = 38$–90 were found to be endohedral, while fullerenes were non-endohedral. Annealing processes in the LaC_n^+ fullerenes for larger clusters led to formation of fullerenes and graphite sheets. The graphite sheet was found to be the main isomerization product for clusters with 30–34 carbon atoms, while for clusters with more than 38 atoms >90% of the rings are converted into metallofullerenes [11]. In the case of $La_2C_n^+$ [13] the efficiency of encapsulation of a second La atom inside a fullerene cage was found to be substantially lower than that of the first. Both diendohedral fullerenes and fullerenes with one non-endohedral metal atom were observed for $La_2C_n^+$ clusters. The authors suggested that the reduced efficiency for encapsulating the second La could also result from stabilization of the $La(La@C_n)^+$ or $La@C_nLa^+$ geometry by the endohedral La atom.

M. Liu and J.M. Cowley [14,15] studied the encapsulation of lanthanum carbide in carbon nanotubes and nanoparticles. The samples were studied by high-resolution electron microscopy (HREM), scanning transmission electron microscopy (STEM), selected-area electron diffraction (SAED) and electron nanodiffraction. The compounds most likely to be formed inside nanotubes include α-La(hcp), β-La(fcc), La_2C_3(bcc), α-LaC_2(bc tetragonal) and β-LaC_2(fcc). For α-LaC_2 it was found that two crystals could be formed within a tube or a particle. The angle (orientation difference) between the two encapsulated neighboring α-LaC_2 crystals was approximately 15°. The crystal in the middle region had the 002 fringes perpendicular to the tube wall while the one above has the 002 fringes slightly tilted with respect to the tube wall. The accompanying numerous polyhedral nanoparticles showed pentagonal cross-sections in projection. All crystals encapsulated inside the nanotubes were observed to be located at or near the tube end. The preliminary examination of the α-LaC_2 samples by the nanodiffraction technique has given no indication of the existence of intermediate layers between carbon atoms and the encapsulated material.

H. Funasaka et al. [16] reported the synthesis of lanthanum compounds encapsulated within carbon nanoparticles. The encapsulation procedures were carried out by varying the lanthanum compounds (La_2O_3, LaB_6 and LaN) filled in the positive graphite electrode. The form of the core materials in the graphite cage was revealed to vary with the composite anode prior to arc discharge. For a La_2O_3/graphite composite anode, a LaN/graphite composite anode and a LaB_6/graphite composite anode the corresponding encapsulated forms were LaC_2, La and LaB_6, respectively.

M. Ata et al. [17] used X-ray diffraction, high-resolution electron microscopy (HREM) and magnetic characterization for an investigation of carbon nanotubes filled with gadolinium carbide crystals. According to these measurements the gadolinium metal was incorporated in the form of GdC_2 as single crystals as well as an amorphous carbide in the same nanotube. The growth mechanisms of metal carbide-filled carbon nanotubes was discussed.

2.2. Cyclopentadienyl complexes

2.2.1. Mono(cyclopentadienyl) complexes

S.J. Swamy and H. Schumann [18] reported the synthesis and characterization of 9-(pentamethylcyclopentadienyl)lanthanidefluorene complexes. The compounds were obtained by the one pot reaction of $LnCl_3$ (Ln = Sm, Yb, Lu) with NaC_5Me_5 followed by treatment with the TMED adduct of 2,2′-dilithiobiphenyl (Scheme 1). The complexes were characterized by elemental analyses as well as their IR and ^1H NMR spectra.

M.N. Bochkarev et al. [19] investigated reactions of cyclopentadienyl naphthalene complexes of lutetium with C- and N-unsaturated compounds. Reaction of $CpLuC_{10}H_8(THF)_2$ with azobenzene in THF led to a binuclear diphenylhydrazido complex, $[CpLu(THF)]_2(Ph_2N_2)_2$. Similar treatment of $CpLuC_{10}H_8(DME)$ with diphenylacetylene in DME yielded the binuclear complex $[CpLu(DME)]_2[1,1\text{-}\mu\text{-}4,4\text{-}\mu\text{-}(Ph)C(Ph)C{=}C(Ph)C(Ph)]$, which was structurally characterized. In the structure (Fig. 7) the two Lu atoms of the CpLu(DME) fragments are bound by a bridging $[C_4Ph_4]^{4-}$ ligand. The central C_4 fragment is planar (within 0.03 Å). Lu–μ_2–$C(C_4Ph_4)$ σ-bond lengths are 2.280(7) and 2.336(7) Å

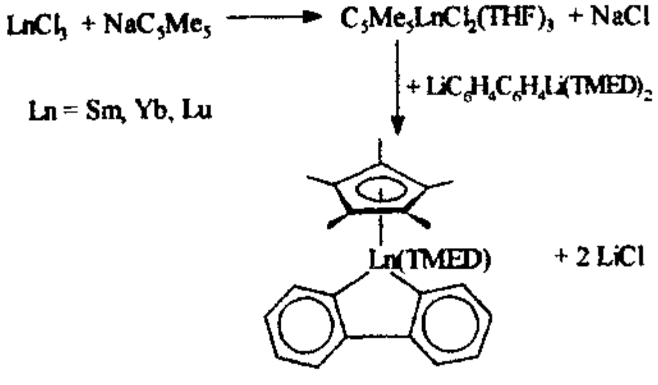

Scheme 1.

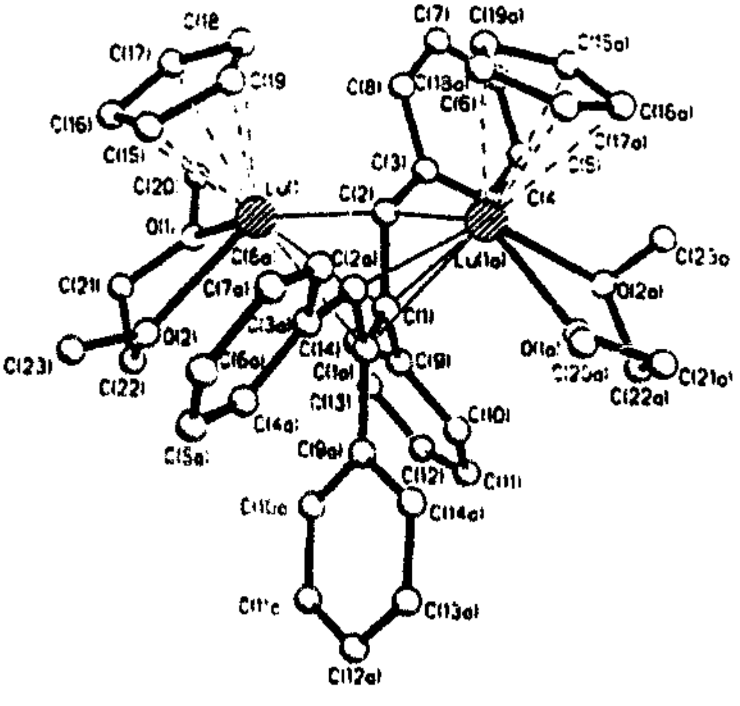

Fig. 7. Molecular structure of [CpLu(DME)]$_2$[1,1-μ-4,4-μ-(Ph)C(Ph)C=C(Ph)C(Ph)].

and the average Lu–C(Cp) distance is 2.62 Å. The C$_4$Ph$_4$ ligand has an asymmetrical propeller-like structure, which provides chirality to the molecule on the whole. Two enantiomeric forms of the molecules were found in the crystal of [CpLu(DME)]$_2$[1,1-μ-4,4-μ-(Ph)C(Ph)C=C(Ph)C(Ph)]. The authors suggested that the Lu central atoms in the molecule are bonded by two alkylidene type carbon bridges $>C^2$ connected by the ethene group.

$$2CpLuC_{10}H_8(THF)_2 + 2Ph_2N_2 \xrightarrow{THF} [CpLu(THF)]_2(Ph_2N_2)_2 + 2C_{10}H_8$$

$$2CpLuC_{10}H_8(DME) + 2PhC \equiv CPh \rightarrow$$
$$[CpLu(DME)]_2[\mu-(Ph)C(Ph)C=C(Ph)C(Ph)] + 2C_{10}H_8$$

W. Kretschmer und K.-H. Thiele [20] prepared a series of cyclopentadienyllanthanide 1,3-butadiene complexes including $(C_5Me_5)La(C_4H_6) \cdot MgI_2 \cdot 3THF$, $(C_5Me_5)Ce(C_4H_6) \cdot MgBr_2 \cdot 2THF$, $(C_5Me_5)Nd(C_4H_6) \cdot MgCl_2 \cdot 2THF$, $[1,3\text{-}(t\text{-}C_4H_9)_2C_5H_3]Nd(C_4H_6) \cdot MgCl_2 \cdot 2THF$, $(C_5H_5)Er(C_4H_6) \cdot MgCl_2 \cdot 2THF$, $[1,3\text{-}(t\text{-}C_4H_9)_2C_5H_3]Lu(C_4H_6) \cdot MgCl_2 \cdot 2THF$ by the reaction of the appropriate cyclopentadienyllanthanide dihalides with $(C_4H_6)Mg(THF)_2$. Subsequent reactions of $(C_5Me_5)Nd(C_4H_6) \cdot MgCl_2 \cdot 2THF$ with diphenylamine and of $(C_5Me_5)Ce(C_4H_6) \cdot MgBr_2 \cdot 2THF$ with carbon dioxide were also investigated. The products were characterized by elemental analyses, IR, ^1H and ^{13}C NMR and EI-MS spectroscopy.

$$Cp^*LnX_2(THF)_x + (C_4H_6)Mg(THF)_2 \xrightarrow{THF} Cp^*Ln(C_4H_6) \cdot MgX_2 \cdot nTHF$$

$$Cp^* = C_5H_5,\ C_5Me_5 \text{ or } 1,3-(t-C_4H_9)_2C_5H_3,$$

$$Ln = La,\ Ce,\ Nd,\ Er \text{ or } Lu;\ X = Cl,\ Br \text{ or } I;\ n = 2 \text{ or } 3$$

$$(C_5Me_5)Nd(C_4H_6) \cdot MgCl_2 \cdot 2THF + 3HNPh_2 \xrightarrow[MgCl_2,\ C_4H_8,\ 2THF]{THF}$$

$$(C_5Me_5)Nd(NPh_2)_2 \cdot HNPh_2$$

$$(C_5Me_5)Ce(C_4H_6) \cdot MgBr_2 \cdot 2THF + 2CO_2 \xrightarrow[MgBr_2,\ 2THF]{DMF}$$

$$(C_5Me_5)Ce(O_2CC_4H_6CO_2)_2$$

X. Zhou et al. [21] reported the synthesis and structure of a new organolanthanide oxo complex, $(MeC_5H_4)_3Yb_4(\mu\text{-}Cl)_6(\mu_3\text{-}Cl)(\mu_4\text{-}O)(THF)_3$. The compound was obtained from the reaction of $Na(C_5H_4Me)$ with $YbCl_3$ and YbOCl in THF. In the structure of $(MeC_5H_4)_3Yb_4(\mu\text{-}Cl)_6(\mu_3\text{-}Cl)(\mu_4\text{-}O)(THF)_3$ (Fig. 8) the four Yb atoms form a distorted tetrahedron. Three Yb atoms are coordinated by one bridging oxygen atom, four bridging chlorine atoms and a C_5H_4Me-ligand to give a distorted octahedral geometry, while the fourth Yb atom is coordinated by one bridging oxygen atom, three bridging chlorine atoms and three tetrahydrofuran molecules. The average Yb–C(Cp-ring) distance is 2.59(2) Å, the triply bridging Yb–Cl distances are 2.79(4)–2.81(4) Å, the doubly bridging Yb–Cl bond lengths are 2.60(4)–2.71(4) Å and the Yb–O(μ_4-oxide) distances are 2.13(1)–2.29(1) Å.

2.2.2. *Bis(cyclopentadienyl) complexes*

M.-R. Spirlet and J. Goffart [22] prepared the ytterbium complex $[Yb(\eta^5\text{-}C_5H_4SiMe_3)_2(\mu\text{-}Cl)]_2$ by the reaction of $YbCl_3$ with $Li(C_5H_4SiMe_3)$ in THF. According to X-ray diffraction the compound has a typical dimeric structure with two bridging chlorine atoms. The Yb–Cl bond lengths are 2.643(2) and 2.659(2) Å, the Yb–C distances range from 2.570(9) to 2.634(8) Å.

X. Zhou et al. [23] investigated the thermolytic reactivity of Cp_2HoCl and published the structure of $[(C_5H_3CH{=}CHCH_2C{=}CHC_5H_4)_2Ho_2Cl_2]_\infty$. The latter compound was obtained by sublimation of Cp_2HoCl at 235 °C. The polymeric

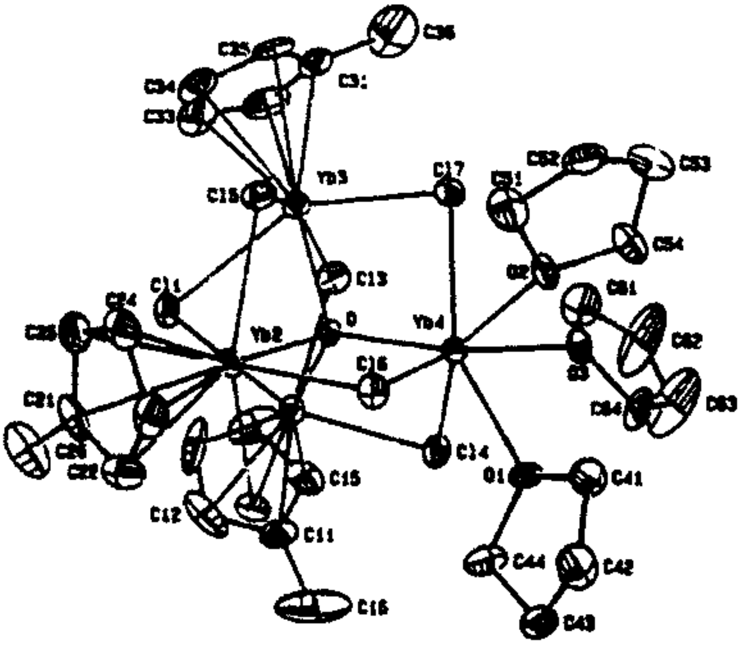

Fig. 8. Molecular structure of $(MeC_5H_4)_3Yb_4(\mu\text{-}Cl)_6(\mu_3\text{-}Cl)(\mu_4\text{-}O)(THF)_3$.

two-dimensional infinite network of the compound consists of $(C_5H_3CH=CHCH_2C=CHC_5H_4)_2Ho_2Cl_2$ units, in which each holmium atom is coordinated by a monosubstituted η^5-Cp group, a disubstituted η^5-Cp group and two bridging chlorine atoms. The cyclopentadienyl groups are cross-linked together by μ_3-"open cyclopentadiene" trialkenyl chains. The average Ho–C(monosubstituted η^5-Cp) distances and Ho–Cl bond lengths are 2.63(2) and 2.67(1) Å, respectively.

H. Schumann et al. [24] reported the reactions of $LnCl_3$ (Ln = Ho, Tm, Lu) with $Na(C_5Me_4H)$ in THF to give the corresponding dicyclopentadienyl complexes $(C_5Me_4H)_2LnCl(THF)$. The Ln(II)-complexes $(C_5Me_4H)_2Ln(THF)_2$ (Ln = Sm, Yb) were also synthesized by the reactions of the appropriate LnI_2 with two equivalents of $Na(C_5Me_4H)$ in THF. The obtained complexes were characterized by elemental analyses, as well as EI-MS, ^1H and ^{13}C NMR spectra.

H. Schumann et al. [25] also prepared lanthanide metallocene complexes containing the ethyltetramethylcyclopentadienyl ligand. Reactions of $LnCl_3(THF)_x$ (Ln = Y, Nd, Sm, Lu) with $Na(C_5Me_4Et)$ in THF gave the corresponding $(C_5Me_4Et)_2LnCl(THF)$ complexes. The bis(ethyltetramethylcyclopentadienyl)lanthanide chlorides were converted into the amides $(C_5Me_4Et)_2Ln[N(SiMe_3)_2]$ or alkyl complexes $(C_5Me_4Et)_2Ln[CH(SiMe_3)_2]$ by reaction with equimolar amounts of either $NaN(SiMe_3)_2$ or $LiCH(SiMe_3)_2$ in toluene. The compounds $(C_5Me_4Et)_2Y[N(SiMe_3)_2]$ and $(C_5Me_4Et)_2Sm[CH(SiMe_3)_2]$ were characterized by X-ray crystallography. In $(C_5Me_4Et)_2Y[N(SiMe_3)_2]$ the yttrium atom is coordinated by two C_5Me_4Et ligands and one bis(trimethylsilyl)amido ligand and has a pseudo-trigonal planar arrangement. The average Y–C(η^5) distances and Y–N bond lengths are 2.678(2) and 2.276(3) Å, respectively. In $(C_5Me_4Et)_2Sm[CH(SiMe_3)_2]$ (Fig. 9) the samarium atom also adopts a pseudo-trigonal planar coordination

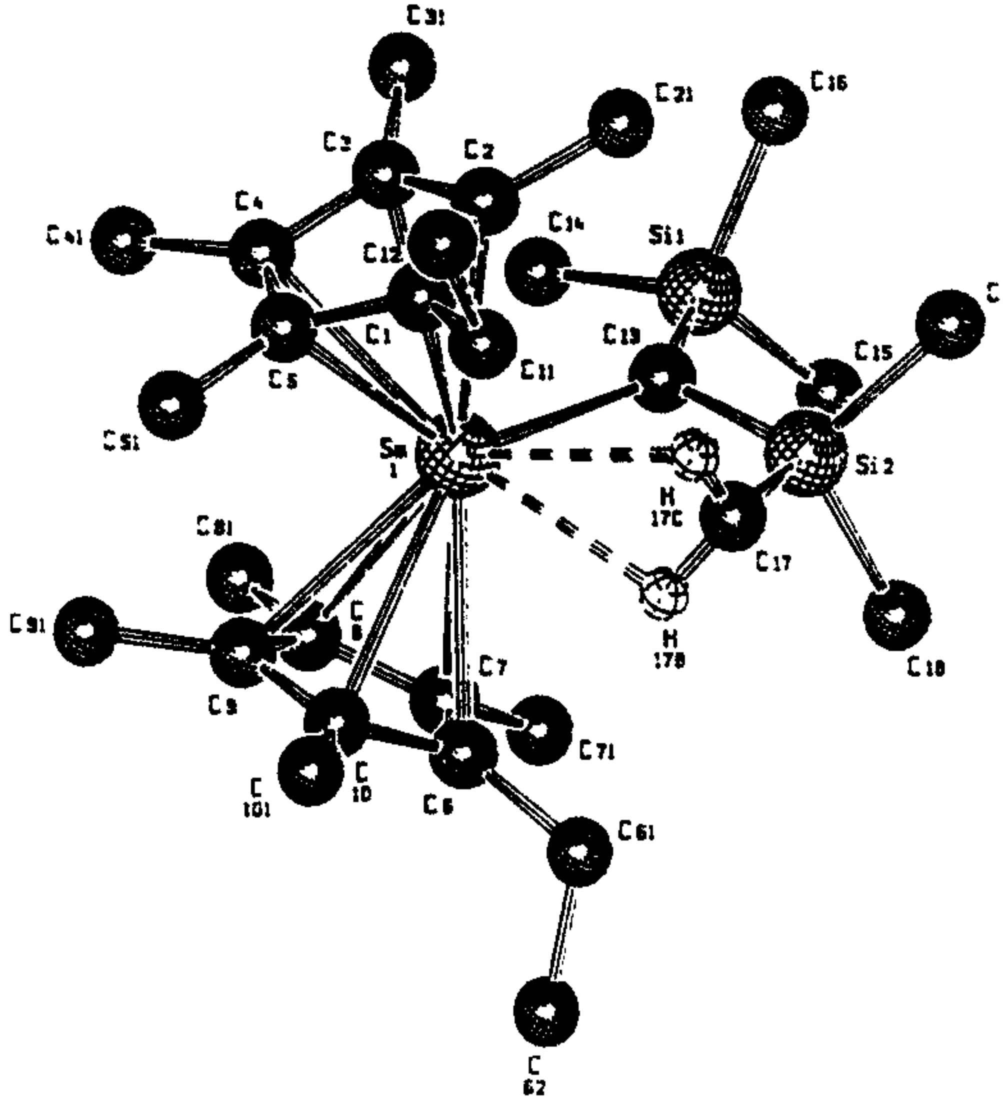

Fig. 9. Molecular structure of [$(C_5Me_4Et)_2Sm\{CH(SiMe_3)_2\}$].

sphere with two C_5Me_4Et-ligands and one $CH(SiMe_3)_2$-ligand. The average Sm–C(η^5-C_5Me_4Et) distances are 2.732(3) and 2.740(3) Å, and the Sm–C($CH(SiMe_3)_2$) σ-bond length is 2.502(3) Å. The authors presume γ-agostic bonds between the methyl groups of the $N(SiMe_3)_2$ or $CH(SiMe_3)_2$ ligands and the lanthanide center in both structures.

$$LnCl_3(THF)_x + 2Na(C_5Me_4Et) \rightarrow (C_5Me_4Et)_2LnCl(THF) + 2NaCl$$

$$(C_5Me_4Et)_2LnCl(THF) + NaN(SiMe_3)_2 \rightarrow$$
$$(C_5Me_4Et)_2Ln[N(SiMe_3)_2] + NaCl$$

$$(C_5Me_4Et)_2LnCl(THF) + LiCH(SiMe_3)_2 \rightarrow$$
$$(C_5Me_4Et)_2Ln[CH(SiMe_3)_2] + LiCl \quad Ln = Y, Nd, Sm, Lu$$

H. Schumann et al. [26] also used the sodium salt of the ethyltetramethylcyclopentadienyl ligand for the synthesis of the correspondent samarium(II) and ytterbium(II) complexes, $(C_5Me_4Et)_2Ln(THF)$ ($Ln = Sm$ or Yb). The compounds were characterized by NMR and MS spectroscopy and the structure of $(C_5Me_4Et)_2Yb(THF)$ was determined by X-ray diffraction. The ytterbium complex has a typical bent metallocene structure, in which the Yb atom is coordinated by two η^5-C_5Me_4Et-ligands and one oxygen atom of the solvating THF. Ytterbium has the formal coordination number 7. The average Yb–C(ring) distance is 2.692(7) Å and the angle Cp_c–Yb–Cp_c is 144.5°.

$$LnI_2(THF)_x + 2Na(C_5Me_4Et) \xrightarrow{THF} (C_5Me_4Et)_2Ln(THF) + 2NaI$$

M.G. Silva-Valenzuela et al. [27] reported the synthesis and characterization of a tetramethylurea adduct of a bis(cyclopentadienyl) ytterbium(II) complex, $Cp_2Yb(TMU)_2$ (TMU = 1,1,3,3-tetramethylurea). The compound was obtained by addition of $(CH_3)_2NCON(CH_3)_2$ to $Cp_2Yb(THF)_2$, which was previously synthesized by reduction of $Cp_2YbCl(THF)$ with sodium naphthalenide. The complex was characterized by metal analysis, IR and ^1H NMR spectra and by single-crystal X-ray diffraction. In the structure (Fig. 10) the ytterbium atom has a distorted tetrahedral arrangement formed by the two η^5-Cp rings and two oxygen atoms of the TMU ligands. The Yb–C distances range from 2.708(9) to 2.760(9) Å, while the Yb–O distance is 2.325(5) Å.

D.J. Schwartz and R.A. Andersen [28] investigated interactions of Cp^*_2Yb ($Cp^* = C_5Me_5$) with trialkylphosphines (Me_3P, Et_3P, $Me_2PCH_2PMe_2$ and $1,2\text{-}(Me_2P)_2C_6H_4$) and R_3PX derivatives (Me_3PO, Et_3PNH, $Me_2PhPCHSiMe_3$, Me_2PhPCH_2) in solution. The interactions and the obtained adducts, $Cp^*_2Yb(PMe_3)_2$, $Cp^*_2Yb(PMe_3)$, $Cp^*_2Yb(PEt_3)$, $Cp^*_2Yb(Me_2PCH_2PMe_2)$, $Cp^*_2Yb[1,2\text{-}(Me_2P)_2C_6H_4]$, $Cp^*_2Yb(OPMe_3)$, $Cp^*_2Yb(HNPEt_3)$, $Cp^*_2Yb(OPMe_3)_2$,

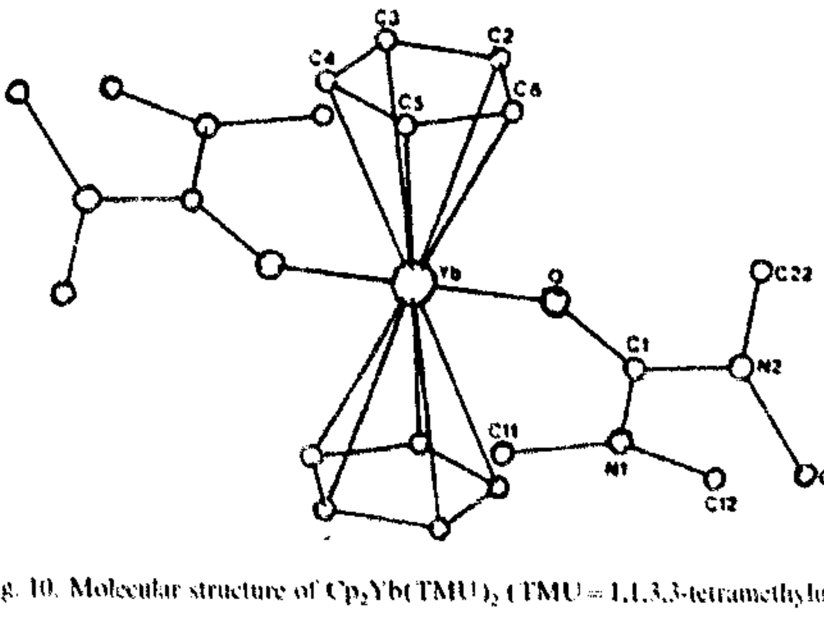

Fig. 10. Molecular structure of $Cp_2Yb(TMU)_2$ (TMU = 1,1,3,3-tetramethylurea).

$Cp^*_2Yb(HNPEt_3)_2$, $Cp^*_2Yb(Me_2PhPCHSiMe_3)$ and $Cp^*_2Yb(Me_2PhPCH_2)$, have been investigated by ^1H, ^{13}C, ^{31}P, ^{171}Yb and variable-temperature NMR spectroscopy. It was found that $^1J_{YbP}$ is significantly reduced for 1:2 phosphine adducts, relative to the 1:1 adducts. The barrier for the intermolecular exchange for phosphine oxide and imine adducts is much higher and the $^2J_{YbP}$ values for 1:1 adducts are one order of magnitude smaller than the analogous one-bond values for the phosphine derivatives. The ylide adduct $Cp^*_2Yb(Me_2PhPCHSiMe_3)$ was also characterized by X-ray crystallography. In the structure (Fig. 11) the Yb–C21 distance (2.69(2) Å) and other parameters indicate a direct Yb–C interaction, supplemented by a secondary γ-CH_3 interaction.

The same authors and G.E. Ball [29] also studied interactions of Cp^*_2Yb ($Cp^* = C_5Me_5$) with *cis*-P_2PtX_2 complexes (P_2 = chelating phosphine; X = H, CH_3). The obtained complexes, [{*cis*-$(Me_3C)_2PCH_2CH_2P(CMe_3)_2$}$Pt(\mu\text{-}H)_2YbCp^*_2$], [{*cis*-$(Cy)_2PCH_2CH_2P(Cy)_2$}$Pt(\mu\text{-}H)_2YbCp^*_2$], [{*cis*-$(^iPr)_2PCH_2CH_2P(^iPr)_2$}$Pt(\mu\text{-}CH_3)_2YbCp^*_2$] and [{*cis*-$(^iPr)_2PCH_2CH_2P(^iPr)_2$}$Pt(\mu\text{-}CH_3)(\mu\text{-}H)YbCp^*_2$] have been investigated by NMR spectroscopy. The latter two compounds were characterized also by their X-ray structures. In the structure of [{*cis*-$(^iPr)_2PCH_2CH_2P(^iPr)_2$}$Pt(\mu\text{-}CH_3)_2YbCp^*_2$] (Fig. 12) the Pt and Yb atoms are connected via the two bridging methyl groups. The Pt···Yb separation is 4.0391(5) Å, the Yb–C(μ-CH_3) distances are 2.908(8) and 2.88(1) Å, and the Pt–C–Yb angles are 106.8(3)° and 107.5(4)°. There was found a rare agostic C–H–Yb bonding mode for the bridging methyl groups. The Yb–H(μ–CH_3) distances are ranging from 2.30 to 3.80 Å. For the structure of [{*cis*-$(^iPr)_2PCH_2CH_2P(^iPr)_2$}$Pt(\mu\text{-}CH_3)(\mu\text{-}H)YbCp^*_2$] the hydrogen atoms on the bridging methyl group and the hydride ligand were not located. In this structure the Pt–Yb separation is 3.388(9) Å and the Yb–C(μ–CH_3) distance is 2.79(2) Å. In contrast to the agostic interactions observed for the previous structure, structural

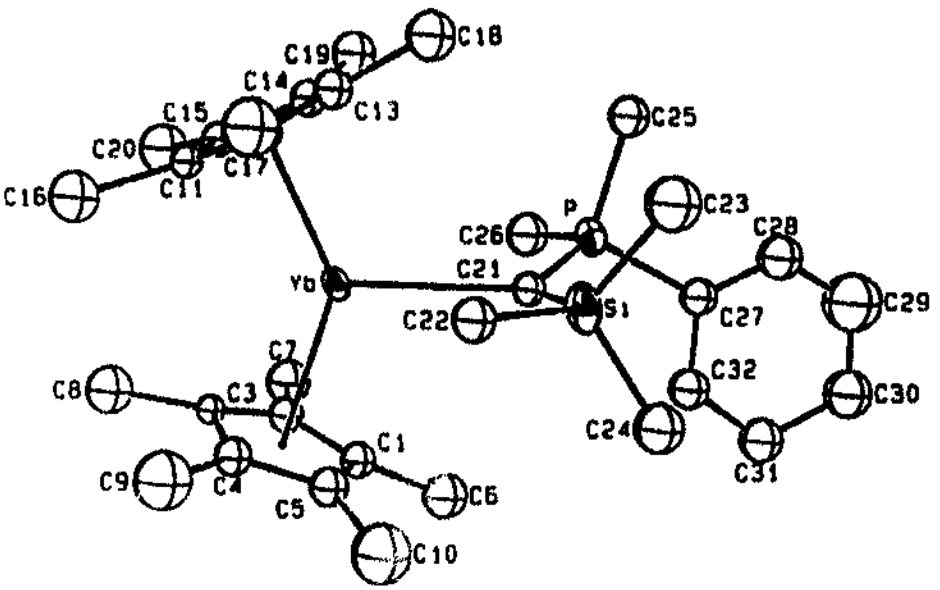

Fig. 11. Molecular structure of $Cp^*_2Yb(Me_2PhPCHSiMe_3)$.

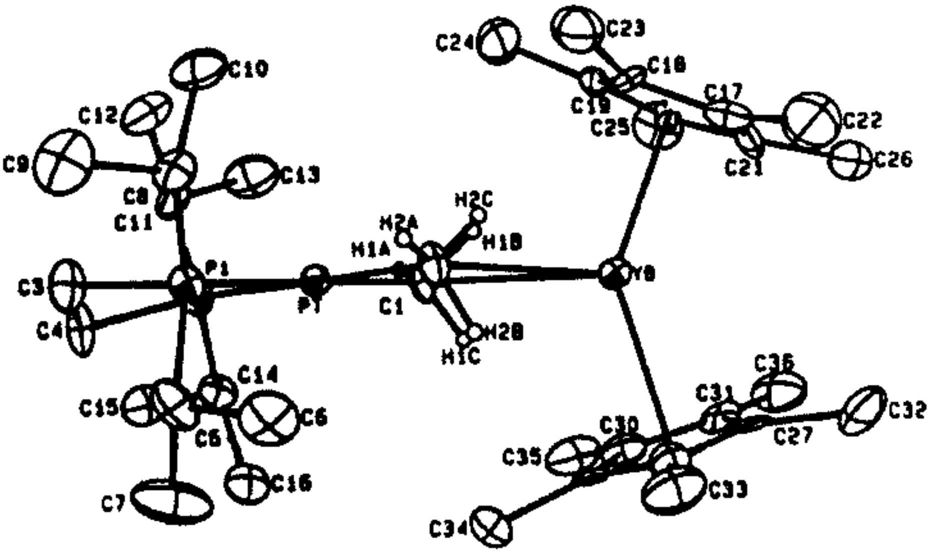

Fig. 12. Molecular structure of [{*cis*-(^{i}Pr)$_2$PCH$_2$CH$_2$P(^{i}Pr)$_2$}Pt(μ-CH$_3$)$_2$YbCp$^*_2$].

parameters for [{*cis*-(^{i}Pr)$_2$PCH$_2$CH$_2$P(^{i}Pr)$_2$}Pt(μ-CH$_3$)(μ-H)YbCp$^*_2$] were found to be consistent with a Pt–C–Yb interaction.

K.-H. Thiele and R. Seifert [30] prepared a series of permethyllanthanocene and lutetiocene vinyl complexes, [Li(DME)$_3$][Cp$^*_2$La(C$_4$H$_6$)], Cp$^*_2$LaCPh=CMe$_2$·2THF, Cp$^*_2$Lu(CH=CH$_2$)·LiCl·DME and Cp$^*_2$LuCPh=CMe$_2$·2MgCl$_2$·DME. The compounds were obtained by reactions of the appropriate precursors Cp$^*_2$Ln(μ-Cl)$_2$K(DME)$_2$ (Ln=La or Lu) with LiCH=CH$_2$ or with MgBrCPh=CMe$_2$. The complexes were characterized by ^{1}H and ^{13}C NMR spectroscopy.

$$\mathrm{Cp^*_2La(\mu-Cl)_2K(DME)_2 + LiCH{=}CH_2 \xrightarrow[-78\,^\circ C]{DME}}$$

$$\mathrm{[Li(DME)_3][Cp^*_2La(C_4H_6)] + LiCl + KCl}$$

$$\mathrm{Cp^*_2La(\mu-Cl)_2K(DME)_2 + MgBrCPh{=}CMe_2 \xrightarrow[2DME]{THF/OEt_2}}$$

$$\mathrm{Cp^*_2LaCPh{=}CMe_2 \cdot 2THF + MgBrCl + KCl}$$

$$\mathrm{Cp^*_2Lu(\mu-Cl)_2K(DME)_2 + LiCH{=}CH_2 \xrightarrow{DME}}$$

$$\mathrm{Cp^*_2Lu(CH{=}CH_2) \cdot LiCl \cdot DME + KCl + DME}$$

K.-H. Thiele and coworkers [31] also published the synthesis and characterization of some Cp$^*_2$Ln(DAD)-complexes. The reaction of Cp$^*_2$La(μ-Cl)$_2$K(DME)$_2$ with one equivalent of Na$_2$(DAD) [DAD=(Ph)N=C(Ph)C(Ph)=N(Ph)] in the presence of DAD or with two equivalents of Na(DAD) gave the ionic complex [Na(DAD)][Cp$^*_2$La(DAD)] (Scheme 2). The interaction of Cp$^*_2$Y(μ-Cl)$_2$Li(OEt$_2$)$_2$ with Na(DAD) [DAD=N(C$_6$H$_4$-4-Me)=C(Ph)C(Ph)=N(C$_6$H$_4$-4-Me)] led to the Cp$^*_2$Y(DAD) complex, which was structurally characterized. The DAD ligand in the complex is reduced to the radical anion. In the structure (Fig. 13) the yttrium atom has a pseudo-tetrahedral coordination arrangement formed by the two Cp*-groups and two N atoms of the *cis*-1,4-diazadiene. The Y–(η^5-Cp*-ring) and Y–N distances are 2.408(4) and 2.362(6) Å, respectively. The metallacycle Y(N–C–C–N) is planar.

K. Jacob et al. [32] reported the synthesis and structure of the novel heterotrimetallic complex $Li[Cp_2Y(FcN)_2]$ (FcN = 2-dimethylaminomethylferrocenyl). The compound was obtained by the reaction of $[Cp_2YCl]_2$ with two equivalents of 2-dimethylamino-methylferrocenyl lithium in THF solution. In the structure (Fig. 14) the central Y atom is pseudo-tetrahedrally coordinated by two η^5-C_5H_5-ligands and by two η^1-σ-bonded cyclopentadienyl rings from the dimethylaminomethylferrocenyl groups. The Y–C(η^1–σ–Cp) distance is 2.534(3) Å and the angle (η^1–σ–Cp)C–Y–C(η^1–σ–Cp) is 89.37(11)°. The lithium atom also adopts a tetrahedral arrangement which is formed by the two N atoms of the Me_2NCH_2-substituents and by the C atoms of the Cp rings.

$$[Cp_2YCl]_2 + 4Li(FcN) \rightarrow 2Li[Cp_2Y(FcN)_2] + 2LiCl$$

F. Shen et al. [33] prepared new bis(cyclopentadienyl)lanthanide complexes with the 2-naphthoyltrifluoroacetonato chelating ligand, $Cp_2Ln(C_{10}H_7COCHCOCF_3)(THF)$ (Ln = Ho, Fr) and $Cp_2Ln(C_{10}H_7COCHCOCF_3)$(Ln = Pr, Sm). The complexes were characterized by elemental analyses and IR spectroscopy, and the structure of $Cp_2Ho(C_{10}H_7COCHCOCF_3)(THF)$ was determined by X-ray diffraction. In the structure (Fig. 15) the central Ho atom is coordinated by two η^5-C_5H_5-ligands, two oxygen atoms of the 2-naphthoyltrifluoroacetonato ligand and one oxygen of a THF molecule. The Ho–Cp(cent.) distances are 2.402 and 2.371 Å and the Ho–$O(C_{10}H_7COCHCOCF_3)$ distances are 2.250(3) and 2.306(4) Å.

G. Lin and W.-T. Wong [34] reported the synthesis and crystal structure of the divalent ytterbium complex $(\eta^5$-$C_5H_4PPh_2)_2Yb(DME)$. The compound was

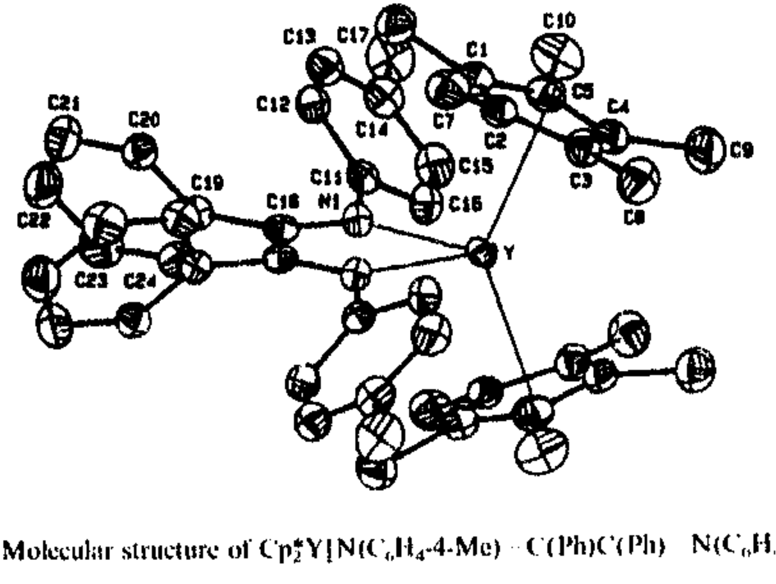

Fig. 13. Molecular structure of $Cp^*_2Y[N(C_6H_4\text{-}4\text{-}Me)$–C(Ph)C(Ph)–$N(C_6H_4\text{-}4\text{-}Me)]$.

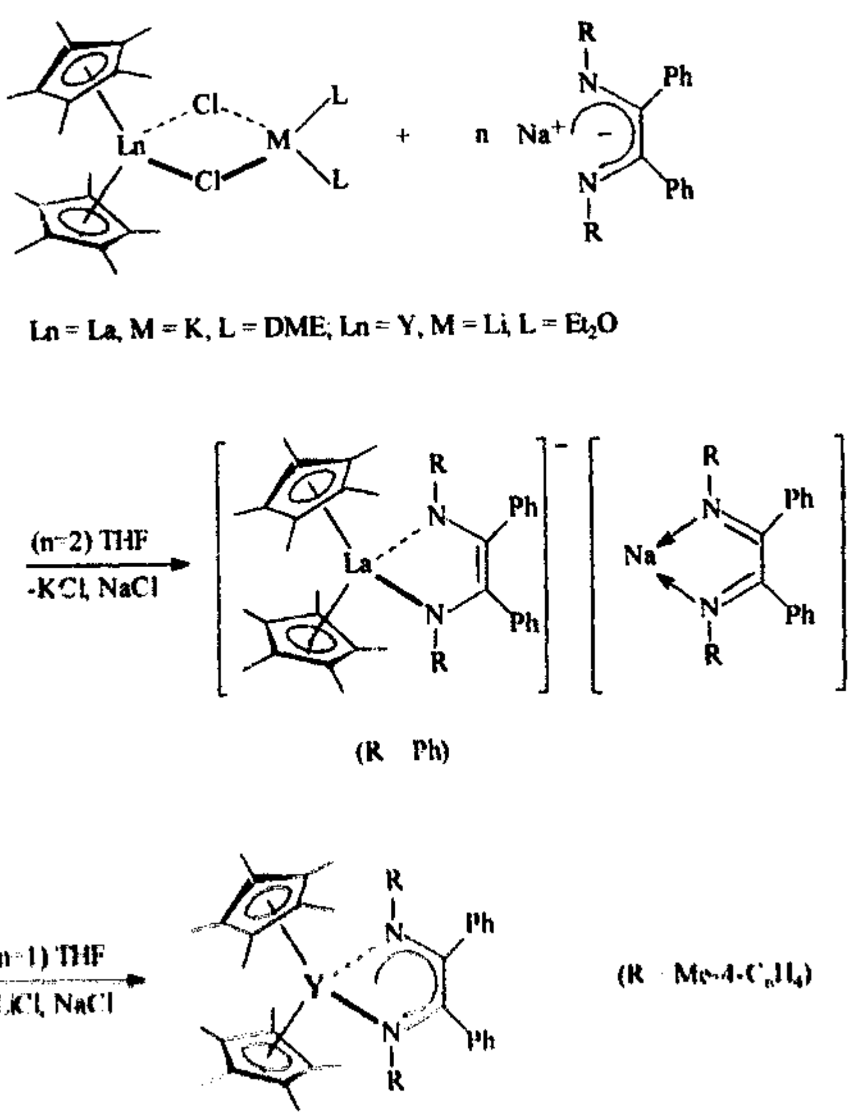

Scheme 2.

obtained by reaction between the thallium derivative $[(\eta^5{:}\eta^5\text{-}C_5H_4PPh_2)Tl]_x$ and excess of metallic ytterbium in THF followed by extraction with DME. According to an X-ray structure determination in the molecule $(\eta^5\text{-}C_5H_4PPh_2)_2Yb(DME)$ the Yb atom is coordinated by two $\eta^5\text{-}C_5H_4PPh_2$-rings and by two oxygen atoms of the solvent DME molecule, but Yb is not coordinated by the phosphorus atoms of the substituents. Thus, the ytterbium has a distorted tetrahedral coordination arrangement. The Yb–C distances are ranged from 2.666 to 2.747 Å with a mean value of 2.710 Å.

The same authors [35] also prepared the trigonal organoerbium cluster $[Na(DME)_3]^+[\{(Ph_2PC_5H_4)_2Er\}_3(\mu_3\text{-}O)(\mu\text{-}OH)_2]^-$ by reaction of $ErCl_3$ with $Ph_2PC_5H_4Na$ in the presence of traces of water. The compound was characterized by elemental analysis, IR, ^{31}P NMR and single-crystal X-ray diffraction. The structure consists of discrete cation $[Na(DME)_3]^+$ and anion

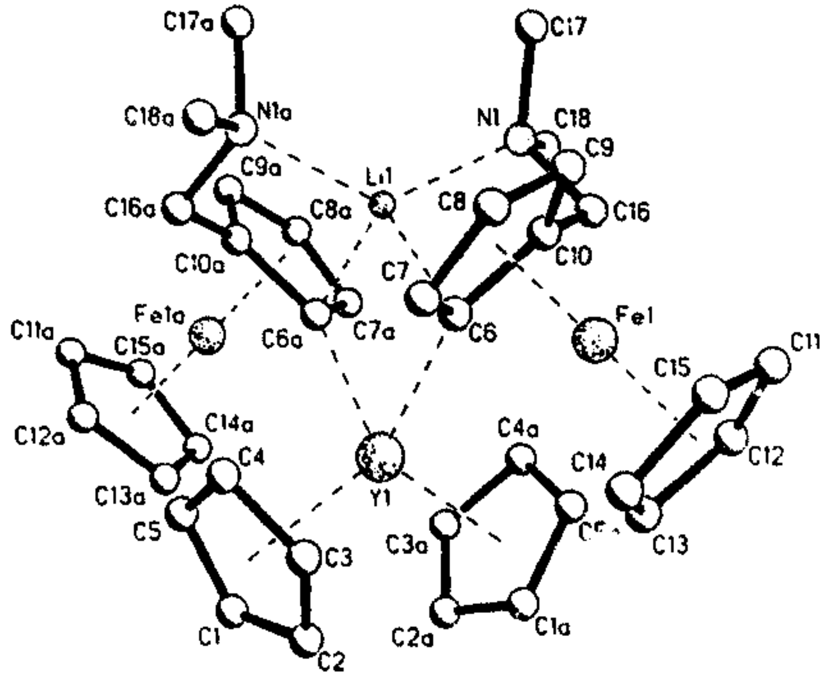

Fig. 14. Molecular structure of $Li[Cp_2Y(FeN)_2]$ (FeN = 2-dimethylaminomethylferrocenyl).

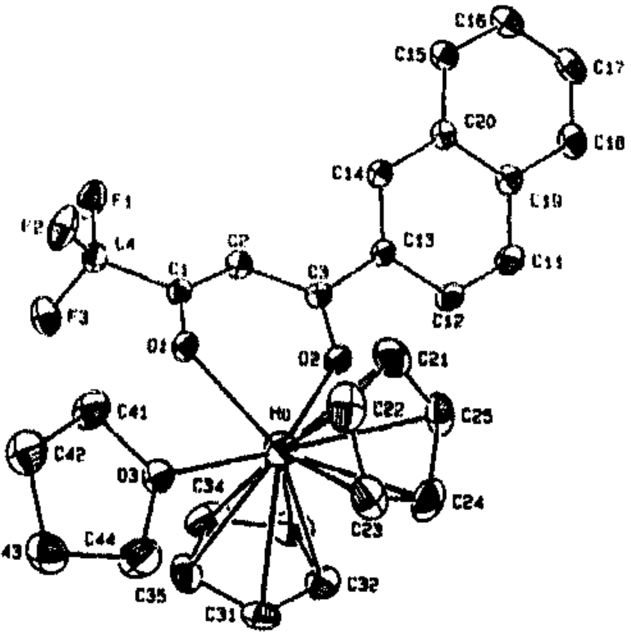

Fig. 15. Molecular structure of $Cp_2Ho(C_{10}H_7COCHCOCF_3)(THF)$.

$[\{(Ph_2PC_5H_4)_2Er\}_3(\mu_3-O)(\mu_3-OH)_2]$ pairs. In the anion (Fig. 16) three $(Ph_2PC_5H_4)_2Er$ fragments are linked by one μ_3-oxygen and two μ_2-hydroxy groups in a triangular array. Two erbium atoms have a coordination number of eight, while the third erbium atom is nine-coordinated. The average Er–C($Ph_2PC_5H_4$) and Er–O distances are 2.72 and 2.16(2) Å, respectively.

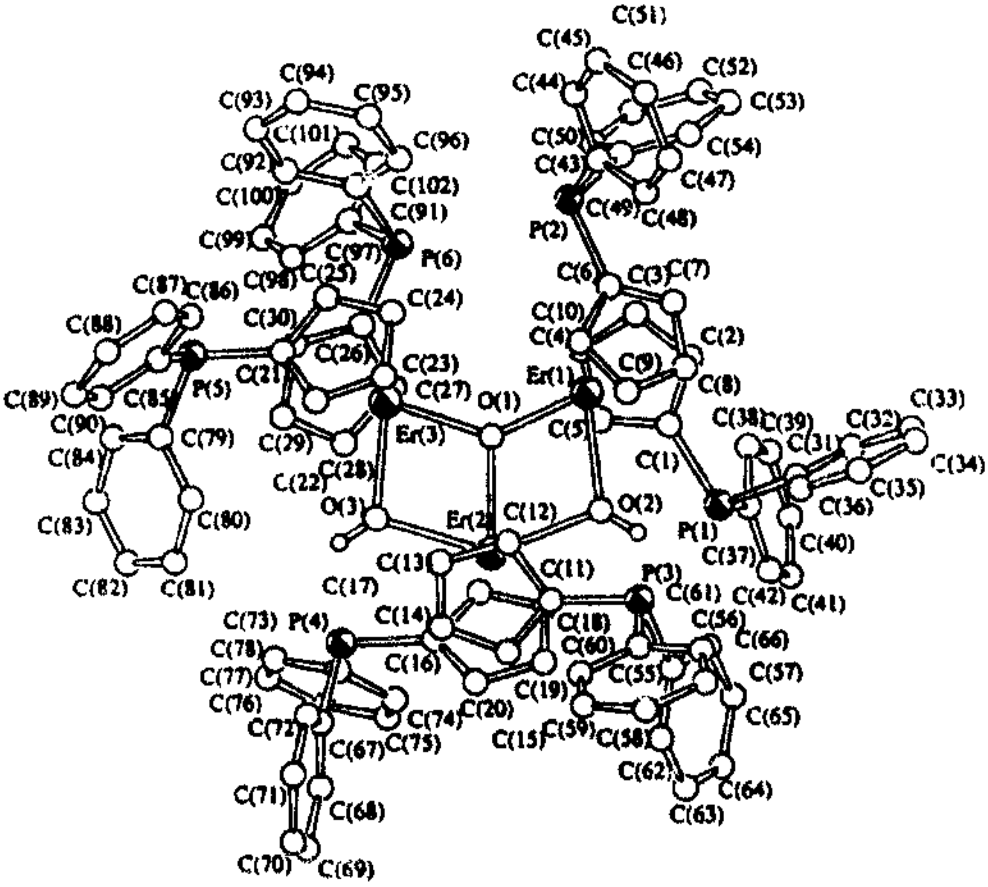

Fig. 16. Structure of the [{(Ph$_2$PC$_5$H$_4$)$_2$Er}$_3$(μ_3-O)(μ-OH)$_3$]$^-$ anion.

J.S. Xia et al. [36] published a new synthetic route to Cp$_2$Yb(THF)$_2$. The complex was obtained by reduction of Cp$_2$YbCl(THF) with cyclooctadienyl potassium. The compound was characterized by elemental analyses, IR spectroscopy and X-ray crystallography.

K. Takaki et al. [37] reported the generation of organosamarium η^3-allyl complexes by reductive cleavage of allylic ethers with Cp$^*_2$Sm(THF)$_n$ (Scheme 3). The second product of these reactions is the samarium benzyloxide Cp$^*_2$SmOCH$_2$Ph.

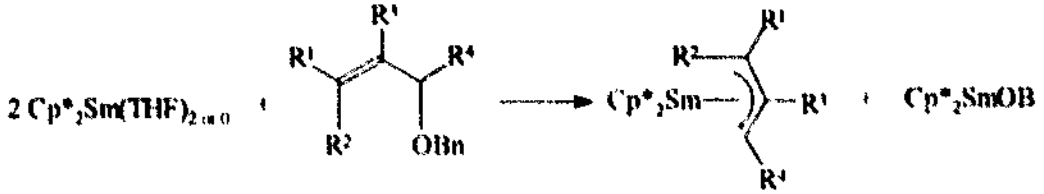

R^1 = H, Me or Ph, R^2 = H or Me, R^3 = H or Me, R^4 = H or Me, OBn = OCH$_2$Ph

Scheme 3.

K. Takaki and coworkers [38] also published the generation of allenic samarium complexes from propargylic benzyl ethers and Cp$^*_2$Sm(THF)$_2$ (Scheme 4).

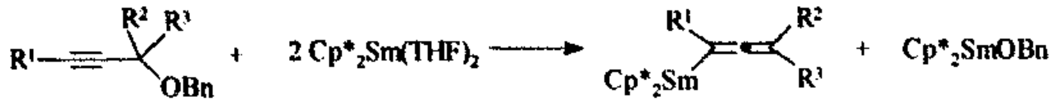

R^1 = Ph or ^{n}Bu ; R^2 = H, Me, Ph or ^{n}Bu; R^3 = H or Me; OBn = OCH_2Ph

Scheme 4.

W.J. Evans et al. [39] reported the synthesis and structure of the mixed-metal complexes $[PPh_4][(Cp^{\ddagger}_2Sm)_2Mo(\mu\text{-}S)_4]$ and $[PPh_4][Cp^{\ddagger}_2Sm(\mu\text{-}S)_2WS_2]$. The compounds were obtained by reaction of $Cp^{\ddagger}_2Sm(THF)_2$ with $[PPh_4]_2MoS_4$ and $[PPh_4]_2WS_4$. According to an X-ray structure determination (Fig. 17) the cation $[(Cp^{\ddagger}_2Sm)_2Mo(\mu\text{-}S)_4\}]^-$ contains two essentially identical $Cp^{\ddagger}_2Sm(\mu\text{-}S)_2$ units with eight-coordinated Sm(III) atoms. The Sm–S distances are 2.784(2)–2.796(2) Å. In the structure of cation $[Cp^{\ddagger}_2Sm(\mu\text{-}S)_2WS_2]^-$ the Sm atom is bound to the tungsten center by two bridging sulfur atoms. The Sm–S distances are 2.817(8)–2.841(7) Å.

W.J. Evans and coworkers [40] also published the synthesis and structure of a nonclassical 7-norbornadienyl carbocation, $Cp^{\ddagger}_2Sm(O_2C_7Me_5)$, which was obtained by the reaction of $Cp^{\ddagger}_3Sm$ and CO in toluene. According to X-ray data the compound (Fig. 18) contains a $O_2C_7Me_5$-ligand, which originates from the five ring carbon atoms of a Cp* group and the carbon atoms of two CO molecules. The seven non-methyl carbon atoms of the ligand adopt a norbornadiene structure. The symmetry-equivalent Sm–O bonds are 2.347(2) Å, the average Sm–C(C_5Me_5) distance is 2.73 Å.

$$Cp^{*}_3Sm + 2CO \rightarrow Cp^{*}_2Sm(O_2C_7Me_5)$$

J.H. Teuben et al. [41] reported the activation of ethers and sulfides by organolan-

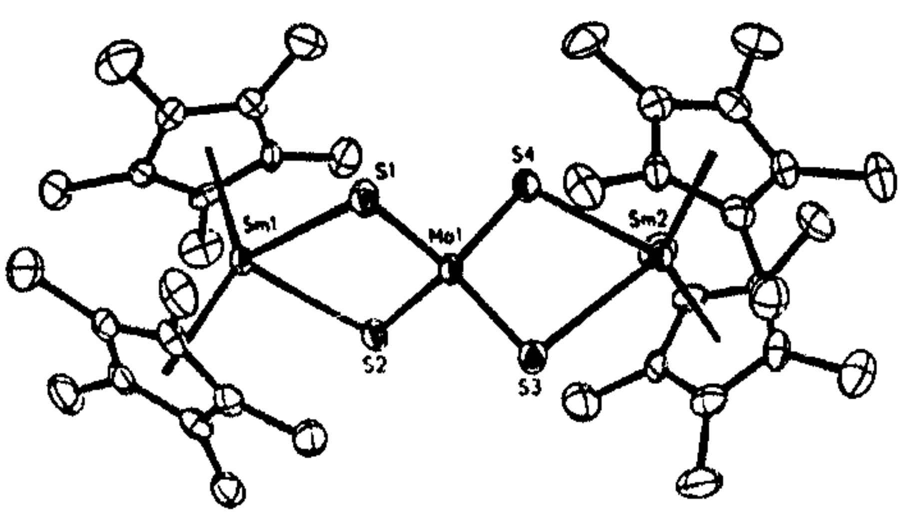

Fig. 17. Structure of $\{[Cp^{\ddagger}_2Sm]_2Mo(\mu\text{-}S)_4\}$ cation.

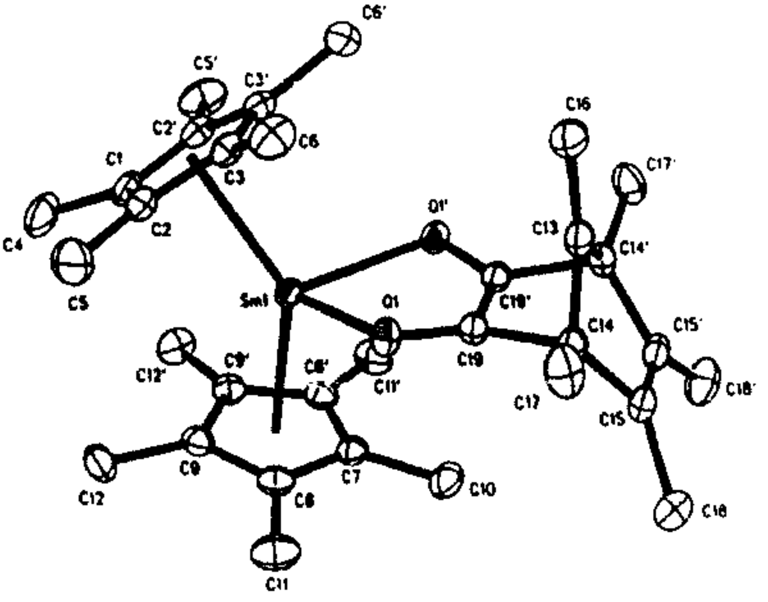

Fig. 18. Structure of $Cp^*_2Sm(O_2C_7Me_5)$.

thanide hydrides. $(Cp^*_2LnH)_2$ (Ln = Y, La, Ce; Cp* = C_5Me_5) cleave dialkyl ethers ROR′ to form alkoxides Cp^*_2LnOR and Cp^*_2LnOR', and alkanes. The interactions of $(Cp^*_2LnH)_2$ with Et_2O, ${}^tBuOMe$, ${}^tBuOEt$, ${}^nBuOEt$, THF, 1,4-dioxane, furan, ethyl vinyl ether and allyl ethyl ether were studied. The authors used NMR tube experiments for monitoring the reactions. The product of the reaction between $(Cp^*_2YH)_2$ and 1,4-dioxane (Scheme 5), $(Cp^*_2Y)_2(\mu\text{-}OCH_2CH_2O)(THF)_2$, was characterized by X-ray crystallography. In the structure (Fig. 19) two $Cp^*_2Y(THF)$ units

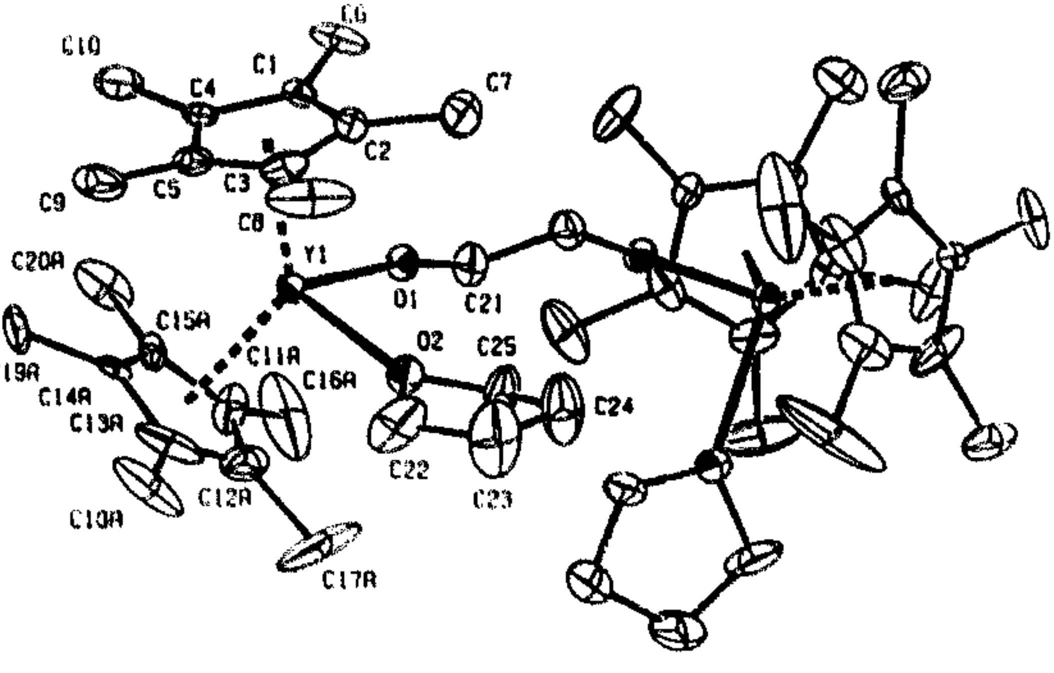

Fig. 19. Structure of $(Cp^*_2Y)_2(\mu\text{-}OCH_2CH_2O)(THF)_2$.

with distorted tetrahedral arrangement are bridged by a glycolate ligand. The Y–O(μ–OCH_2CH_2O) distance is 2.042(4) Å, the Y–Cp*(centroid) distances are 2.413(3) and 2.421(7) Å.

C–O bonds of alkoxides such as Cp^*_2LnOEt were cleaved also by $(Cp^*_2LnH)_2$ to give bimetallic complexes $(Cp^*_2Ln)_2$(μ-O). The structure of the THF adduct $(Cp^*_2Ce)_2$(μ-O)$(THF)_2$ was determined by X-ray diffraction. The complex consists of two Cp^*_2Ce fragments linked by a nearly linear oxygen bridge. The Ce–O(μ-) distances are equal (2.185(4) and 2.183(5) Å), the angle Ce1–O–Ce2 is 175.9(2)°. In contrast to ethers, activation of organic sulfides by $(Cp^*_2YH)_2$ led to the corresponding metalation products (Scheme 6).

$$(Cp^*_2LnH)_2 + 2\ ROR' \rightarrow Cp^*_2LnOR + Cp^*_2LnOR' + RH + R'H$$

Ln = Y, La, Ce; Cp* = C_5Me_5

Scheme 5.

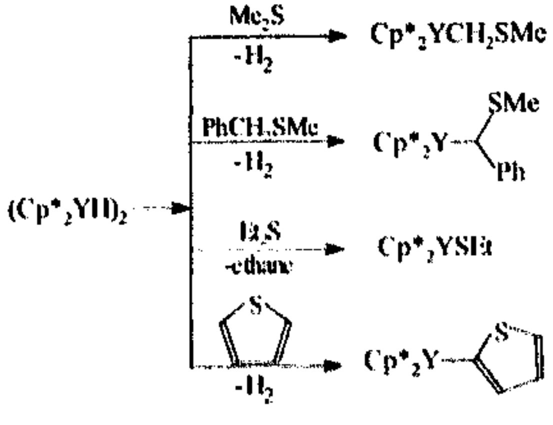

Scheme 6.

J.H. Teuben et al. [42] also described reactions of $(Cp^*_2LnH)_2$ (Ln = Y, La) and $Cp^*_2Y(2\text{-}C_6H_4CH_2NMe_2)$ with esters (ethyl acetate, ethyl benzoate, ethylacrylate, ethyl 2-methylpropanoate) and amides (*N*,*N*-dimethylacetamide) (Scheme 7). The molecular structure of the product of the reaction of $Cp^*_2Y(2\text{-}C_6H_4CH_2NMe_2)$ with ethyl acetate, $[Cp^*_2Y(\mu\text{-}OCMe{=}CHC(OEt)O)]_2$, was determined by X-ray diffraction. The structure (Fig. 20) is dimeric with two equivalent $Cp^*_2Y(\mu\text{-}OCMe{=}CHC(OEt)O)$-fragments. The Y–O distances are 2.179(2) and 2.292(2) Å.

$$(Cp^*_2LnH)_2 + MeCOOEt \rightarrow 2Cp^*_2LnOEt$$

$$(Cp^*_2LnH)_2 + PhCOOEt \rightarrow 2Cp^*_2LnOEt + Cp^*_2LnOCH_2Ph$$

Y.K. Gun'ko et al. [43] reported the activation of a C–O bond in dimethoxyethane (DME) by reaction of a tris(cyclopentadienyl)lanthanide complex with an alkali

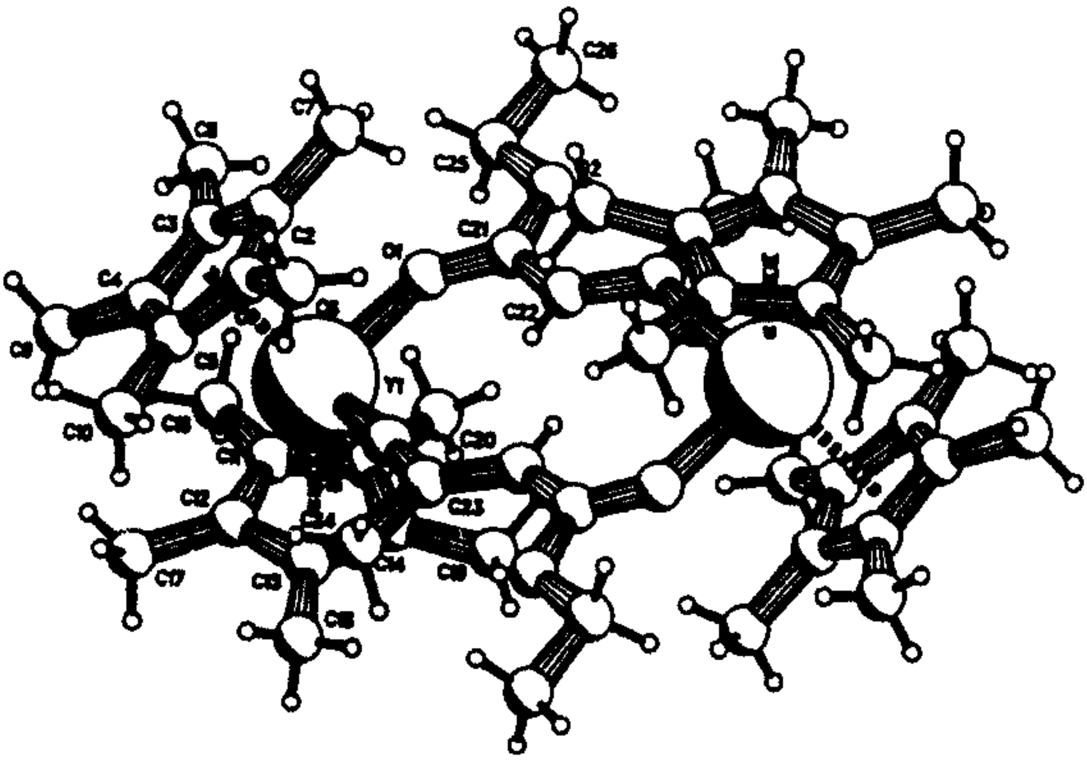

Fig. 20. Molecular structure of $[Cp^*_2Y(\mu\text{-}OCMe\}\{CbCHC(OEt)O)]_2$.

metal in DME. The interaction of $[LnCp''_3]$ (Ln = Ce, Cp″ = η-$C_5H_3^tBu_2$-1,3 or η-$C_5H_3(SiMe)_3$; Ln = Nd, Cp″ = η-$C_5H_3(SiMe)_3$) with metallic lithium or potassium in DME led to the formation of alkoxide complexes, $[\{LnCp''_2(\mu\text{-}OMe)\}_2]$ and $[Nd\{\eta\text{-}C_5H_3(SiMe_3)_2\text{-}1,3\}_2(\mu\text{-}OMe)_2Li(DME)]$. The latter complex and $[\{Ce(\eta\text{-}C_5H_3^tBu_2\text{-}1,3)_2(\mu\text{-}OMe)\}_2]$ were characterized by X-ray crystallography. In the dimeric structure of $[\{Ce(\eta\text{-}C_5H_3^tBu_2\text{-}1,3)_2(\mu\text{-}OMe)\}_2]$ two Cp''_2Ce fragments are bound by two bridging OMe-groups. The mean Ce–O bond distance is 2.376(4) Å and the Ce–Cp″(centroid) distances are 2.596 and 2.564 Å. The structure of $[Nd\{\eta\text{-}C_5H_3(SiMe_3)_2\text{-}1,3\}_2(\mu\text{-}OMe)_2Li(DME)]$ (Fig. 21) contains one Cp''_2Nd-fragment connected with the Li ion via two OMe-bridges. The central four-membered NdOLiO ring is almost planar. The Nd–O bond length and Nd–Cp″(centroid) distances are 2.25(1) and 2.58 Å, respectively.

$$[LnCp''_3] + M + DME \xrightarrow{DME} [\{LnCp''_2(\mu-OMe)\}_2]$$

Ln = Ce, Cp″ = η – $C_5H_3^tBu_2$ – 1,3 or η – $C_5H_3(SiMe)_3$, M = Li, K;

Ln = Nd, Cp″ = η – $C_5H_3(SiMe)_3$, M = K

$$[Nd\{\eta-C_5H_3(SiMe)_3\}_3] + Li + DME \xrightarrow{DME}$$

$$[Nd\{\eta-C_5H_3(SiMe_3)_2\}_2(\mu-OMe)_2Li(DME)]$$

W.J. Evans et al. [44] published the synthesis and structure of

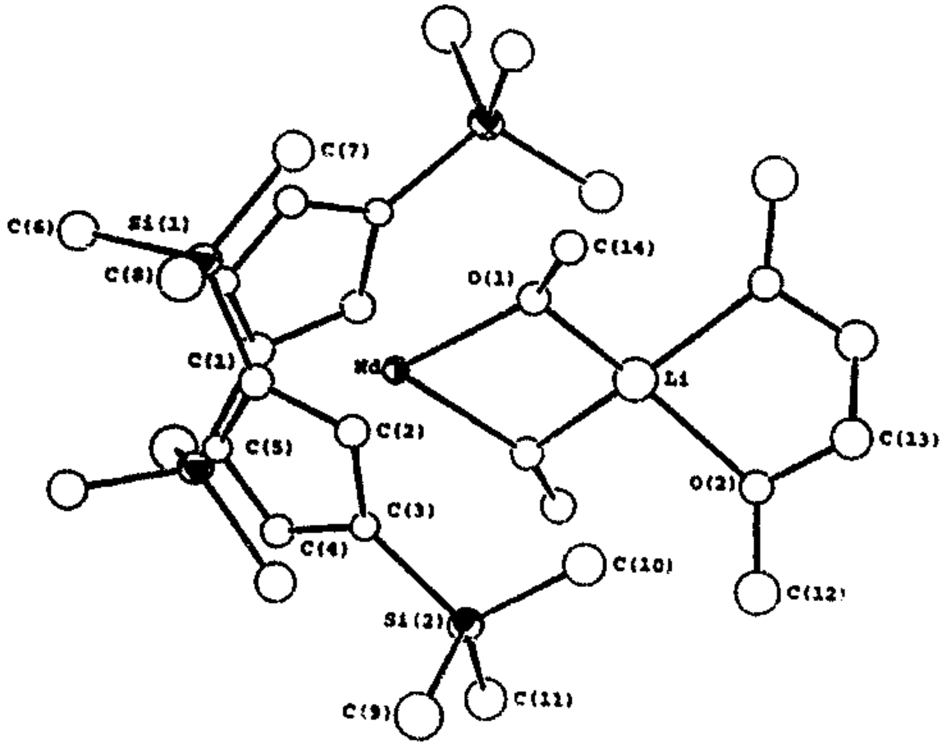

Fig. 21. Molecular structure of [Nd{η-C$_5$H$_3$(SiMe$_3$)$_2$-1,3}$_2$(μ-OMe)$_2$Li(DME)].

{K[(μ-Cp)$_2$Nd(μ-O-C$_6$H$_3$Me$_2$-2,6)$_2$]}$_n$, which was obtained by the reaction of KCp with [Nd(OAr)$_3$(THF)$_2$]$_2$ (Ar = C$_6$H$_3$Me$_2$-2,6) in THF. According to X-ray diffraction studies (Fig. 22) the [Cp$_2$Nd(OAr)$_2$]$^-$ anions in the complex are connected to give a two-dimensional layered structure by K$^+$ cations bridged by arene and cyclopentadienyl rings. Each potassium atom connects four different [Cp$_2$Nd(OAr)$_2$]$^-$ anions and is surrounded by two bridging Cp-groups and two

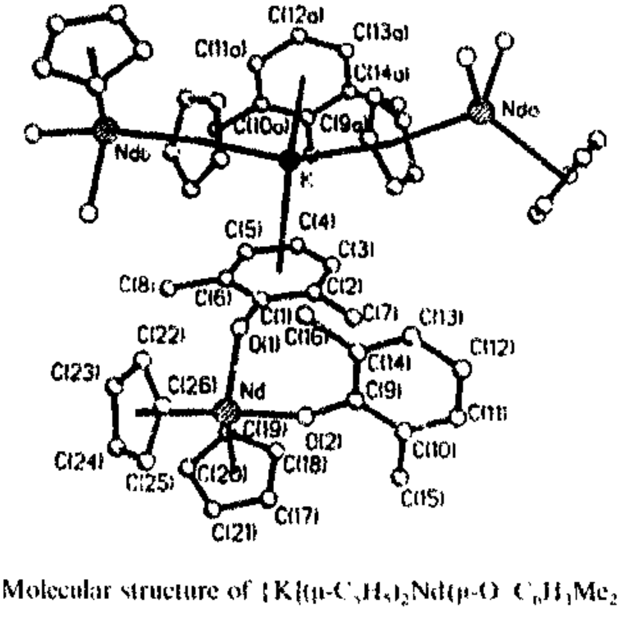

Fig. 22. Molecular structure of {K[(μ-C$_5$H$_5$)$_2$Nd(μ-O-C$_6$H$_3$Me$_2$-2,6)$_2$]}$_n$.

bridging arenes. The K–C(Cp) and the K–C(arene) distances range from 3.01(2) to 3.37(2) Å and from 3.17(2) to 3.54(2) Å, respectively. The neodymium atom in the $[Cp_2Nd(OAr)_2]^-$ anions has a distorted tetrahedral arrangement. The Nd–CCp distances are in the range of 2.75(5)–2.82(2) Å (2.79(6) Å average) and the Nd–O(OAr) bond lengths are 2.206(12) and 2.194(11) Å.

$$(1/2)[Nd(OAr)_3(THF)_2]_2 + 2KCp$$
$$\rightarrow (1/n)\{K[(\mu-Cp)_2Nd(\mu-OAr)_2]\}_n + KOAr\ (Ar = C_6H_3Me_2-2,6)$$

Y.H. Lin et al. [45] reported syntheses and crystal structures of $Cp^*_2Nd(\mu\text{-}Cl)_2Na(DME)_2$ and $Cp^*_2Nd(\mu\text{-}OMe)_2Na(DME)_2$. The first complex was obtained by reaction of $NdCl_3$ with NaCp*. Methoxylation of $Cp^*_2(Nd(\mu\text{-}Cl)_2Na(DME)_2$ led to the methoxide derivative $Cp^*_2Nd(\mu\text{-}OMe)_2Na(DME)_2$. Both of the complexes were structurally characterized.

$$(Cp^*_2LnH)_2 + MeCOOEt \longrightarrow 2\ Cp^*_2LnOEt$$

$$(Cp^*_2LnH)_2 + PhCOOEt \longrightarrow 2\ Cp^*_2LnOEt + Cp^*_2LnOCH_2Ph$$

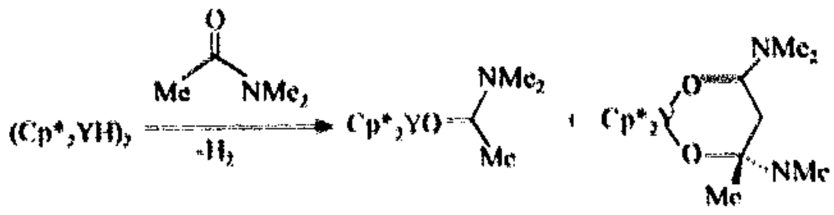

Scheme 7.

Z.-Z. Wu et al. [46] published the synthesis, characterization and study of the thermal stability of dimeric bis(cyclopentadienyl)lanthanide furylmethoxide complexes.

These compounds were obtained by the metathetical reaction of the appropriate Cp_3Ln with furfuryl alcohol in THF solution. The complexes were characterized by elemental analyses, IR, MS and X-ray photoelectron spectra. Investigation of the thermal stability of the compounds has shown that they decompose into Cp_3Ln and $Ln(OR)_3$.

Z.-Z. Wu et al. [47] also prepared the binuclear organolanthanide alkoxides $[Cp_2Yb(\mu\text{-}OCH_2CH_2CH_2CH_2CH_3)]_2$ and $[Cp_2Ln(\mu\text{-}OCH_2CH_2CHMe_2)]_2$ (Ln = Dy, Yb) by the similar reaction of Cp_3Ln with an equimolar amount of the alcohol HOR ($R = CH_2CH_2CH_2CH_2CH_3$ or $CH_2CH_2CHMe_2$). The complexes $[Cp_2Yb(\mu\text{-}OCH_2CH_2CH_2CH_2CH_3)]_2$ and $[Cp_2Yb(\mu\text{-}OCH_2CH_2CHMe_2)]_2$ (Fig. 23) were characterized by X-ray crystallography. In the two dimeric structures the ytterbium atom is coordinated by two Cp ligands and two oxygen atoms of alkoxide ligands to form a distorted tetrahedral geometry. The central Yb_2O_2 metallacycles

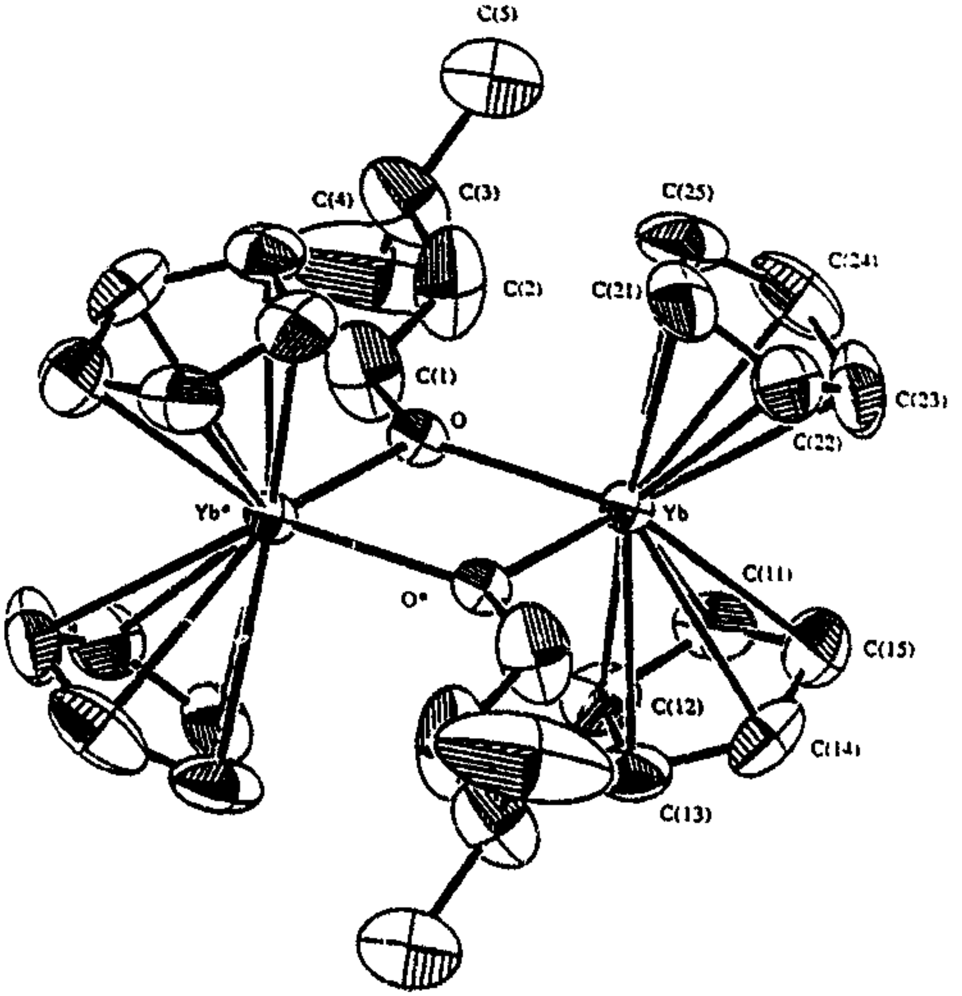

Fig. 23. Molecular structure of $[Cp_2Yb(\mu\text{-}OCH_2CH_2CHMe_2)]_2$.

in the two molecules are completely planar. The Yb–O bond lengths and the average Yb–C(Cp) distance for $[Cp_2Yb(\mu\text{-}OCH_2CH_2CH_2CH_2CH_3)]_2$ are 2.17(1), 2.19(1) and 2.59(2) Å, respectively. The same parameters for $[Cp_2Yb(\mu\text{-}OCH_2CH_2CHMe_2)]_2$ are 2.210(6), 2.184(7) and 2.60(2) Å, respectively.

Z.-Z. Wu et al. [48] also used the related reaction of Cp_3Ln (Ln = Pr, Gd, Dy and Yb) with an equimolar amount of acetoxime for the synthesis of bis(cyclopentadienyl) lanthanide acetoximate derivatives, $[Cp_2Ln(\mu,\eta^2\text{-}ONCMe_2)]_2$. The complex $[Cp_2Gd(\mu,\eta^2\text{-}ONCMe_2)]_2$ was characterized by X-ray diffraction. In the binuclear structure (Fig. 24) each Gd atom is coordinated by two Cp-ligands, two oxygen atoms and one nitrogen atom of $ONCMe_2$ to form a distorted trigonal bipyramidal arrangement (oxygen and nitrogen atoms in the axial positions). The gadolinium has the formal coordination number nine. The Gd–O bond lengths are in the range from 2.25(1) to 2.38(1) Å. The average Gd–C(Cp) and Gd–N distances are 2.68(2) and 2.42(1) Å, respectively.

$$2Cp_3Ln + 2HONCMe_2 \xrightarrow{THF} [Cp_2Ln(\mu,\eta^2-ONCMe_2)]_2 + 2C_5H_6$$

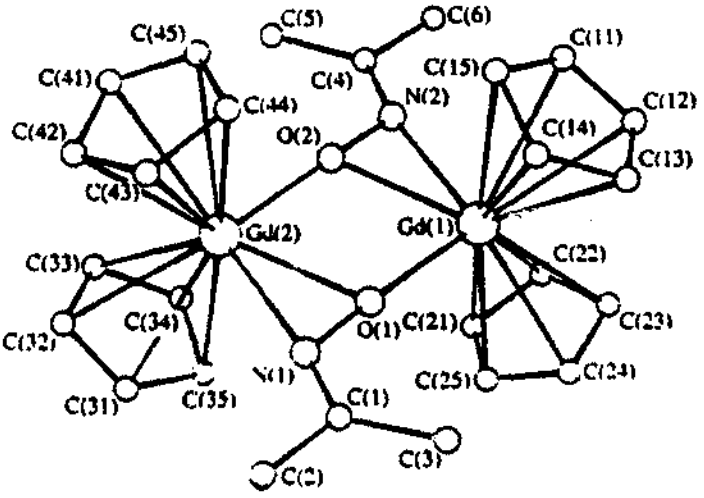

Fig. 24. Molecular structure of $[Cp_2Gd(\mu,\eta^2\text{-}ONCMe_2)]_2$.

G.B. Deacon et al. [49] reported the synthesis and structure of ytterbiocene acetato complexes. The complex $(\eta^5\text{-}C_5H_4PPh_2)_2Yb(\mu\text{-}O_2CMe)$ was obtained by the oxidation of $Yb(C_5H_4PPh_2)_2$ with $Hg(O_2CMe)_2$ in THF. The structures of $(\eta^5\text{-}C_5H_4PPh_2)_2Yb(\mu\text{-}O_2CMe)$ and analogously obtained $Cp_2Yb(\mu\text{-}O_2CMe)$ (Fig. 25) were determined by X-ray diffraction. Both complexes have a dimeric structure with two acetate bridges. However, the crystal structure of $(\eta^5\text{-}C_5H_4PPh_2)_2Yb(\mu\text{-}O_2CMe)$ contains one dimer, while $(\eta^5\text{-}CpP)_2Yb(\mu\text{-}O_2CMe)$ has two similar but independent dimers A and B. The ytterbium atom in both complexes is formally nine-coordinated by two η^5-cyclopentadienyl ligands, two oxygen atoms from the chelating and bridging acetato ligand, and one oxygen atom from the other. Thus, the O_2CMe-ligand is involved in a bridging tridentate coordination. The Yb–O distances the $(\eta^5\text{-}C_5H_4PPh_2)_2Yb(\mu\text{-}O_2CMe)$ range from 2.282(4) to 2.454(4) Å and the Yb–Cp(cent.) distances are 2.332 and 2.323 Å. The Yb–O distances for $Cp_2Yb(\mu\text{-}O_2CMe)$ range from 2.25(1) to 2.42(1) and the Yb–Cp(cent.)

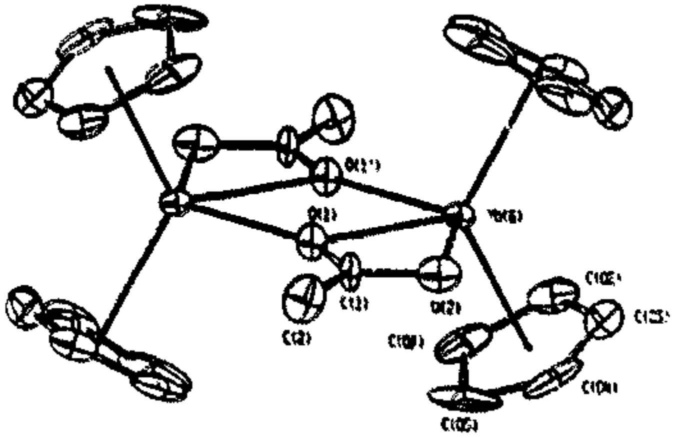

Fig. 25. Molecular structure of $[Cp_2Yb(\mu\text{-}O_2CMe)]_2$.

distances are 2.324 and 2.287 Å for the different A and B molecules.

$$2Yb(C_5H_4PPh_2)_2+Hg(O_2CMe)_2 \rightarrow 2(C_5H_4PPh_2)_2Yb(O_2CMe)+Hg\downarrow$$

F.T. Edelmann et al. [50] prepared bis(η^5-cyclopentadienyl)lanthanide(III) complexes with bulky alkoxide and thiolate ligands. The alkoxide complexes $Cp_2Yb(THF)(OR_F)$ [Ln = Nd, Sm, Yb; R_F = 2,4,6-tris(trifluoromethyl)phenyl, $-C_6H_2(CF_3)_3$-2,4,6] were obtained by reaction of the appropriate Cp_3Ln with 2,4,6-tris(trifluoromethyl)phenol (R_FOH) (Scheme 8). The thiolate complex $Cp_2Yb(THF)(SR_F)$ was prepared analogously from Cp_3Yb and R_FSH. According to X-ray diffraction studies $Cp_2Yb(THF)(SR_F)$ (Fig. 26) is a monomer, in which the ytterbium atom is coordinated by two η^5-Cp-rings, one sulfur of the $SC_6H_2(CF_3)_3$-2,4,6-ligand and one oxygen of a solvating THF molecule. Thus the ytterbium has a pseudo-tetrahedral coordination arrangement and the formal coordination number 8. The average Yb C distances and Yb S bond lengths are 2.306 and 2.639(3) Å, respectively.

S.A. Vinogradov et al. [51] synthesized new organolanthanide complexes contain-

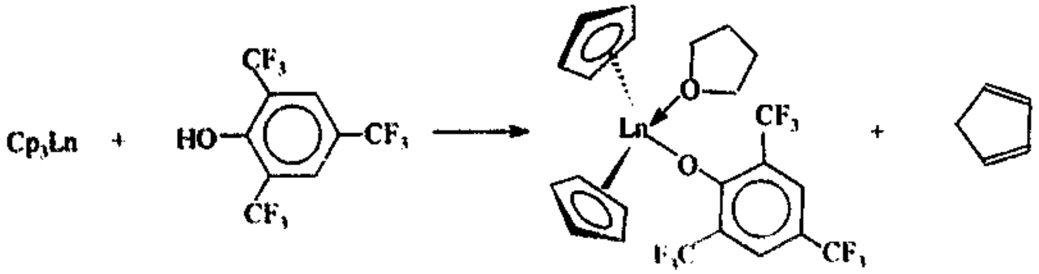

Ln = Nd, Sm, Yb

Scheme 8.

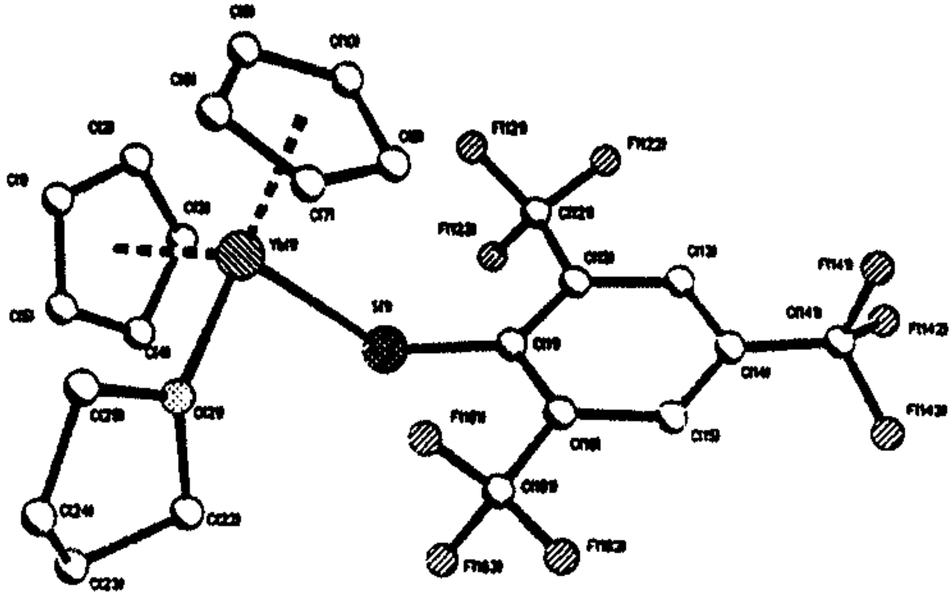

Fig. 26. Molecular structure of $Cp_2Yb(THF)(SR_F)$.

ing a σ-bonded 1,3-dithiane, $[Ln(C_5H_4Bu^t)_2(C_4H_7S_2\text{-}1,3)]\cdot LiCl\cdot 2THF$ (Ln = Lu or Y; THF = tetrahydrofuran). The compounds were obtained according to Scheme 9 and have been characterized by single-crystal X-ray diffraction. In $[Lu(C_5H_4Bu^t)_2(C_4H_7S_2\text{-}1,3)]\cdot LiCl\cdot 2THF$ (Fig. 27) the Lu atom is coordinated by two η^5-$C_5H_4Bu^t$-rings, a bridging chlorine ligand and the σ-bonded carbon atom of 1,3-dithiane to form a pseudo-tetrahedral coordination arrangement. The central fragment of the structure is a pentagon, formed by the Lu atom, 1,3-dithiane and one LiCl unit. The Lu C(η^5) distances are in the range from 2.56(2) to 2.70(2) Å, the Lu-Cl and Lu-C(1,3-dithiane) distances are 2.570(5) and 2.45(2) Å, respectively. The structure of $[Y(C_5H_4Bu^t)_2(C_4H_7S_2\text{-}1,3)]\cdot LiCl\cdot 2THF$ is similar to that of the lutetium analogue. The average Y–C(η^5) distances are 2.65(3) and 2.68(3) Å and the Y–Cl and Y–C(1,3-dithiane) distances are 2.638(6) and 2.47(3) Å, respectively.

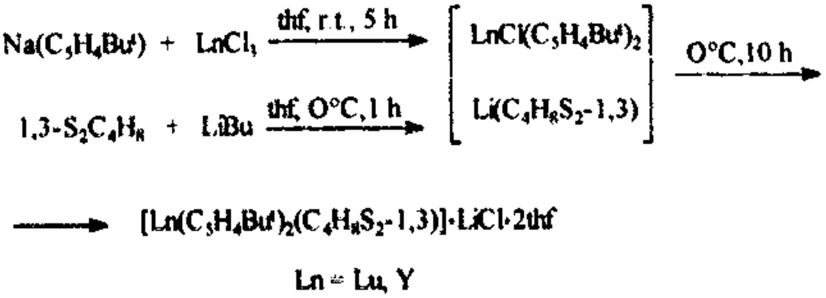

$$\left.\begin{array}{l} 2\,Na(C_5H_4Bu^t) + LnCl_3 \xrightarrow{\text{thf, r.t., 5 h}} \\ 1,3\text{-}S_2C_4H_8 + LiBu \xrightarrow{\text{thf, 0°C, 1 h}} \end{array}\right. \left[\begin{array}{l} LnCl(C_5H_4Bu^t)_2 \\ Li(C_4H_8S_2\text{-}1,3) \end{array}\right] \xrightarrow{\text{0°C, 10 h}}$$

$$\longrightarrow [Ln(C_5H_4Bu^t)_2(C_4H_8S_2\text{-}1,3)]\cdot LiCl\cdot 2thf$$

$$Ln = Lu, Y$$

Scheme 9.

W.A. King and T.J. Marks [52] reported measurements of metal silicon bond disruption enthalpies for a series of metallocene complexes including $Cp^{\ddagger}_2SmSiH(SiMe_3)_2$. The complexes were studied by iodinolytic titration calorimetry. The treatment of $Cp^{\ddagger}_2SmSiH(SiMe_3)_2$ with a stoichiometric amount of MeI gave $MeSiH(SiMe_3)_2$ and $(Cp^{\ddagger}_2SmI)_x$.

$$Cp^*_2SmSiH(SiMe_3)_2 + MeI \rightarrow 1/x(Cp^*_2SmI)_x + MeSiH(SiMe_3)_2$$

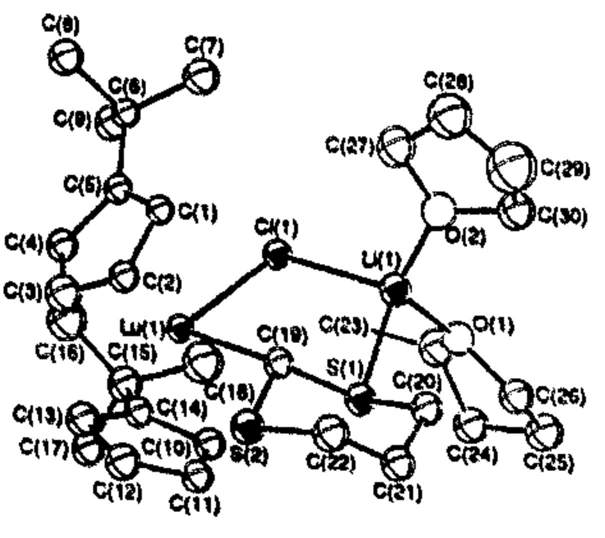

Fig. 27. Molecular structure of $[Lu(C_5H_4Bu^t)_2(C_4H_7S_2\text{-}1,3)]\cdot LiCl\cdot 2THF$.

The resulting D(Sm–Si) value of 43(5) kcal mol^{-1} was calculated from the equation:

$$\begin{aligned}&\mathrm{D[Cp_2^*Sm-SiH(SiMe_3)_2]} = D\mathrm{[Cp_2^*Sm-I]}\\&\quad + D\mathrm{[(SiMe_3)_2HSi-Me]} + \Delta H_{\mathrm{rxn}} - D\mathrm{[Me-I]}\\&\quad (\text{where } \Delta H_{\mathrm{rxn}} = -52(1)\ \mathrm{kcal\ mol^{-1}})\end{aligned}$$

T.V. Timofeeva et al. [53] calculated and reproduced molecular conformations of the bent sandwich metallocenes MCp_2 including $LnCp_2^*$ (Ln = Sm, Eu, Yb). The molecular mechanics calculations were carried out with the MM3 program, using standard optimization procedures. The calculations revealed that the bending is mainly a result of nonbonding interactions, especially attraction between the Cp-ligands. Crystal packing forces are not a major factor determining the degree of bending. When the interplanar distances between the planes of Cp rings are short (i.e. for metals with a small ionic radius), the ligands have parallel orientation. When the metal atom in MCp_2 has a large ionic radius, the interplanar distances are longer and the ligand planes do not stay parallel. The influence of bulky substituents on the bending angle was also elucidated.

2.2.3. *Tris(cyclopentadienyl) complexes*

W. de Oliveira et al. [54] prepared tris(cyclopentadienyl) lanthanides Cp_3Ln (Ln = Nd, Yb) by the reaction of anhydrous lanthanide(III) methanesulphonates $Ln(OSO_2CF_3)_3$ with NaCp in THF. The obtained compounds were characterized by elemental analysis, inductively coupled argon plasma atomic and IR spectrometry.

T.P. Hanusa et al. [55] reported a cyclopentadienyl ring metathesis of Cp_3Ln (Ln = La, Nd, Sm) with bis(pentamethylcyclopentadienyl)calcium Cp_2^*Ca in toluene to give mixed ring organolanthanide complexes Cp_2^*LnCp. According to X-ray diffraction crystallography the compound Cp_2^*NdCp consists of monomeric units, in which the Nd atom is coordinated by two η^5-C_5Me_5 and one η^5-C_5H_5 rings. The average Nd–C distances for both the C_5Me_5 and C_5H_5 rings are 2.76–2.79 Å.

$$\mathrm{Cp_2^*Ca + Cp_3Ln \xrightarrow{toluene} Cp_2^*LnCp + Cp_2Ca}$$

D.C. Chadwick and R.A. Andersen [56] published the synthesis and crystal structure of $[(Me_3C)_2C_5H_3]_3Ce$. This complex as well as $[(Me_3Si)_2C_5H_3]_3Ce$ were obtained by reaction of $Ce(OSO_2CF_3)_3$ with the corresponding magnesium cyclopentadienides $Mg(R_2C_5H_3)_2$ (R = $SiMe_3$, Bu^t) in THF. According to X-ray diffraction $[(Me_3C)_2C_5H_3]_3Ce$ has a monomeric structure with three ordered $(Me_3C)_2C_5H_3$ rings and C_{3h} symmetry. The average Ce–ring(centroid) distance and Cent.–Ce–Cent. angle are 2.59 Å and 120°, respectively.

$$\mathrm{2Ce(OSO_2CF_3)_3 + 3Mg(R_2C_5H_3)_2 \rightarrow 2Ce(R_2C_5H_3)_3 + 3Mg(OSO_2CF_3)_2}$$

$$\mathrm{R = SiMe_3,\ Bu^t}$$

H. Schumann et al. [24] prepared the homoleptic tris(tetramethylcyclopentadienyl) complexes $Ln(C_5Me_4H)_3$ (Ln = La, Nd, Sm, Tb) by reaction of $LnCl_3$ with

$Na(C_5Me_4H)$ in THF. The complexes $Ln(C_5Me_4H)_3$ ($Ln = La$, Sm) were characterized by X-ray crystallography. The compounds have typical monomeric structures. The $Ln–C_5Me_4H$(cent.) distances are 261.6(6) pm for lanthanum and 248.9(8) pm for the samarium complex.

W.-K. Wong et al. [57] synthesized neodymium ylide complexes of the type $(C_5H_4R)_3NdCH_2P(Me)Ph_2$ ($R = H$, Bu^t) by refluxing of $(C_5H_4R)_3NdCl \cdot LiCl$ with one equivalent of $Li[(CH_2)(CH_2)PPh_2]$ in THF. The compounds were characterized by single-crystal X-ray diffraction. In $(C_5H_5)_3NdCH_2P(Me)Ph_2$ (Fig. 28) the Nd adopts a distorted tetrahedral geometry formed by three η^5-Cp-rings and one carbon atom of the $CH_2P(Me)Ph_2$ ligand. The mean Nd–C(Cp) distances are 2.76, 2.78 and 2.79 Å, and the $Nd–C(CH_2P(Me)Ph_2)$ distance is 2.64(2) Å. The complex $(C_5H_4Bu^t)_3NdCH_2P(Me)Ph_2$ has a similar structure in which the average Nd–C(Cp) distances are 2.82, 2.86 and 2.87 Å, and the $Nd–C(CH_2P(Me)Ph_2)$ distance is 2.66(2) Å. Solution dynamics of the compounds were also studied. The authors suggest that there exists an equilibrium in solution:

$$(C_5H_4R)_3Nd \leftarrow CH_2P(Me)Ph_2 + THF \leftrightarrow (C_5H_4R)_3Nd(THF) + CH_2{=}P(Me)Ph_2$$

$$(R = H, Bu^t)$$

M. Shimizu et al. [58] used tris(isopropylcyclopentadienyl)lanthanum $La(i\text{-}C_3H_7C_5H_4)_3$ as a precursor for the preparation of ferroelectric lanthanum-modified lead zirconate titanate (PLZT) thin films by metalorganic chemical vapor deposition (MOCVD). Liquid $La(i\text{-}C_3H_7C_5H_4)_3$ is a promising precursor for MOCVD because it is very easy to control its vapor pressure in the process.

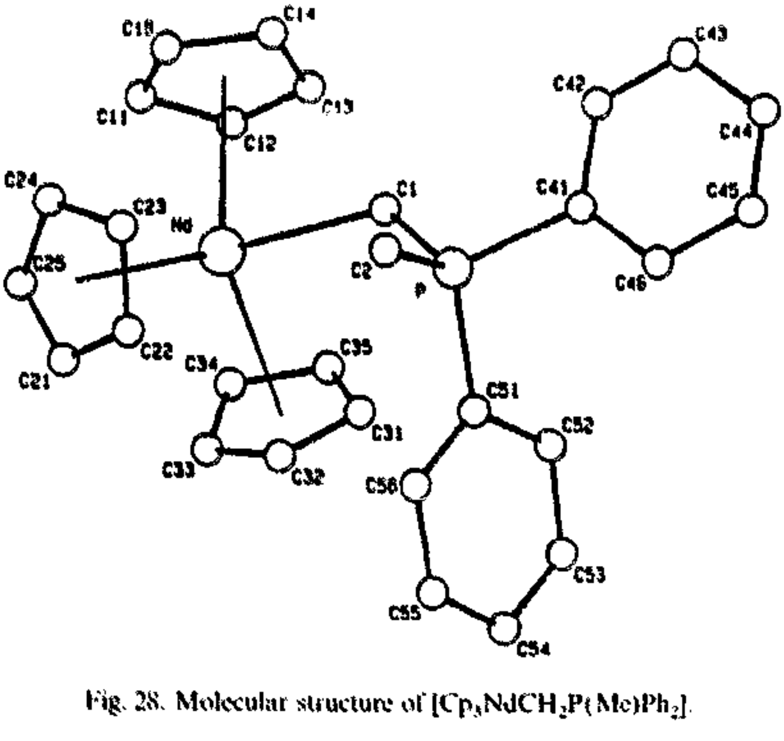

Fig. 28. Molecular structure of $[Cp_3NdCH_2P(Me)Ph_2]$.

2.2.4. Complexes with cyclopentadienyl and cyclooctatetraenyl ligands

W.J. Evans et al. [59] reported the synthesis and structure of a cyclooctatetraenyl sandwich complex of europium(II), $[Cp^*(THF)_2Eu]_2(\mu\text{-}C_8H_8)$. The compound was synthesized by the reaction of $K_2C_8H_8$ with $EuCl_3$ followed by interaction with KCp* in THF. According to X-ray diffraction the complex has an inverse sandwich structure (Fig. 29), in which the COT ring is located symmetrically between two Eu(II) atoms. Each europium is coordinated by one η^8-C_8H_8 ring, one η^5-C_5Me_5 group and two solvating THF molecules and has a formal coordination number of 10. The Eu–C(C_5Me_5) average distances are 2.86(2) and 2.878(7) Å. The average distances Eu–C(C_8H_8) for the two europium centers are 2.92(3) and 2.91(6) Å. The planar C_8H_8 ring is nearly perpendicular to the Eu–Eu vector and the (C_8H_8-cent.)–Eu–(C_5Me_5-cent.) angles are 139.1 and 137.9°.

$$EuCl_3 \xrightarrow[2.\ KC_5Me_5]{1.\ K_2C_8H_8} [(C_5Me_5)(THF)_2Eu]_2[\mu-(\eta^8:\eta^8-C_8H_8)]$$

The ylidic olefin complex $(C_8H_8)YCp^*CH_2{=}C\overline{N(Me)C(Me){=}C(Me)N}(Me)$ was prepared by H. Schumann et al. [60] using the reaction of $(C_8H_8)YCp^*$ with 1,3,4,5-tetramethyl-2-methylenimidazoline (Scheme 10). The compound was characterized by X-ray diffraction. In the structure (Fig. 30) the yttrium atom is coordinated by one η^8-C_8H_8 ring and one η^5-C_5Me_5 ligand and the exocyclic carbon atom of the 1,3,4,5-tetramethyl-2-methylenimidazoline ligand ($C_8H_{14}N_2$). The Y–(C_8H_8-cent.), Y–(C_5Me_5-cent.) and Y–C($C_8H_{14}N_2$) distances are 1.895(15), 2.410(13) and 2.624(11) Å, respectively.

J. Jin et al. [61] published syntheses and crystal structures of $(C_8H_8)Nd(C_5H_9C_5H_4)(THF)_2$ and $[(C_8H_8)Gd(C_5H_9C_5H_4)(THF)][(C_8H_8)Gd(C_5H_9C_5H_4)(THF)_2]$. The complexes were obtained by the reaction between the

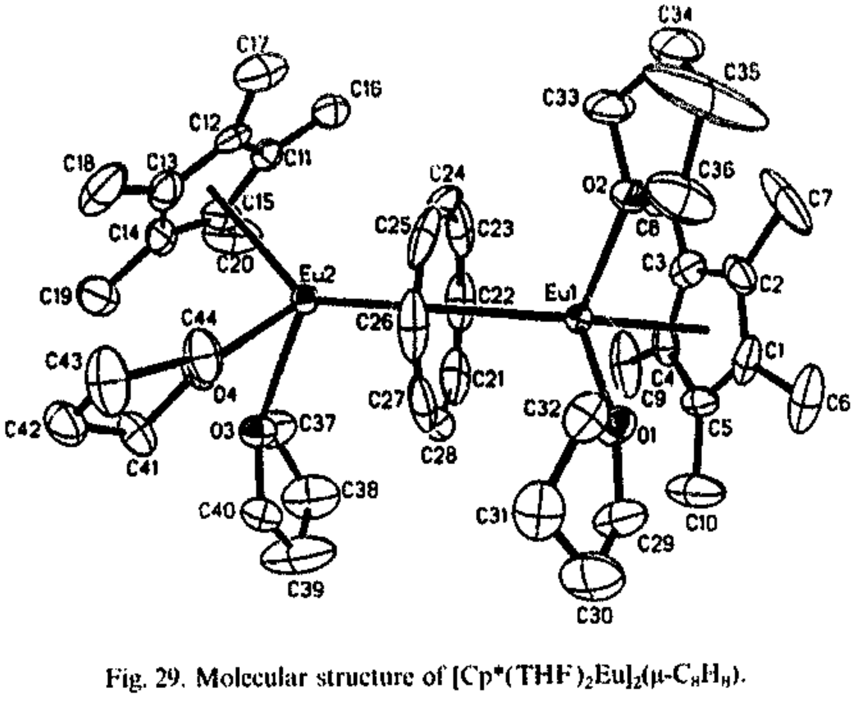

Fig. 29. Molecular structure of $[Cp^*(THF)_2Eu]_2(\mu\text{-}C_8H_8)$.

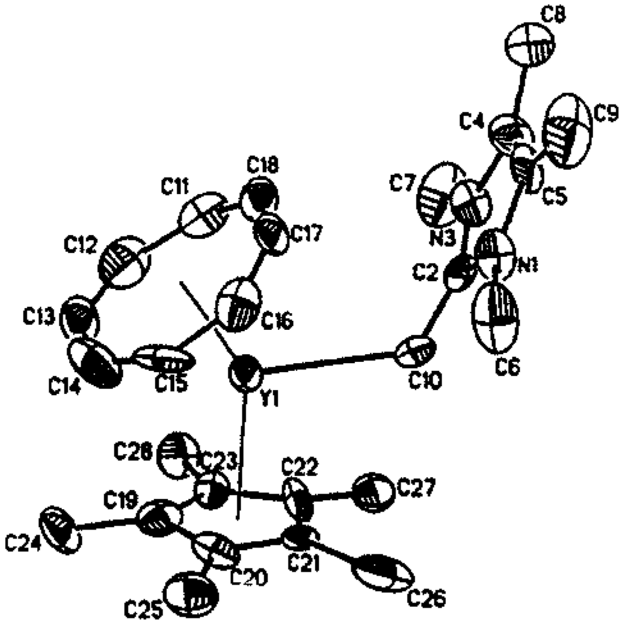

Fig. 30. Molecular structure of (C$_8$H$_8$)YCp*[CH$_2$=CN(Me)C(Me)=C(Me)N(Me)].

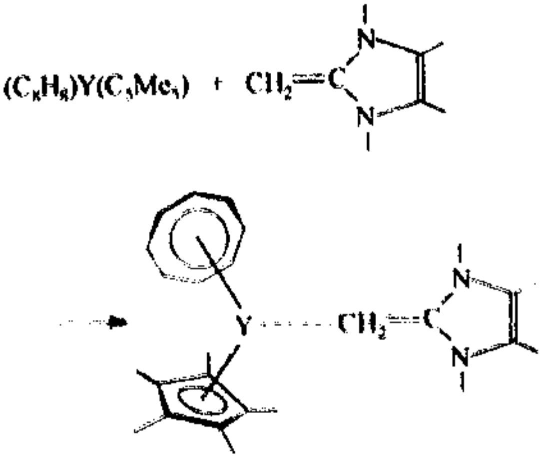

Scheme 10.

appropriate anhydrous LnCl$_3$ (Ln = Nd, Gd) and C$_5$H$_9$C$_5$H$_4$Na (or K$_2$C$_8$H$_8$) in THF (C$_5$H$_9$C$_5$H$_4$ = cyclopentylcyclopentadienyl) followed by reaction with K$_2$C$_8$H$_8$ (or C$_5$H$_9$C$_5$H$_4$Na) in THF (Scheme 11). In the structure of (C$_8$H$_8$)Nd(C$_5$H$_9$C$_5$H$_4$)(THF)$_2$ (Fig. 31) the Nd atom is coordinated by one η^8-C$_8$H$_8$ ring, one η^5-C$_5$H$_9$C$_5$H$_4$ ligand and two oxygen atoms of solvating THF molecules. The Nd atom has a formal coordination number of 10 and a twisted pseudo-tetrahedral coordination arrangement. The Nd–(C$_8$H$_8$-cent.) and Nd–(C$_5$H$_9$C$_5$H$_4$-cent.) distances are 2.011 and 2.540 Å, respectively, while the two Nd–O(THF) distances are 2.654 and 2.619 Å. The crystal structure of [(C$_8$H$_8$)Gd(C$_5$H$_9$C$_5$H$_4$)(THF)][(C$_8$H$_8$)Gd(C$_5$H$_9$C$_5$H$_4$)(THF)$_2$] consists of two independent complexes, (C$_8$H$_8$)Gd(C$_5$H$_9$C$_5$H$_4$)(THF) and (C$_8$H$_8$)Gd(C$_5$H$_9$C$_5$H$_4$)

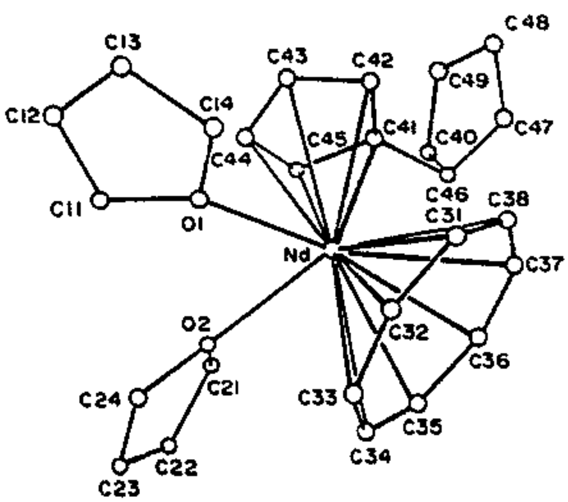

Fig. 31. Molecular structure of $(C_8H_8)Nd(C_5H_9C_5H_4)(THF)_2$.

$(THF)_2$. The latter complex has a structure similar to the above-mentioned neodymium analogue. The correspondent Gd–(C_8H_8-cent.) and Gd–($C_5H_9C_5H_4$-cent.) distances are 1.958 and 2.464 Å, the two Gd–O(THF) distances are 2.629 and 2.617 Å. In the molecule of $(C_8H_8)Gd(C_5H_9C_5H_4)(THF)$ the Gd atom is coordinated by one η^8-C_8H_8- and one η^5-$C_5H_9C_5H_4$-ligand and an oxygen of only one THF molecule. The Gd atom has a pseudo-triangular arrangement and a formal coordination number of 9. Here the Gd–(C_8H_8-cent.), Gd–($C_5H_9C_5H_4$-cent.) and Gd–O(THF) distances are 1.875, 2.419 and 2.469 Å, respectively.

$$LnCl_3 + C_5H_9C_5H_4Na \xrightarrow{THF} (C_5H_9C_5H_4)LnCl_2(THF)_n$$

$$\xrightarrow{1\ K_2C_8H_8} (C_8H_8)Ln(C_5H_9C_5H_4)(THF)$$

$$Ln = Nd, Gd$$

Scheme 11.

2.3. Indenyl complexes

W.J. Evans et al. [62] investigated the reactivity of samarium(II) in a bis(indenyl) coordination environment and compared it with that of $Cp_2^*Sm(THF)_2$. Reaction of the organosamarium(II) indenyl complex $(C_9H_7)_2Sm(THF)_x$ with excess N_2O yielded the complexes $[(C_9H_7)_2Sm(THF)]_2(\mu$-$O)$ and $(C_9H_7)_3Sm(THF)$. Treatment of two equivalents of $(C_9H_7)_2Sm(THF)_x$ with 1,2-diiodoethane gave $(C_9H_7)_3Sm(THF)$ and $(C_9H_7)SmI_2(THF)_2$. These two compounds could be synthesized also by reaction of $SmCl_3$ with three equivalents of KC_9H_7 in THF for $(C_9H_7)_3Sm(THF)$ and by reaction of SmI_3 with one equivalent of KC_9H_7 in THF for $(C_9H_7)SmI_2(THF)_2$, respectively. Two equivalents of $(C_9H_7)_2Sm(THF)_x$ also react with one equivalent of 1,3,5,7-cyclooctatetraene (C_8H_8) to form

$(C_9H_7)_3Sm(THF)$ and $(C_9H_7)Sm(C_8H_8)(THF)_x$. Reaction of two equivalents of $(C_9H_7)_2Sm(THF)_x$ with one equivalent of azobenzene led to $(C_9H_7)_3Sm(THF)$ and $[(C_9H_7)Sm(N_2Ph_2)(THF)]_x$. The complexes $[(C_9H_7)_2Sm(THF)]_2(\mu\text{-}O)$, $(C_9H_7)_3Sm(THF)$, $(C_9H_7)SmI_2(THF)_3$ and the 2,2′-bipyridine adduct $(C_9H_7)Sm(C_8H_8)(C_{10}H_8N_2)$ were characterized by X-ray diffraction. In the structure of $[(C_9H_7)_2Sm(THF)]_2(\mu\text{-}O)$ (Fig. 32) two $(C_9H_7)_2Sm(THF)$ fragments are bound by a bridging oxygen ligand. Each samarium is formally eight-coordinated. The average Sm–C(C_9H_7) and Sm–(μ–O) distances are 2.79(6) and 2.078(1) Å, respectively. The structure of $(C_9H_7)_3Sm(THF)$ is similar to that of other tris(cyclopenta-

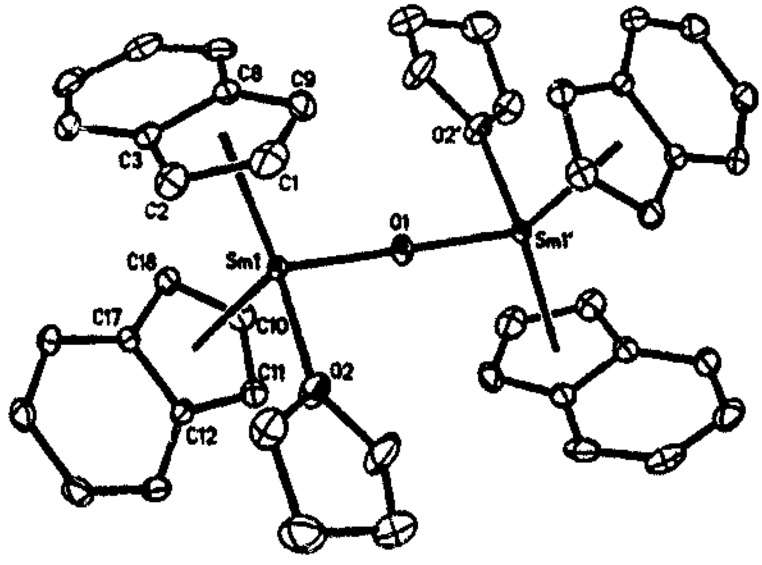

Fig. 32. Molecular structure of $[(C_9H_7)_2Sm(THF)]_2(\mu\text{-}O)$.

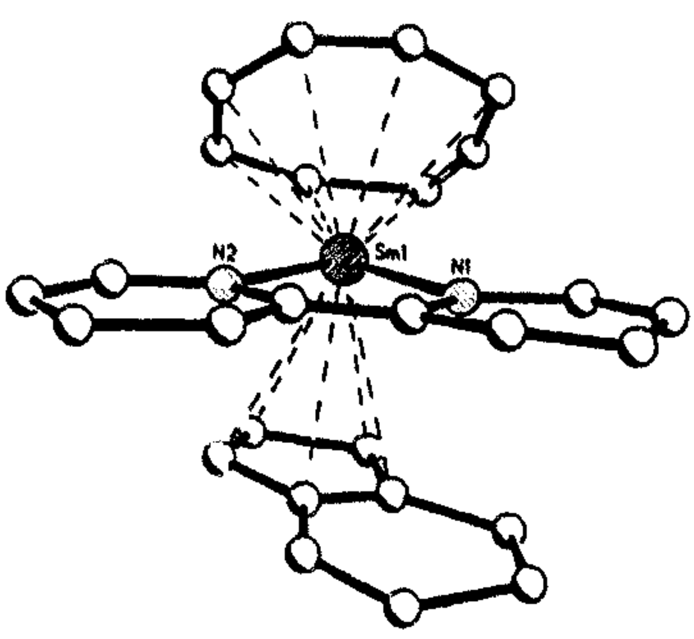

Fig. 33. Structure of $(C_9H_7)Sm(C_8H_8)(C_{10}H_8N_2)$.

dienyl)lanthanide complexes solvated with THF. The average Sm–C(C_9H_7) distance is 2.80(12) Å. The complex $(C_9H_7)SmI_2(THF)_3$ crystallizes with two molecules in the unit cell. In the structure the Sm atom has a distorted octahedral arrangement with the C_9H_7-rings and iodine atoms in a *mer-trans* orientation. The average Sm–C(C_9H_7) distance is 2.75(2) Å and the two Sm–I bond lengths are 3.130(6) and 3.113(13) Å. The ball and stick structure of $(C_9H_7)Sm(C_8H_8)(C_{10}H_8N_2)$ is shown in Fig. 33.

$$(C_9H_7)_2Sm(THF)_x + N_2O \xrightarrow{\text{THF, 15 min}} [(C_9H_7)_2Sm(THF)]_2(\mu-O) + (C_9H_7)_3Sm(THF)$$

$$2(C_9H_7)_2Sm(THF)_x + ICH_2CH_2I \xrightarrow{\text{THF, 10 min}} (C_9H_7)_3Sm(THF) + (C_9H_7)SmI_2(THF)_2$$

$$2(C_9H_7)_2Sm(THF)_x + C_8H_8 \xrightarrow{\text{THF, 15 min}} (C_9H_7)Sm(C_8H_8)(THF)_x + (C_9H_7)_3Sm(THF)$$

$$2(C_9H_7)_2Sm(THF)_x + PhN{=}NPh \xrightarrow{\text{THF, 1 h}} (C_9H_7)_3Sm(THF) + [(C_9H_7)Sm(N_2Ph_2)(THF)]_x$$

Z. Ye et al. [63] reported the synthesis and molecular structure of $[Na(THF)_6][(\eta^5\text{-}C_9H_7)_3Pr(\mu\text{-}Cl)Pr(\eta^5\text{-}C_9H_7)_3]$. The complex was obtained by the reaction of $PrCl_3$ with sodium indenide (molar ratio 1:0.8) in THF. The structure consists of the $[(\eta^5\text{-}C_9H_7)_3Pr(\mu\text{-}Cl)Pr(\eta^5\text{-}C_9H_7)_3]$ anion and a $[Na(THF)_6]^+$ cation. In the anion two praseodymium metal centers are bound by the bridging chlorine atom. Each Pr atom is coordinated by three indenyl and one chloride ligand to form a distorted pseudo-tetrahedral geometry. The Pr–C(C_9H_7) distances range from 2.730(9) to 2.937(7) Å while the Pr–Cl bond length is 2.8272(6) Å.

The same authors [64] prepared the complex tris(indenyl)(tetrahydrofuran)-praseodymium, $(C_9H_7)_3Pr(THF)$, by reaction of $PrCl_3$ with sodium indenide in a 1:0.8 molar ratio in THF solution. The complex crystallizes with two disconnected structural isomers in one asymmetrical unit $[(C_9H_7)_3Pr(1)OC_4H_8]$ $[(C_9H_7)_3Pr(2)OC_4H_8]$ (Fig. 34). Each Pr atom is coordinated by three $\eta^5\text{-}C_9H_7$ ligands and one THF molecule and has a distorted pseudo-tetrahedral arrangement. The average Pr(1)–C(C_9H_7) and Pr(2)–C(C_9H_7) distances are equal with 2.836 Å. The Pr(1)–O(THF) and Pr(2)–O(THF) distances are 2.553(4) and 2.542(4) Å.

2.4. *Complexes with heteroatom five-membered ring ligands*

H. Schumann et al. [65] reported the synthesis and X-ray structure of the monopyrrolyl complex $(pyr^*)YbCl_2(THF)_2$ ($pyr^* = NC_4H_2{}^tBu_2$-2,5). The compound was obtained by the reaction of $YbCl_3(THF)_3$ with Na[pyr*] in THF. In the structure (Fig. 35) the Yb atom is coordinated by the azacyclopentadienyl ligand ($NC_4H_2{}^tBu_2$-2,5) in π-fashion, two chlorine ligands and two THF molecules. The Yb has a distorted trigonal bipyramidal coordination environment with both chloride

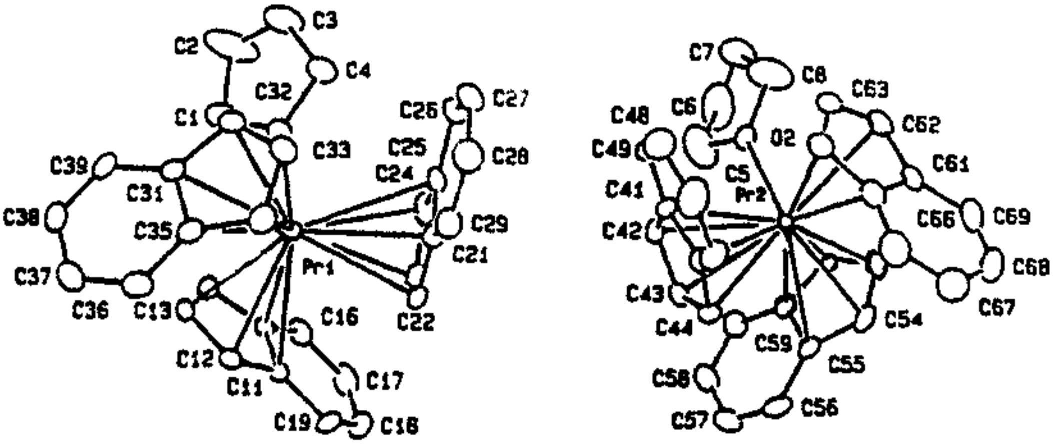

Fig. 34. Structure of [$(C_9H_7)_3Pr(1)OC_4H_8$][$(C_9H_7)_3Pr(2)OC_4H_8$].

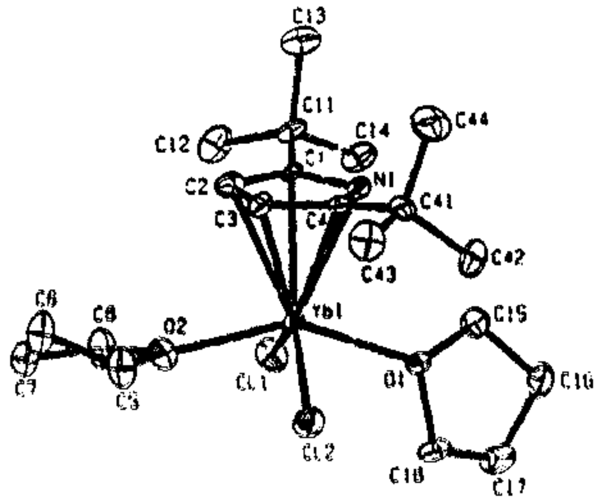

Fig. 35. Molecular structure of [(pyr*)$YbCl_2(THF)_2$] (pyr* = $NC_4H_2^tBu_2$-2,5).

and pyrrolyl ligands in the equatorial and the oxygen atoms of the two THF groups in axial positions. The Yb–pyr*(cent.) distance is 232.6 pm, the two Yb–Cl bond lengths are 251.2(1) and 252.1(2) pm, and the Yb–O(THF) distances are 229.5(3) and 232.0(3) pm.

$$YbCl_3(THF)_3 + Na[pyr^*] \rightarrow (pyr^*)YbCl_2(THF)_2 + NaCl$$

$$(pyr^* = NC_4H_2^tBu_2-2,5)$$

F. Mathey et al. [66] prepared and characterized by X-ray diffraction several phospholylsamarium(III) complexes. Reaction of KTmp (Tmp = 2,3,4,5-tetramethylphospholyl) with $SmCl_3$ in a 3:1 molar ratio in toluene yielded the complex $[(Tmp)_6Sm_2(KCl)_2(C_7H_8)_3]_n$. According to X-ray crystallography the compound has a polymeric structure (Fig. 36), which is made up of two crystallographically different eight-membered rings $[Sm1-P11-K1-Cl1]_2$ and $[Sm2-P45-K2-Cl2]_2$ connected by [Sm1–P6–K2] and [Sm2–P40–K1] links. Each

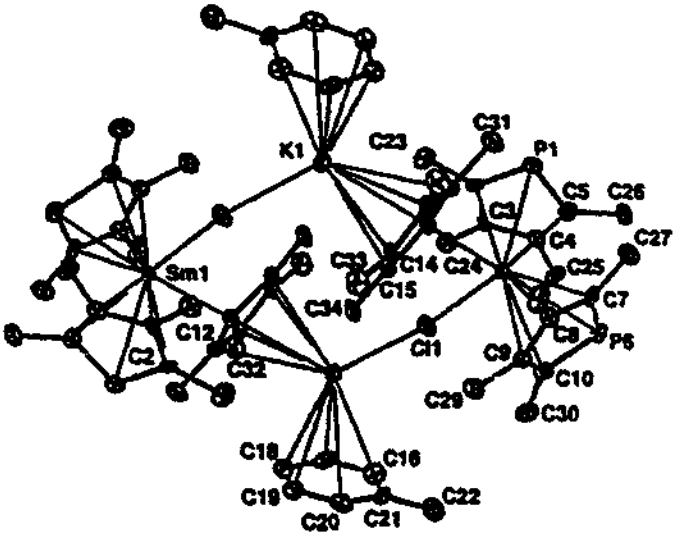

Fig. 36. Structure of $[(Tmp)_6Sm_2(KCl)_2(C_7H_8)_2]_n$.

Sm atom is coordinated by two Tmp ligands in π-fashion, one Tmp ligand through the phosphorus atom and one bridging Cl atom to give a pseudo-tetrahedral arrangement. The Sm–P bond lengths range from 2.92 to 2.95 Å. The K atom also has a pseudo-tetrahedral environment formed by the one π-coordinated Tmp ligand, one π-toluene molecule, one bridging chlorine atom and one phosphorus atom of the Tmp ligand from another unit. The K–C(toluene) bond lengths range from 3.17 to 3.55 Å and the K–Cl distance is 3.00 Å. The complex $[(\eta^5\text{-Dmp})_4\{\mu\text{-}(\eta^5,\eta^1)\text{-Dmp}\}_2Sm_2]$ (Dmp = 3,4-dimethylphospholyl) was synthesized in a similar manner from KDmp and $SmCl_3$ in a 3:1 molar ratio in toluene. According to an X-ray diffraction study the compound has a dimeric structure in which two $(\eta^5\text{-Dmp})_2Sm$ fragments are bridged by two $\mu\text{-}(\eta^5,\eta^1)$-Dmp ligands. Once again each Sm atom has a pseudo-tetrahedral coordination arrangement.

2.5. *Complexes with cyclooctatetraenyl ligands*

H. Schumann and F.T. Edelmann et al. [67] published the synthesis and characterization of monomeric (cyclooctatetraenyl)lanthanide benzamidinate complexes of the type $(C_8H_8)Ln[4\text{-}RC_6H_4C(NSiMe_3)_2](THF)$ (R = H, OMe; Ln = Y, Ce, Pr, Nd, Sm, Tm, Lu; R = CF_3; Ln = Y, Tm, Lu). The compounds were synthesized by reactions of $[(C_8H_8)Ln(\mu\text{-}Cl)(THF)_2]_2$ or $[(C_8H_8)Ln(\mu\text{-}O_3SCF_3)(THF)_2]_2$ with $Na[4\text{-}RC_6H_4C(NSiMe_3)_2]$ (R = H, OMe, CF_3) or $Li[PhC(NSiMe_3)_2]$ in THF (Scheme 12). $[(C_8H_8)Ln(\mu\text{-}Cl)(THF)_2]_2$ (Ln = Ce, Pr, Nd, Sm) was also reacted with $Li[Ph_2P(NSiMe_3)_2]$ in THF to give the correspondent (cyclooctatetraenyl) [diphenyl-bis(trimethylsilylimino)phosphinato] complexes $(C_8H_8)Ln[Ph_2P(NSiMe_3)_2](THF)$. The molecular structures of $(C_8H_8)Tm[PhC(NSiMe_3)_2](THF)$, $(C_8H_8)Lu[4\text{-}MeOC_6H_4C(NSiMe_3)_2](THF)$ and $(C_8H_8)Nd[Ph_2P(NSiMe_3)_2](THF)$ were determined by single-crystal X-ray diffraction. The crystal structures of $(C_8H_8)Tm[PhC(NSiMe_3)_2](THF)$ and $(C_8H_8)Lu[4\text{-}MeOC_6H_4C$

$(NSiMe_3)_2](THF)$ (Fig. 37) are similar with the exception that the thulium compound contains solvent molecules (toluene) in the unit cell. In both complexes the Ln^{+3} ion is coordinated by one η^8-C_8H_8 ring, two nitrogen atoms of the chelating benzamidinato ligand and one THF molecule. In the thulium complex the Tm–C_8H_8(cent.) distance is 179.0 pm and the two Tm–N bond lengths are 234.0(4) and 234.7(3) pm. In the lutetium compound the corresponding Lu–C_8H_8(cent.) and Lu–N bond lengths are 175.6, 230.8(3) and 232.4(3) pm, respectively. In the structure of $(C_8H_8)Nd[Ph_2P(NSiMe_3)_2](THF)$ (Fig. 38) the neodymium is also coordinated by one η^8-C_8H_8 ring, two nitrogen atoms of the chelating diphenyl-bis(trimethylsilylimino)phosphinate anion and one THF molecule. The PN_2Nd-cycle is almost planar. The Nd–C_8H_8(cent.) distance is 195.5 pm and the two Nd–N bond lengths are equal (247.2(3) and 247.3(3) pm). The isolated complexes were also fully characterized by ^1H, ^{13}C, ^{29}Si, ^{31}P NMR, MS and Raman spectra.

M. Dolg et al. [68] carried out large-scale state-average multi-configuration self-consistent field, configuration interaction, averaged coupled-pair functional and

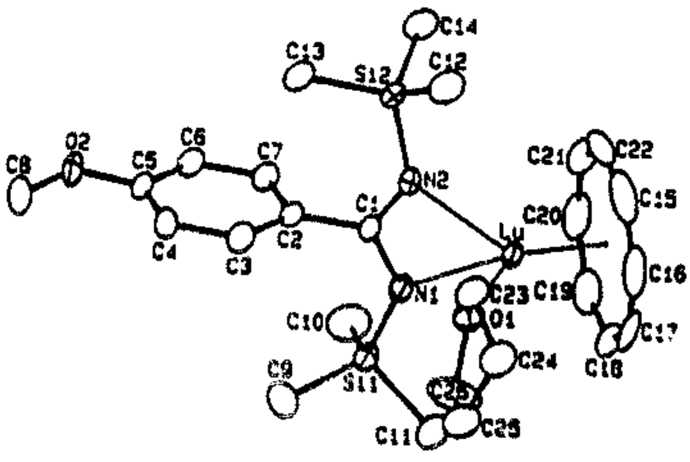

Fig. 37. Structure of $(C_8H_8)Lu[4\text{-}MeOC_6H_4C(NSiMe_3)_2](THF)$.

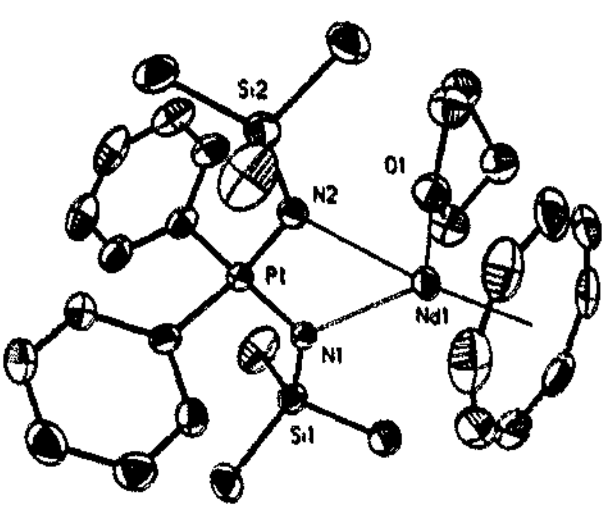

Fig. 38. Structure of $(C_8H_8)Nd[Ph_2P(NSiMe_3)_2](THF)$.

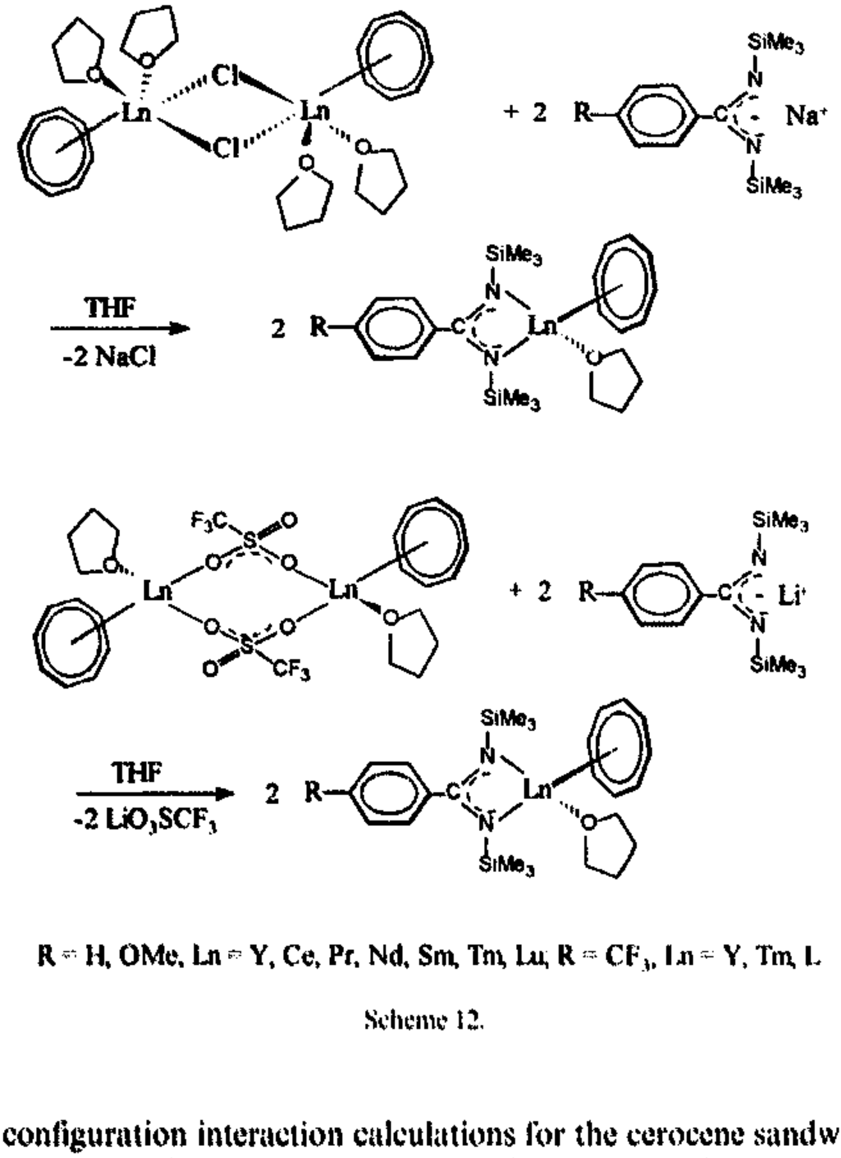

R = H, OMe, Ln = Y, Ce, Pr, Nd, Sm, Tm, Lu; R = CF_3, Ln = Y, Tm, L

Scheme 12.

spin–orbit configuration interaction calculations for the cerocene sandwich complex $Ce(C_8H_8)_2$. On the basis of these calculations the authors concluded that $Ce(C_8H_8)_2$ is essentially a Ce(III) compound, i.e. a Ce^{3+} ion with a $4f^1$ configuration and two $C_8H_8^{1.5-}$ ligands. The covalent contributions to metal–ring bonding in $Ce(C_8H_8)_2$ result mainly from the cerium 5d orbitals, whereas the 4f orbitals retain an atomic-like character in the molecular environment. The calculated $Ce–C_8H_8$(ring) distance of 2.05 Å still shows a substantial error when compared to the experimental value of 1.97 Å.

2.6. *Organolanthanide complexes in organic synthesis*

R.M. Giuliano et al. [69] used methylcerium compounds for additions to pentodialdo-1,4-furanoses. The addition of a methylcerium unit to incorporate the branching methyl group at C-3 in a 2-deoxyfuranosid-3-ulose was found to be superior to either Grignard reagents or methyllitium.

J.W. Timberlake et al. [70] reported the use of CH_3CeCl_2 for the preparation of

2-(2,4,6-trimethylphenyl)-2-propanol and 2,4,6-trimethylacetophenone. It was found that a single addition of CH_3CeCl_2 to 2,4,6-trimethylbenzonitrile led to the imine, while it was necessary to add CH_3CeCl_2 twice to *p*-methylbenzonitrile in order to obtain the corresponding imine, (Scheme 13).

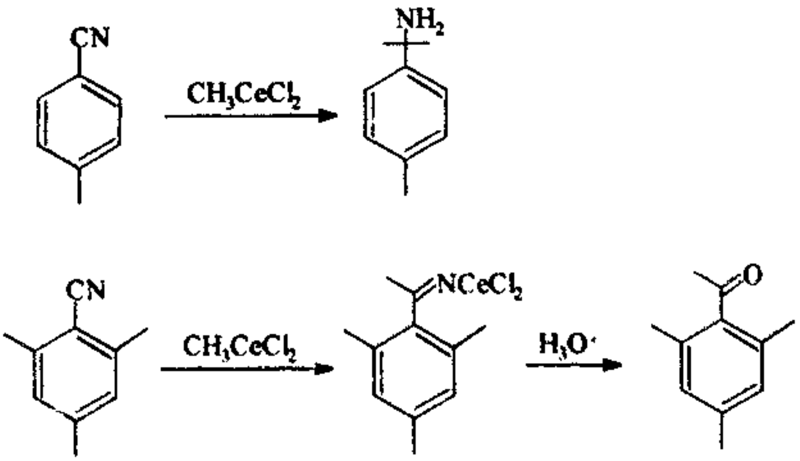

Scheme 13.

J. Betz and M. Heuschmann [71] reported the formation of homoallylic amines (*Z*-diastereomers) from the appropriate imines in the presence of vinylcerium dichloride (Scheme 14). The intermediate $CH_2{=}CHCeCl_2$ was prepared from $CH_2{=}CHMgBr$ and $CeCl_3$. The use of $CH_2{=}CHCeCl_2$ enabled the authors also to transform some chiral imines to *l*-products with high diastereoselectivity.

R^1 = Me, Ph, or 4-$MeOC_6H_4$, R^2 = Me, or H,

R^3 = CH_2Ph, Bu, CH*i*Pr-CH_2OMe or CHMe-CH_2OMe

Scheme 14.

G. Ulibarri et al. [72] reported the reaction of dichlorocerium trimethylsilylacetylide with an β,γ-unsaturated ketone (Scheme 15).

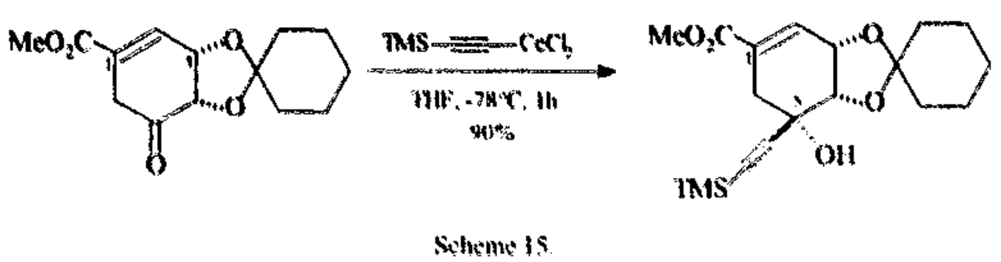

Scheme 15.

P.M.J. Jung et al. [73] also employed cerium trimethylsilylacetylide additions to 3'-ketonucleosides (Scheme 16). The ethynylcerium reagents ($RCeCl_2$) gave the best yields and the highest degree of diastereoselectivity for ribo- and xylo-derivatives, respectively.

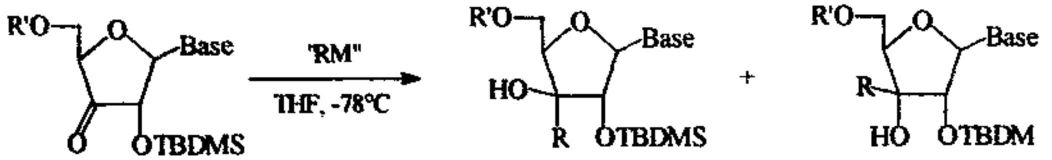

R' = TBDMS or H ; R = TMS-C≡C-; Base = Adenine or Uracil

TBDMS = tert-butyldimethylsilyl-; "RM" = RLi, R_2CeCl or $RCeCl_2$

Scheme 16.

M. Kunishima et al. [74] found alkynylsamarium derivatives to be involved as intermediates in SmI_2-mediated coupling reactions between iodoalkynes and ketones or aldehydes (Scheme 17). The reactions led to the formation of propargyl alcohols.

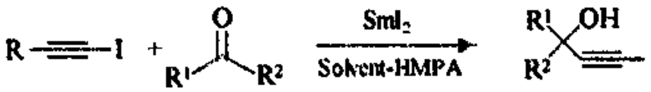

R = n-C_8H_{17}, $R^1 = R^2$ = Bu

Scheme 17.

H. Yasuda et al. [75] used $Cp_2^*SmMe(THF)$ as initiator for syntheses of monodispersed methyl methacrylate (MMA) oligomers ($M_n \approx 2500$; $M_w/M_n < 1.10$). The oligomerization proceeds via a samarium enolate as the propagating species, and the reaction of the living oligomer with *p*-tolualdehyde produced *p*-tolyl hydroxymethyl-terminated oligoMMA (Scheme 18).

2.7. *Organolanthanide catalysis*

X. Yang et al. [76] patented the organolanthanide hydrides $[(C_5Me_5)_2LnH]_2$ (Ln = Sm, Lu) as catalysts for the copolymerization of methylenecyclopropane and simple olefins (ethylene, propylene or styrene). The polymerization goes via a lanthanide-mediated β-alkyl shift ring-opening process and results exomethylene functionalized polyolefins of the type $\{-(CH_2CHR)_x-[CH_2CH_2C(CH_2)]_y-\}$ (R = H, CH_3 or Ph).

P.-F. Fu and T.J. Marks [77] reported that $PhSiH_3$ is an efficient and selective chain transfer agent in α-olefin polymerization and copolymerization catalyzed by $[Cp_2^*LnH]_2$ (Ln = Y, La, Sm, Lu) and $[Me_2Si(C_5Me_4)_2]LnCH(SiMe_3)_2$ (Ln = Sm, Nd). Some characteristic data of the ethylene polymerization are presented in Table 1. Organolanthanide-catalyzed ethylene/1-hexene and ethylene/styrene copolymerization processes were also investigated.

T.J. Marks et al. [78] investigated the stereocontrol in the polymerization of methyl methacrylate mediated by chiral organolanthanide metallocenes. Hydride, hydrocarbyl and amide bis(cyclopentadienyl) complexes (Scheme 19) were used as

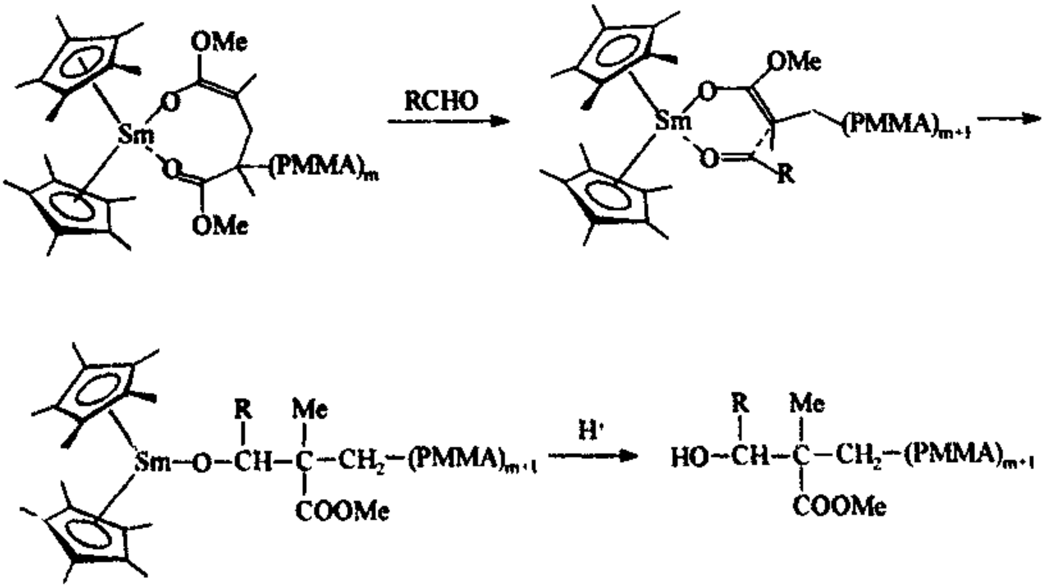

Scheme 18.

Table 1
Ethylene polymerization catalyzed by organolanthanide complexes in the presence of $PhSiH_3$ [77]

Catalyst/ precatalyst	$PhSiH_3$ (M)	Reaction time (min)	Yield (g)	Activity (kg of PE/mol of Ln atm h)	M_n ($\times 10^{-3}$)	M_w/M_n
$[\mathrm{Cp}^*_2\mathrm{SmH}]_2$	0.02	3	1.30	897	98.6	1.8
$[\mathrm{Cp}^*_2\mathrm{SmH}]_2$	0.03	4	1.55	776	75.1	2.1
$[\mathrm{Cp}^*_2\mathrm{SmH}]_2$	0.05	2	0.69	713	57.0	2.1
$[\mathrm{Cp}^*_2\mathrm{SmH}]_2$	0.24	2	0.80	827	7.6	4.2
$[\mathrm{Cp}^*_2\mathrm{SmH}]_2$	0.74	2	0.33	342	4.4	4.3
$[\mathrm{Cp}^*_2\mathrm{LuH}]_2$	0.74	4	0.50	274	2.6	
$[\mathrm{Cp}^*_2\mathrm{YH}]_2$	0.74	2	0.35	300	4.9	2.2
$[\mathrm{Cp}^*_2\mathrm{LaH}]_2$	0.74	1.5	0.59	828	4.1	3.5
$[\mathrm{Me_2Si(C_5Me_4)_2}]\mathrm{Sm{-}CH(SiMe_3)_2}$	0.74	25	0.24		2.6	2.9

precatalysts in these processes. The achiral hydride precatalysts yielded syndiotactic PMMA with narrow polydispersities ($M_w/M_n = 1.02$–1.05). The polydispersity of PMMA from the chiral and achiral hydrocarbyl precatalysts are larger than those from the hydride precatalysts, and amide precatalysts gave the highest polydispersities.

W.J. Evans et al. [79] studied the samarium-catalyzed polymerization of ethylene under hydrogen by field desorption mass spectrometry (FD-MS). The complexes $\mathrm{Cp}^*_2\mathrm{Sm}$, $\mathrm{Cp}^*_2\mathrm{Sm(THF)_2}$, $[\mathrm{Cp}^*_2\mathrm{Sm}(\mu\text{-H})]_2$, $[\mathrm{Cp}^*_2\mathrm{Sm}]_2(\mathrm{PhCHCHPh})$, $[\mathrm{Cp}^*_2\mathrm{Sm}]_2(\mathrm{PhC_2Ph})$ and $[\mathrm{Cp}^*_2\mathrm{Sm}]_2(\mathrm{PhC_4Ph})$ were used as catalysts. According to FD-MS the variety of precursors gave the same FD-MS data, which confirmed the existence of one common primary catalytic cycle for all of these samarium complexes. The mechanism of the polymerization process is presented in Scheme 20. The FD-MS

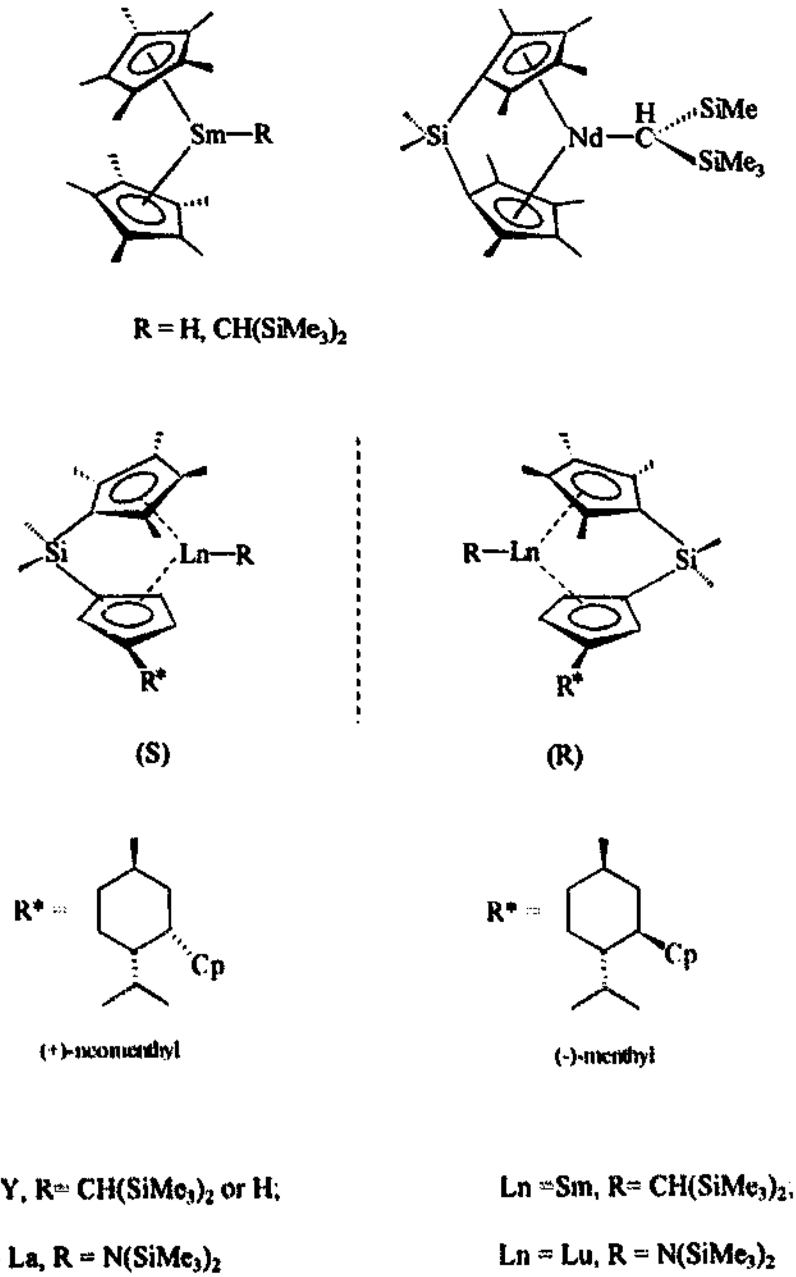

Scheme 19.

and NMR data on the formation of D–$(CH_2CH_2)_n$–D from $CH_2{=}CH_2$ under D_2 and H–$(CH_2CH_2)_n$–H from $CD_2{=}CD_2$ under H_2 were consistent with the termination of the polymerization by hydrogenolysis. The β-hydrogen elimination is not competing with hydrogenolysis as a termination mechanism. The data showed also no evidence for radical-based polymerization in the system. Styrene was not polymerized by these compounds but according to FD MS styrene could be incorporated into the polyethylene.

H. Yasuda et al. [80,81] also used $Cp^*_2SmMe(THF)$ and $Cp^*_2YMe(THF)$ as catalysts for living polymerizations and copolymerizations of alkyl acrylates. Some

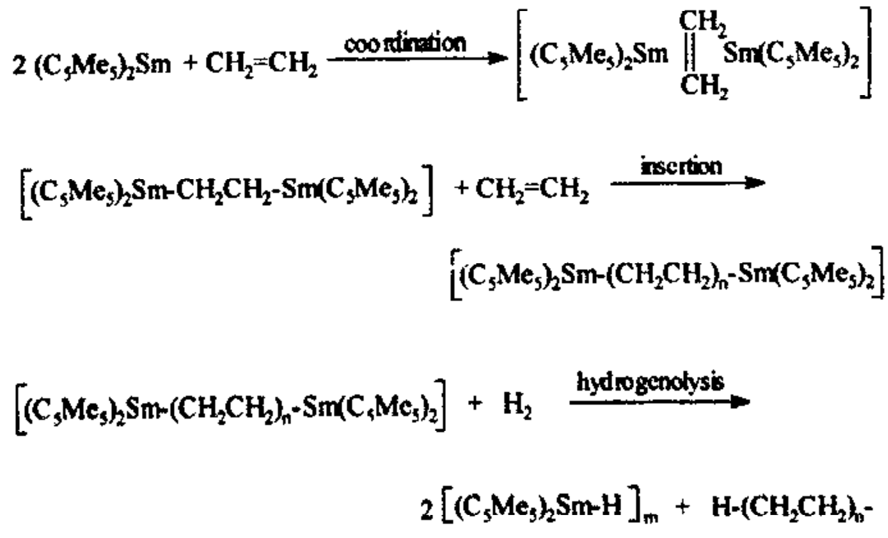

$$2\,(C_5Me_5)_2Sm + CH_2{=}CH_2 \xrightarrow{\text{coordination}} \left[(C_5Me_5)_2Sm \overset{CH_2}{\underset{CH_2}{\|}} Sm(C_5Me_5)_2\right]$$

$$\left[(C_5Me_5)_2Sm\text{-}CH_2CH_2\text{-}Sm(C_5Me_5)_2\right] + CH_2{=}CH_2 \xrightarrow{\text{insertion}} \left[(C_5Me_5)_2Sm\text{-}(CH_2CH_2)_n\text{-}Sm(C_5Me_5)_2\right]$$

$$\left[(C_5Me_5)_2Sm\text{-}(CH_2CH_2)_n\text{-}Sm(C_5Me_5)_2\right] + H_2 \xrightarrow{\text{hydrogenolysis}} 2\left[(C_5Me_5)_2Sm\text{-}H\right]_m + H\text{-}(CH_2CH_2)_n\text{-}$$

Scheme 20.

results of polymerization experiments are presented in Table 2. $Cp^*_2SmMe(THF)$ initiated also the random living copolymerisation of methyl acrylate with *n*-butyl acrylate and block copolymerization of alkyl acrylates with methyl methacrylate to give a triblock copolymer of methyl methacrylate/*n*-butyl acrylate/methyl methacrylate. The thus obtained copolymers exhibited good mechanical properties. Catalyzed by $Cp^*_2SmMe(THF)$ block copolymerization of alkyl acrylates with ε-caprolactone yielded unimodal block copolymers, which contain mainly caprolactone.

B.M. Novak and L.S. Boffa [82] patented the living polymerization of monomers and a two-step method for the formation of triblock copolymers by using bimetallic,

Table 2
Polymerization of alkyl acrylates catalyzed by organolanthanide complexes [80] (A = acrylate, Me = CH_3, Et = C_2H_5, nBu = *n*-C_4H_9, tBu = *t*-C_4H_9)

Initiator	Monomer	M_n ($\times 10^{-3}$)	M_w/M_n	Conversion (%)	Initiator efficiency (%)
$Cp^*_2SmMe(THF)$	MeA	48	1.04	99	89
	EtA	55	1.04	94	86
	EtA^b	56	1.03	96	86
	nBuA	70	1.05	99	91
	nBuA^b	69	1.02	96	89
	tBuA^c	16	1.03	99	79
$Cp^*_2YMe(THF)$	MeA	50	1.07	99	86
	EtA	53	1.05	96	91
	nBuA	72	1.04	98	88
	tBuA^c	17	1.03	99	75

Reaction conditions: ^{a} initiator concentration 0.2 mol% of monomer, toluene, reaction time 10 min, 0 °C; ^{b} initiator concentration 0.2 mol% of monomer, toluene, reaction time 1 h, −78 °C; ^{c} initiator concentration 1.0 mol% of monomer, toluene, reaction time 24 h, 0 °C.

bis-lanthanoid initiators M–L–M (M – organolanthanide complex, L – functionalized linking group that is covalently bound to each of the two metal atoms). The catalyst Cp$^*_2$Sm(μ-η^3-allyl)(μ-η^3-allyl)SmCp$^*_2$ polymerized acrylate esters or lactones (A) to give narrow molecular weight distribution polymers of formula $(A)_n(L)(A)_m$ (L – $(CH_2)_6$). The addition of a second monomer (B) led to triblock copolymers of the type $(B)_o(A)_n(L)(A)_m(B)_p$ (Scheme 21).

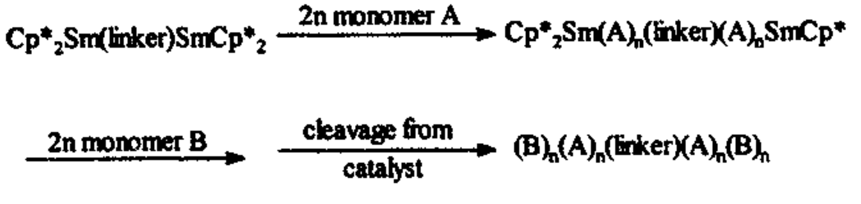

$$Cp^*_2Sm(linker)SmCp^*_2 \xrightarrow{\text{2n monomer A}} Cp^*_2Sm(A)_n(linker)(A)_nSmCp^*$$

$$\xrightarrow{\text{2n monomer B}} \xrightarrow[\text{catalyst}]{\text{cleavage from}} (B)_n(A)_n(linker)(A)_n(B)_n$$

Scheme 21.

H. Yasuda and E. Ihara [83] patented the preparation of a block copolymer of an olefin and an ethylenically unsaturated monomer (α-olefins with 3 and more C-atoms, vinyl and vinylidene compounds) or lactone by using bis(cyclopentadienyl) complexes of the lanthanides, scandium or yttrium with bridged Cp-ligands (Fig. 39), wherein Cp is a cyclopentadienyl ring; R^1 is a substituent on the Cp ring (an alkyl group or a silicon-containing hydrocarbon substituent) having 1 to 20 C-atoms; X is a divalent hydrocarbon or a silicon-containing hydrocarbon unit having 1 to 20 C-atoms; j is an integer from 1 to 5; R^2 is an alkyl group or a silicon-containing hydrocarbon unit having 1 to 12 C-atoms; R^3 is an alkyl group having 1 to 20

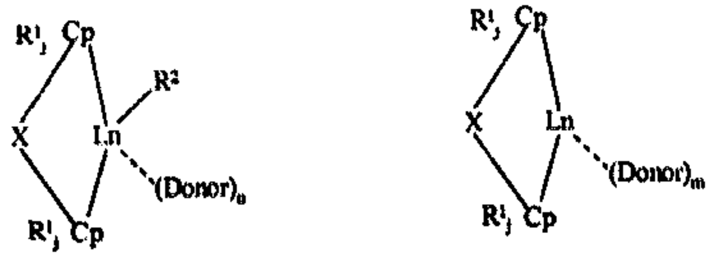

(1)
Ln- a trivalent rare earth metal
(Sc, Y or lanthanide)

(2)
Ln- a divalent rare earth metal
(Sm, Eu or Yb)

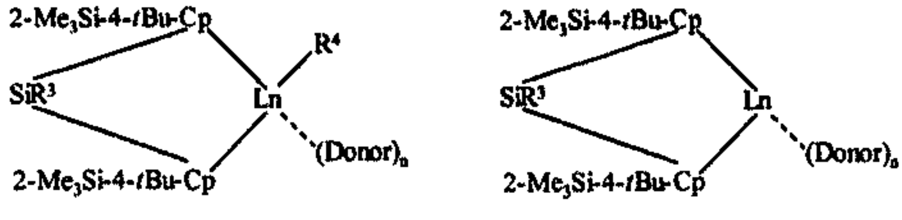

(3)
Ln- a trivalent rare earth metal
(Sc, Y or lanthanide)

(4)
Ln- a divalent rare earth metal
(Sm, Eu or Yb)

Fig. 39. Catalysts for preparing block copolymers of monoolefins.

C-atoms; R^4 is a methyl or a bis(trimethylsilyl)methyl group; Donor is a compound selected from the group consisting of a ketone, an ester, an ether and an amine having 1 to 12 C-atoms; *n* is 0 or 1; *m* is an integer of from 0 to 2.

P. Biagini et al. [9] investigated the catalytic activity of new $Ln(\eta^6\text{-arene})(AlX_3R)_3$ derivatives in the polymerization of butadiene and ethylene. $AlH(\textit{iso}\text{-}Bu)_2$ and $MgBu_2$ were used as cocatalysts. Some results of butadiene and ethylene polymerization with the $MgBu_2$ cocatalyst are presented in Table 3 and Table 4, respectively.

F. Xu et al. [84] published the selective dimerization of butanal to afford butyl butyrate catalyzed by $(C_5H_4Bu^t)_2LnCl$ (Ln = Yb, Er), $(C_5H_4Me)_2YbCl$, $(C_5H_4Bu^t)LnCl_2$ (Ln = Yb, Nd) or $(C_5H_4Me)YbCl_2$ in the presence of *n*-BuLi at 0 °C. The yields of butyl butyrate were found to be dependent on the lanthanocene complex structures.

B.-J. Deelman et al. [85] reported the oligomerization of 2-cycloalken-1-ones catalyzed by organolanthanide hydrides of the type $[Cp^*_2LnH]_2$ (Ln = Y, La). It was found that $[Cp^*_2LaH]_2$ complex showed a higher activity (≥ 150 mmol monomer per mol precatalyst per hour at 25 °C) than the yttrium analogue ($\leq 100\ h^{-1}$). The average degree of oligomerization of 2.7–3.5 at 25 °C increased at higher reaction temperature (by 15 at 100 °C). The authors reported also that the complexes $[Cp^*_2LnH]_2$ (Ln = Y, La) were active catalysts for the oligomerization of 2-cyclohexen-1-one.

Table 3
Butadiene polymerization in the presence of the $ATHAL/MgBu_2$ catalytic system (ATHAL – a toluenic solution of catalyst obtained by the reaction of the parent $Ln(\eta^6\text{-arene})(AlX_4)_3$ with 1.5 equivalents of $AlH(\textit{iso}\text{-}Bu)_3$)

$Ln(\eta^6\text{-arene})(AlX_4)_3$	Time (min)	Conv. (%)	1,4-*cis* (%)	1,4-*trans* (%)	1,2- (%)	M_w ($\times 10^{-3}$)	M_w/M_n
$Pr(\eta^6\text{-}C_6H_5Me)(AlCl_4)_3$	20	92	96.9	2.2	0.9	807	12
$Pr(\eta^6\text{-}C_6H_5Me)(AlI_4)_3$	30	94	88.2	10.8	1.0	408	9
$Nd(\eta^6\text{-}C_6H_5Me)(AlCl_4)_3$	15	73	97.4	1.8	0.8	994	7
$Gd(\eta^6\text{-}C_6H_5Me)(AlCl_4)_3$	15	70	86.8	12.8	0.4	n.d.	n.d.
$Y(\eta^6\text{-}C_6H_5Me)(AlCl_4)_3$	20	87	0.4	99.5	0.1	n.d.	n.d.

Table 4
Ethylene polymerization in the presence of the $ATHAL/MgBu_2$ catalytic system (ATHAL – a toluenic solution of catalyst obtained by the reaction of the parent $Ln(\eta^6\text{-arene})(AlX_4)_3$ with 1.5 equivalents of $AlH(\textit{iso}\text{-}Bu)_3$)

$Ln(\eta^6\text{-arene})(AlX_4)_3$	*T* (°C)	*P* (atm)	Time (min)	Activity	M_w ($\times 10^{-3}$)	M_w/M_n
$Nd(\eta^6\text{-}C_6H_5Me)(AlCl_4)_3$	50	5	60	91	495	11
$Nd(\eta^6\text{-}C_6H_5Me)(AlCl_4)_3$	70	6	30	148	598	32
$Y(\eta^6\text{-}C_6H_5Me)(AlCl_4)_3$	70	6	60	170	616	8

Activity – g polymer × g of $Ln^{-1} \times atm^{-1} \times h^{-1}$.

T. Imori et al. [86] published the dehydropolymerization of secondary stannanes to high molecular weight polystannanes by metallocene catalysts including $Cp^*_2SmCH(SiMe_3)_2$. The latter catalyst produced only small oligomers with $M_n = 600$ and $M_w = 1000$.

T.J. Marks et al. [87] investigated regioselection and enantioselection in olefin hydrosilylation catalyzed by organolanthanide complexes $Cp^*_2LnCH(SiMe_3)_2$ (Ln = Y, La, Nd, Sm, Lu), $Me_2Si(C_5Me_4)_2SmCH(SiMe_3)_2$, $Me_2Si(C_5Me_4)(R^*C_5H_4)SmCH(SiMe_3)_2$ (R^* = chiral auxillary).

According to NMR studies the first Ln–C/Si–H initiation processes are a major pathway for hydrosilylation and warrant additional scrutiny.

$$L_nSmCH(SiMe_3)_2 + PhSiH_3 \rightarrow L_nSmH + PhH_2SiCH(SiMe_3)_2$$

An increasing Ln^{+3} ionic radius correlates with increasing hydrosilylation turnover frequencies and 2,1-regioselectivity for styrenic and related olefins. Opening the metal coordination sphere by connecting the ancillary ligands ($Cp^*_2Ln \rightarrow Me_2Si(C_5Me_4)_2Ln$ or $Me_2Si(C_5Me_4)(R^*C_5H_4)Ln$) also effected a further enhancement in both turnover frequency and regioselectivity. The rate of styrene hydrosilylation was depressed by strongly σ-electron-withdrawing *para* substituents and was slightly accelerated by more π-electron-releasing *para* substituents (e.g. OMe). The observed turnover frequencies were as high as $400\ h^{-1}$ (60 °C) for styrenic olefins and $> 1000\ h^{-1}$ (90 °C) for 1-hexene. The chiral organolanthanide precatalysts $Me_2Si(C_5Me_4)[(-)menthylC_5H_4]SmCH(SiMe_3)_2$ ((*R*)-Sm) and $Me_2Si(C_5Me_4)[(-)menthylC_5H_4]SmCH(SiMe_3)_2$ ((*S*)-Sm) effected the enantioselective hydrogenation of 2-phenyl-1-butene (Scheme 22) with turnover frequencies in the order 9000–$19\,000\ h^{-1}$ at 25 °C and 1.0 atm of H_2. The kinetics of the hydrogenation obey the following equation: $v = k[Sm]^{1/2}[olefin]^0[H_2]^1$. D_2O quenching of the asymmetric hydrosilylation gave $PhCD(CH_3)(CH_2CH_3)$ and $PhSiH_2D$ as products. Cyclohydrosilylation of 1,5-hexadiene catalyzed by the samarium complexes $Cp^*_2SmCH(SiMe_3)_2$, $Me_2Si(C_5Me_4)_2SmCH(SiMe_3)_2$ and $Me_2Si(C_5Me_4)[(-)menthylC_5H_4]SmCH(SiMe_3)_2$ ((*R*)-Sm) yielded four major products (Fig. 40). The probable hydrosilylation mechanism is considered to be that of the analogous olefin

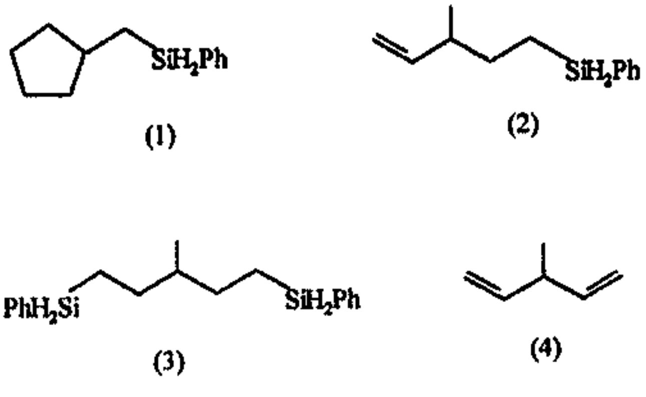

(1) (2)

(3) (4)

Fig. 40. Products of cyclohydrosilylation of 1,5-hexadiene catalyzed by organosamarium complexes.

hydrogenation process, with rapid olefin insertion into the Ln–H bond followed by turnover-limiting Si–H/Ln–C transposition.

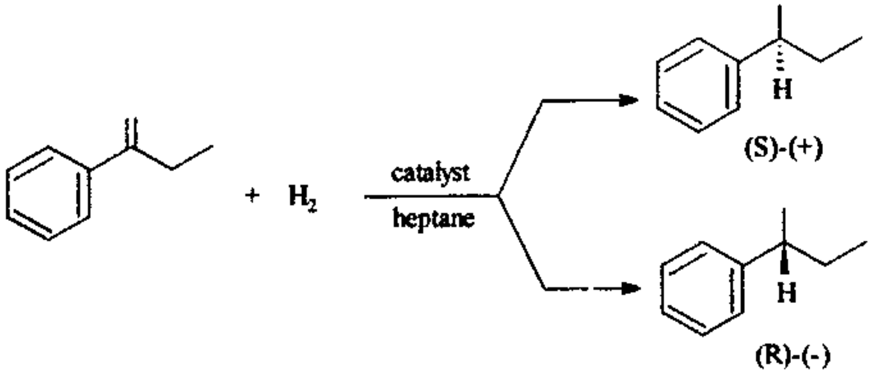

Scheme 22.

G.A. Molander and W.H. Retsch [88] reported the selective hydrosilylation of alkynes catalyzed by the organoyttrium complex $Cp^*_2YMe(THF)$. The hydrosilylation of a symmetrical alkyne (5-decyne) yielded a single stereoisomer (*E*)-alkenylsilane. The reactions of unsymmetrical alkynes gave not only a single stereoisomer but also only one regioisomer in high yield. The proposed catalytic cycle is shown in Scheme 23. The use of $Cp^*_2YbCH(SiMe_3)_2$ as precatalyst enabled to improve the regioselectivity for hydrosilylation of unsymmetrical alkynes.

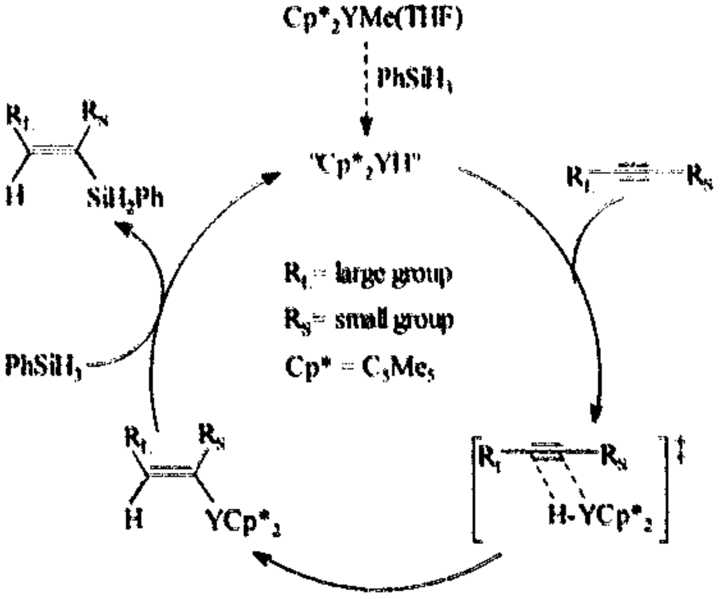

Scheme 23.

G.A. Molander and P.J. Nicols [89] also published sequential cyclization/silylation reactions of 1,5-dienes and 1,6-dienes catalyzed by $Cp^*_2YMe(THF)$. The reaction tolerates a number of functional groups and proceeds with good yields and diastereoselectivities. The obtained phenylsilane products can be easily converted to synthetically more versatile alcohols (Scheme 24).

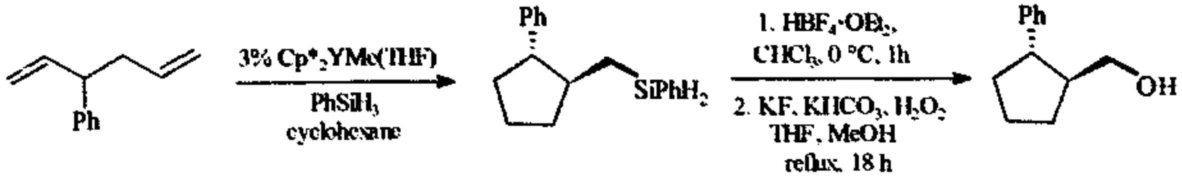

Scheme 24.

J.H. Teuben et al. [90] investigated the organolanthanide complexes $Cp^*_2LnCH(SiMe_3)_2$ (Ln = Y, La), $Cp^*_2YMe(THF)$, $[Cp^*_2YH]_2$, $Cp_2YCH(SiMe_3)_2$ and $Cp_2YCH(SiMe_3)_2(Et_2O)$ as catalysts for the hydroboration of 1-hexene using catecholborane as boration agent (Scheme 25). The complex $Cp^*_2LaCH(SiMe_3)_2$ exhibited the highest activity, but the yttrium analogue was found to be much less active. Other permethylyttrocene compounds such as $Cp^*_2YMe(THF)$ and $[Cp^*_2YH]_2$ were moderately active, while the sterically more accessible $Cp_2YCH(SiMe_3)_2$ and $Cp_2Y[CH(SiMe_3)_2](Et_2O)$ showed an increasing activity. Benzamidinato complexes such as $[PhC(NSiMe_3)_2]_2YCH(SiMe_3)_2$, $[PhC(NSiMe_3)_2]_2YCH_2Ph(THF)$ and $[PhC(NCMe_3)_2]_2YCH(SiMe_3)_2$ were also catalytically active but the activity was essentially lower than that of the $CP^*_2LaCH(SiMe_3)_2$.

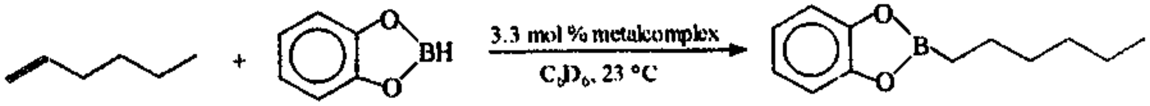

Scheme 25.

N.S. Radu and T. Don Tilley [91] investigated the mechanism of σ-bond metathesis reactions of $Cp^*_2SmCH(SiMe_3)_2$ with silicon hydrogen bonds. The study showed that a seemingly simple σ-bond metathesis process in fact proceeds by a more complex autocatalytic mechanism mediated by a reactive hydride complex (Scheme 26).

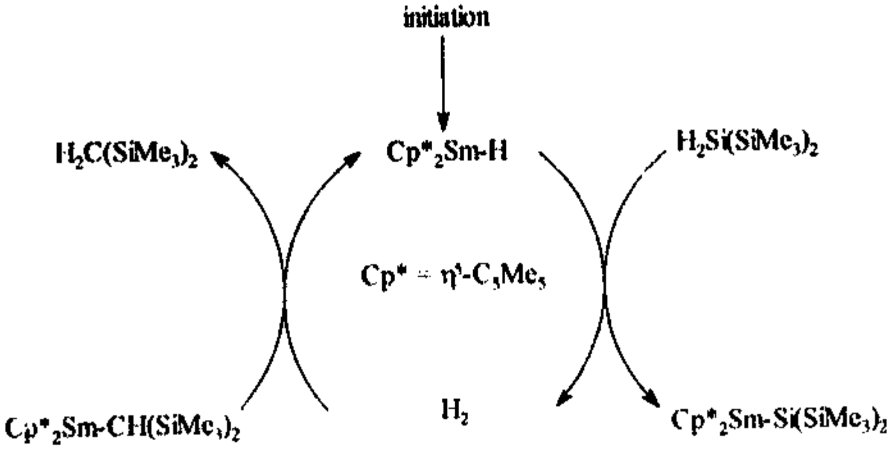

Scheme 26.

M. Takeno et al. [92] reported the organosamarium complex $Cp^*_2Sm(THF)_2$ to act as a catalyst for a new type of coupling reactions of vinyl esters with aldehydes

(Scheme 27). The reactions led to the corresponding diesters in good yields. The proposed mechanism might involve an eight-membered alkoxy samarium intermediate with the subsequent intramolecular hydride shift reaction to give the diesters and regenerated samarium species.

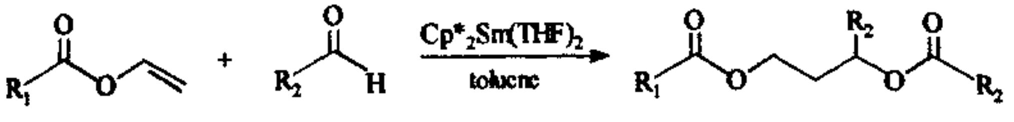

$R_1 = CH_3$, $R_2 = CH_3$, $c\text{-}C_6H_{11}$, $n\text{-}C_3H_7$, $CH(CH_3)_2$, $C(CH_3)_3$,C_6H_5, $2\text{-}CH_3C_6H_4$, $4\text{-}CH_3C_6H_4$, $4\text{-}ClC_6H_4$; $R_1 = n\text{-}C_5H_{11}$, $CH_2{=}CH$, $CH_3CH{=}CH$, $R_2 = C_6H_5$

Scheme 27.

3. Actinides

3.1. *Actinide complexes without supporting cyclopentadienyl ligands*

3.1.1. *Alkynyl and σ-hydrocarbyl complexes*

D. Baudry et al. [93] published the synthesis and reactivity of alkynyl (silylamido)uranium complexes, $[\{N(SiMe_3)_2\}_3U{-}C{\equiv}CR]$ ($R = C(CH_3)_3$, $(CH_2)_nCH_3$, $n = 2$–5). The compounds were obtained by reaction of $[\{N(SiMe_3)_2\}_2UCH_2SiMe_2NSiMe_3]$ with the appropriate terminal alkynes. Treatment of the alkynyl(silylamido)uranium complexes with a stoichiometric amount of acetone led to the corresponding uranium alkoxides $[\{N(SiMe_3)_2\}_3U{-}O{-}CMe_2C{\equiv}CR]$. The following hydrolysis of the latter complexes with aqueous HCl afforded the α-acetylenic alcohols.

$$[\{N(SiMe_3)_2\}_2UCH_2SiMe_2NSiMe_3] + HC{\equiv}CR \rightarrow$$

$$[\{N(SiMe_3)_2\}_3U-C{\equiv}CR] \quad R = C(CH_3)_3, (CH_2)_nCH_3, n = 2-5$$

$$[\{N(SiMe_3)_2\}_3U-C{\equiv}CR] + Me_2C{=}O \rightarrow$$

$$[\{N(SiMe_3)_2\}_3U-O-CMe_2C{\equiv}CR]$$

$$[\{N(SiMe_3)_2\}_3U-O-CMe_2C{\equiv}CR] + H_3O^+ \rightarrow HOCMe_2C{\equiv}CR + [U]$$

A. Pires de Matos et al. [94] reported the synthesis and reactivity of hydrotris (pyrazolyl)borate σ-hydrocarbyl uranium(IV) complexes. The compounds $[UCl_2(2\text{-}CH_2C_6H_4NMe_2)L^*]$ and $[UCl_2(2\text{-}C_6H_4CH_2NMe_2)L^*]$ ($L^* = HB(3,5\text{-}Me_2pz)_3$) were synthesized by treatment of $[UCl_2L^*(THF)]$ with $Li(2\text{-}CH_2C_6H_4NMe_2)$ and $Li(2\text{-}C_6H_4CH_2NMe_2)$, respectively. The isolated compounds were characterized by their elemental analyses, IR and ^1H NMR spectra. The complexes $[UCl_2(2\text{-}CH_2C_6H_4NMe_2)L^*]$ and $[UCl_2(2\text{-}C_6H_4CH_2NMe_2)L^*]$ were found to exhibit fluxional behavior in C_6D_6 solution at room temperature.

$$[UCl_2L^*(THF)] + Li(2-CH_2C_6H_4NMe_2) \rightarrow$$
$$[UCl_2(2-CH_2C_6H_4NMe_2)L^*] + LiCl$$

$$[UCl_2L^*(THF)] + Li(2-C_6H_4CH_2NMe_2) \rightarrow$$
$$[UCl_2(2-C_6H_4CH_2NMe_2)L^*] + LiCl$$

M. Ephritikhine et al. [95] published the synthesis and crystal structure of the novel cycloheptatrienyl sandwich complex $[K(C_{12}H_{24}O_6)][U(\eta\text{-}C_7H_7)_2]$. Reaction between UCl_4, metallic potassium and an excess of cycloheptatriene in THF gave the complex $K[U(\eta\text{-}C_7H_7)_2]$. Subsequent treatment of $K[U(\eta\text{-}C_7H_7)_2]$ with 18-crown-6 in THF yielded crystals of $[K(C_{12}H_{24}O_6)][U(\eta\text{-}C_7H_7)_2]$. The complex was also alternatively prepared from UCl_4 or $U(BH_4)_4$ and four equivalents of KC_7H_9 in THF followed by addition of 18-crown-6 to the filtered solution. According to X-ray diffraction crystallography the complex consists of discrete $[K(18\text{-crown-}6)]^+$ cations and $[U(\eta\text{-}C_7H_7)_2]^-$ anions. The anion $[U(\eta\text{-}C_7H_7)_2]^-$ has a sandwich structure with two parallel cycloheptatrienyl rings in a staggered conformation (Fig. 41). The U–C distances are equal within experimental error with an average value of 2.53(2) Å. The question of the uranium oxidation state in the complex is discussed.

3.2. *Cyclopentadienyl complexes*

3.2.1. *Mono(cyclopentadienyl) complexes*

M.F. Lappert et al. [96] prepared two new mono(cyclopentadienyl)thorium(IV) compounds, $[\{ThCp''Cl_3)_2NaCl(OEt_2)\}_2]$ and $[ThCp''Cl_3(pmdeta)]$ ($Cp'' = \eta\text{-}C_5H_2(SiMe_3)_3\text{-}1,2,4$; pmdeta = $MeN(CH_2CH_2NMe_2)_2$). The complexes were synthesized by reaction of $ThCl_4$ with $NaCp''$ or $[NaCp''(pmdeta)]$. The compound $[\{ThCp''Cl_3)_2NaCl(OEt_2)\}_2]$ was characterized by X-ray diffraction. The structure

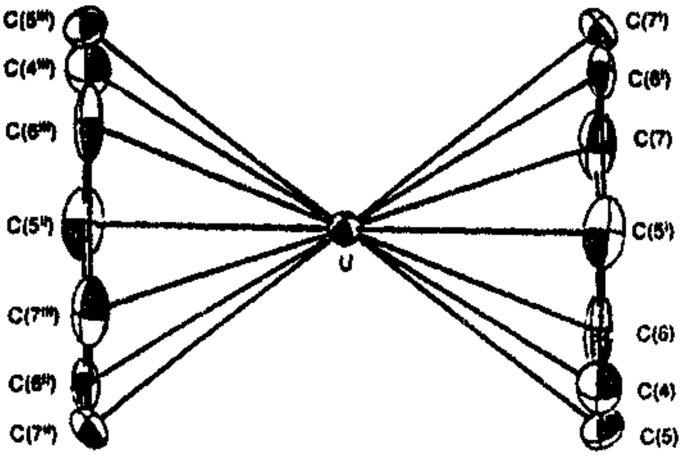

Fig. 41. Structure of $[U(\eta\text{-}C_7H_7)_2]^-$ anion.

is tetranuclear (two Th and two Na atoms) and contains eight μ_2- and two μ_3-bridging chloride ligands. Each thorium atom has a distorted octahedral arrangement. Th is coordinated by a Cp‴ and one triply bridging chloride ligand in axial positions and by four μ_2-bridging chlorides in equatorial positions. The two Th–Cl(μ_3) distances are 2.857(3) and 2.875(2) Å. The Th–Cl(μ_2) bond lengths are 2.849(3) and 2.861(3) Å.

D.M. Barnhart et al. [97] synthesized the mono(cyclopentadienyl)thorium complex $[(\eta\text{-}C_5H_5)Th_2(O\text{-}i\text{-}Pr)_7]_3$ by the reaction between $ThBr_4(THF)_4$ and one equivalent of TlCp in THF followed by addition of three equivalents of KO-*i*-Pr to the mixture. According to X-ray diffraction studies the hexanuclear complex has a cyclic structure in which three binuclear $[(\eta\text{-}C_5H_5)Th_2(O\text{-}i\text{-}Pr)_7]$ units are linked together by the bridging (μ-η^5:η^5)-cyclopentadienyl ligands (Fig. 42). Each thorium is coordinated by an η^5-cyclopentadienyl ring, three bridging and two terminal *iso*-propoxide ligands to give a distorted octahedral geometry. The Th–C(Cp) bond lengths range from 2.95(2) to 3.02(2) Å and the three Th–Cp(cent.) distances are 2.748(3), 2.75(3)

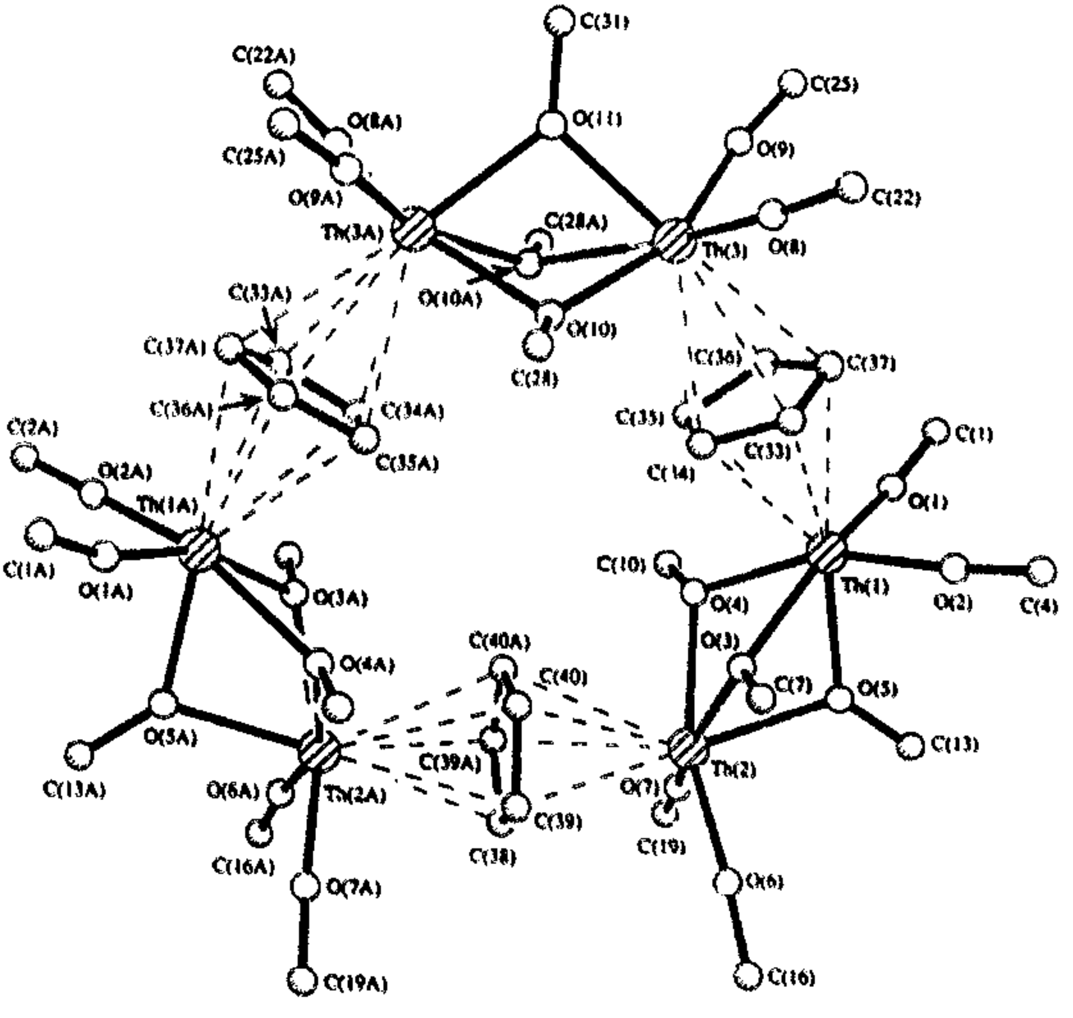

Fig. 42. Molecular structure of $[CpTh_2(O\text{-}i\text{-}Pr)_7]_3$.

and 2.73(3) Å. The average Th–O(term.) distance is 2.14(2) Å, while the average Th–O(bridg.) distance is 2.41(2) Å.

A. Pires de Matos et al. [94] prepared methyl derivatives of monocyclopentadienyl hydrotris(pyrazolyl)borate uranium complexes $[UCl_{2-x}CpMe_xL^*]$ ($L^* = HB(3,5\text{-}Me_2pz)_3$, $x = 1, 2$) by reaction of $[UCl_2CpL^*]$ with the appropriate amount of LiMe in toluene. The compounds were characterized by IR and ^1H NMR spectroscopy.

$$[UCl_2CpL^*] + xLiMe \rightarrow [UCl_{2-x}CpMe_xL^*] + xLiCl$$

$$L^* = HB(3,5-Me_2pz)_3,\ x = 1,2$$

D. Baudry et al. [98] synthesized and characterized by ^1H and ^{11}B NMR the monocyclopentadienyl uranium borohydrides $Cp^*U(BH_4)_3$ ($Cp^* = C_5Me_5$; C_5Me_4H; $C_5Me_4PPh_2$; C_5H_5, $C_5H_4PPh_2$; $C_5Me_4PPh_2(BH_3)$; $C_5H_4PPh_2(BH_3)$). A correlation between the electronic density around the uranium and the chemical shifts of the nuclei were studied. The shift (δ, ppm) of the BH_4-groups for the both ^1H and ^{11}B nuclei was found to increase in the order $C_5Me_5 < C_5Me_4H < C_5Me_4PPh_2 < C_5H_5$, $C_5H_4PPh_2 < C_5Me_4PPh_2(BH_3) < C_5H_4PPh_2(BH_3)$.

M.S. Gill and V.S. Sagoria [99] prepared and characterized by elemental analysis, IR, ^{19}F NMR and MS spectroscopy cyclopentadienyl uranium(IV) β-diketonates and alkoxides, $CpU(L)_3$ ($Cp = C_5H_5$, $L = CH_3COCHCOCF_3^-$, $C_4H_3SCOCHCOCF_3^-$, $CF_3COCHCOCF_3^-$, $C_3HF_6O^-$ and $C_3H_3F_4O^-$). For the complex $CpU(CH_3COCHCOCF_3)_3$ the temperature dependence of the vapor pressure was studied in the temperature range 303–377 K.

D.L. Clark et al. [100] synthesized the mono(pentamethylcyclopentadienyl)uranium(IV) sulfido complex $[Cp^*UI_2(THF)_3]_2S$ by oxidation of $Cp^*UI_2(THF)_3$ with one or two equivalents of CS_2 in toluene. After prolonged standing the solution of $[Cp^*UI_2(THF)_3]_2S$ in THF yielded crystals of $Cp^*_3U_3(\mu_3\text{-}I)(\mu_3\text{-}S)(\mu_2\text{-}I)_3I_3$. X-ray structural characterization of the latter compound has shown that this is a triangular homometallic cluster, in which three uranium atoms are linked by one triply bridging sulfido ligand and three doubly bridging and one triply bridging iodide ligands (Fig. 43). Each uranium atom has a distorted octahedral geometry formed by coordination of one Cp* ring, one μ_3-sulfido ligand, two μ_2-, one μ_3- and one terminal iodide ligands. The average U–C(C_5Me_5) and U–μ_3–S bond lengths are 2.71 and 2.75(2) Å, respectively. The U–I(term.) distances with an average value of 2.952(5) Å are shorter than the U–μ_2–I distances with an average of 3.096(8) Å. The U–μ_3–I distances were found to be significantly different for the three uranium atoms (3.240(5), 3.289(5) and 3.353(4) Å).

$$2Cp^*UI_2(THF)_3 + CS_2 \rightarrow [Cp^*UI_2(THF)_3]_2S$$

M. Ephritikhine et al. [101] prepared the mono(cyclopentadienyl)uranium(V) complex $[Cp^*U(NMe_2)_3(THF)][BPh_4]$ by oxidation of the neutral tetravalent precursor $[Cp^*U(NMe_2)_3]$ by $AgBPh_4$ in THF. The crystal structure of $[Cp^*U(NMe_2)_3(THF)][BPh_4]$ consists of discrete cation–anion pairs. In the cation

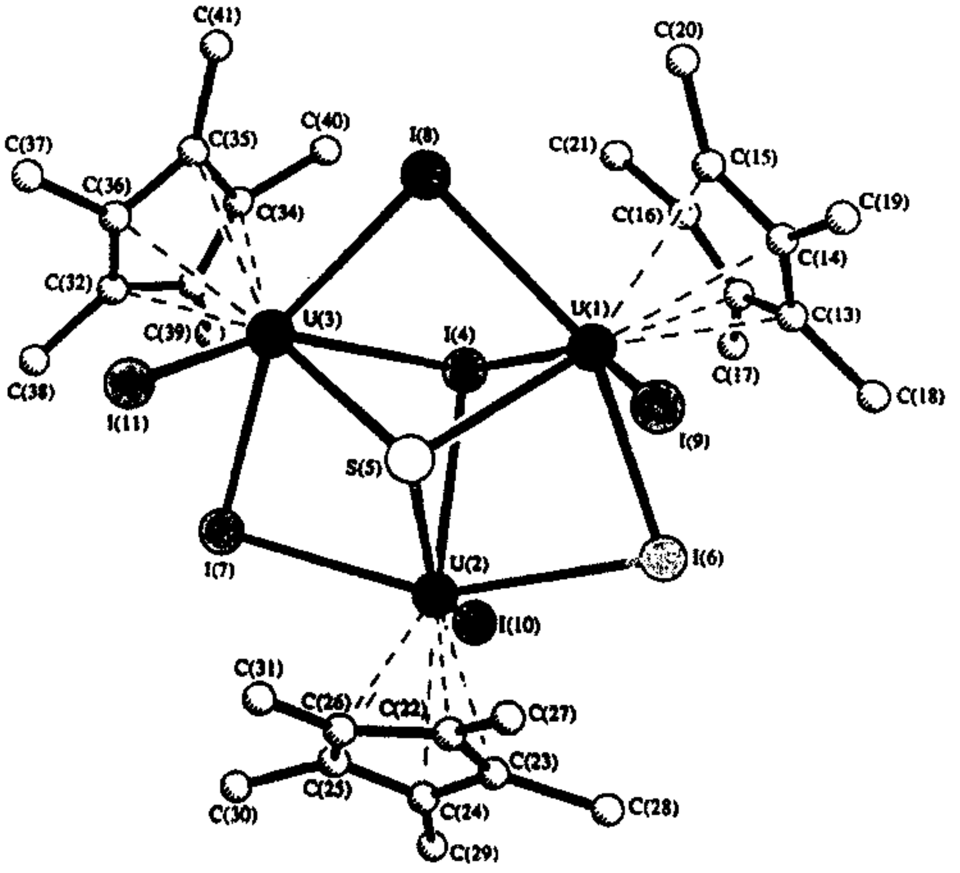

Fig. 43. Molecular structure of $Cp^*_3U_3(\mu_3\text{-}I)(\mu_3\text{-}S)(\mu_2\text{-}I)_3I_3$.

$[Cp^*U(NMe_2)_3(THF)]^+$ (Fig. 44) the uranium atom has a pseudo-trigonal bipyramidal arrangement formed by the centroid of the C_5Me_5-ring and an oxygen atom of THF in apical positions and three nitrogen atoms of the amido groups in equatorial positions. The U–Cp*(cent.) and U–O(THF) distances are 2.47(4) and 2.55(2) Å, respectively. The U–N(NMe_2) bond lengths are 2.25(2), 2.31(3) and 2.358(5) Å.

The same authors [102] reported the synthesis and structure of the ionic uranium(IV) cyclopentadienyl complex $[Cp^*U(NEt_2)_2(THF)_2][BPh_4]$. The compound was obtained by protonolysis of the neutral amide precursor $[Cp^*U(NEt_2)_3]$ with $NHEt_3BPh_4$. In the structure of the cation $[Cp^*U(NEt_2)_2(THF)_2]^+$ the uranium atom is five-coordinated by one Cp*-ring, two nitrogen atoms of the amido groups and two oxygen atoms of solvating THF molecules. The geometry of the cation can be described as a distorted trigonal bipyramid with the Cp*-ring centroid and two nitrogen atoms of NEt_2 groups in equatorial and two oxygen atoms of the THF molecules in orthogonal positions. The U–Cp*(cent.) and the average U–N(NEt_2) distances are 2.50(1) and 2.17(1) Å, respectively.

P. Scott and P.B. Hitchcock [103] prepared a series of amino(triamido) cyclopentadienyl uranium and thorium complexes $[ML(C_5R_5)]$ (M = U, Th; R = H, Me;

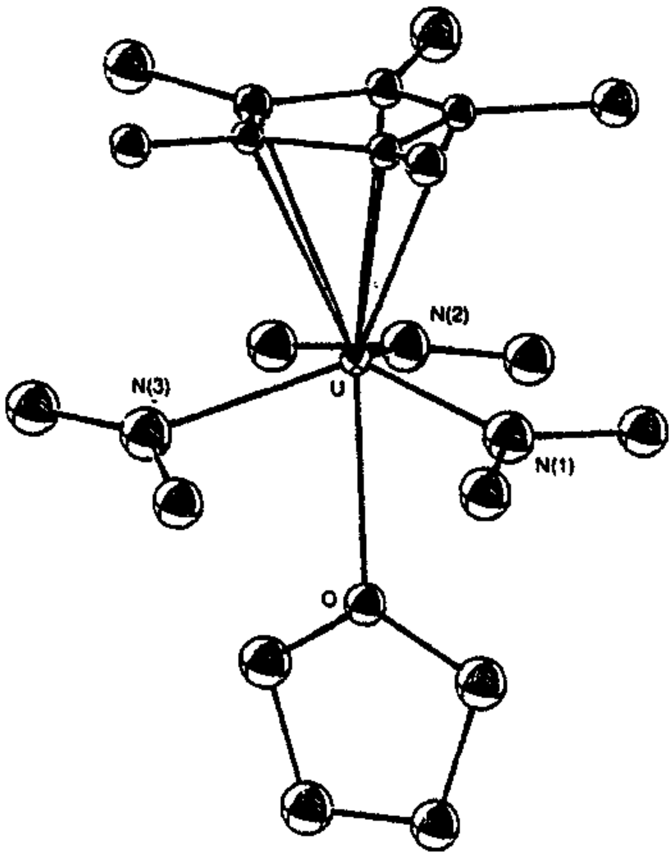

Fig. 44. Structure of $[Cp^{*}U(NMe_2)_3(THF)]^{+}$ cation.

L = $N(CH_2CH_2NSiMe_3)_3$) by reaction of the corresponding chlorides $[\{ML(Cl)\}_2]$ with the appropriate $Na(C_5R_5)$ salts in THF. The complex $[UL(C_5Me_5)]$ was characterized by single-crystal X-ray diffraction. In the structure (Fig. 45) the uranium atom is coordinated by one Cp*-ring and four nitrogens of the $N(CH_2CH_2NSiMe_3)_3$ ligand. The U–Cp*(cent.) distance is 2.58 Å while the U–N distances range from 2.25 to 2.264(15) Å. The complexes $[ML(C_5R_5)]$ were found

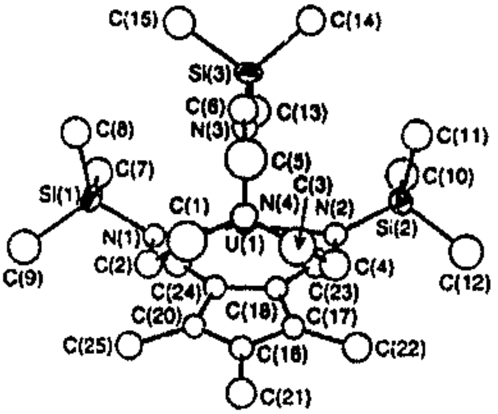

Fig. 45. Molecular structure of $[UL(C_5Me_5)]$ (L = $N(CH_2CH_2NSiMe_3)_3$).

to be fluxional exhibiting apparent three-fold symmetry on the NMR time scale in solution at room temperature.

3.2.2. Bis(cyclopentadienyl) complexes

J.W. Gilje and R.E. Cramer et al. [104] prepared the uranium sufimine derivative $Cp^*_2UCl_2(HNSPh_2)$ by reaction of $Cp^*_2UCl_2$ with $HNSPh_2$. The compound was characterized by single-crystal X-ray diffraction (Fig. 46). In this complex the uranium atom is coordinated by two Cp*-rings, two chloride ligands and one nitrogen of the sufimine ligand. The U–Cp*(cent.) distances are 2.52 and 2.48 Å. The U–Cl bond lengths are 2.648(8) and 2.693(8) Å and the U–N distance is 2.44(3) Å. Hydrolysis of $Cp^*_2UCl_2(HNSPh_2)$ with $HNSPh_2 \cdot H_2O$ led to crystals of the U(IV)/U(V) complex $[Cp^*(Cl)(HNSPh_2)U(\mu_3\text{-}O)(\mu_2\text{-}O)_2U(Cl)(HNSPh_2)_2]_2$. According to X-ray crystallography the compound is a cluster formed by four co-planar uranium atoms, which are linked by two μ_3- and four μ_2-oxygen atoms (Fig. 47). There are two types of uranium atoms in the cluster. Two uranium atoms are bound each to one μ_3- and two μ_2-oxygen atoms, one Cp*-ring, one chloride ligand and one $HNSPh_2$ ligand to give a coordination number of 8. The two other uranium atoms in the cluster have the coordination number 7 caused by the coordination of one chloride ligand, one μ_3- and two μ_2-oxygen atoms and two $HNSPh_2$ ligands to each metal atom.

J.W. Gilje and R.E. Cramer et al. [105] also reported the synthesis and structure of $Cp_2Th[(CH_2)(CH_2)PPh_2]_2$. The complex was obtained by the reaction of Cp_3ThCl with $[Li(CH_2)(CH_2)PPh_2]$. However, as was previously reported, the analogous reaction between Cp_3UCl and $[Li(CH_2)(CH_2)(CH_2)PPh_2]$ led to $Cp_3U{=}CHPPh_2CH_3$. In the molecule of $Cp_2Th[(CH_2)(CH_2)PPh_2]_2$ the thorium atom is coordinated by two η^5-C_5H_5-rings and two bidentate ylide ligands (Fig. 48). The Th atom has a distorted tetrahedral arrangement. The average Th–C(Cp) and Th–Cp(cent.) distances are 2.89(2) and 2.64 Å, respectively. The Th–C($(CH_2)(CH_2)PPh_2$) bond lengths are 2.77(2) and 2.67(1) Å.

D.S.J. Arney and C.J. Burns [106] reported the synthesis and properties of organouranium(IV) and -(VI) imido complexes. Monoimido complexes of uranium(IV) were synthesized by metathesis or direct protonation reactions

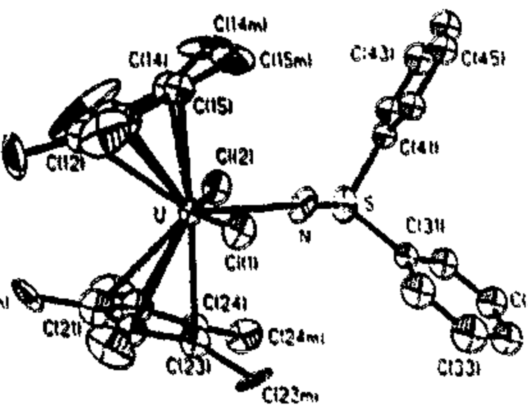

Fig. 46. Molecular structure of $Cp^*_2UCl_2(HNSPh_2)$.

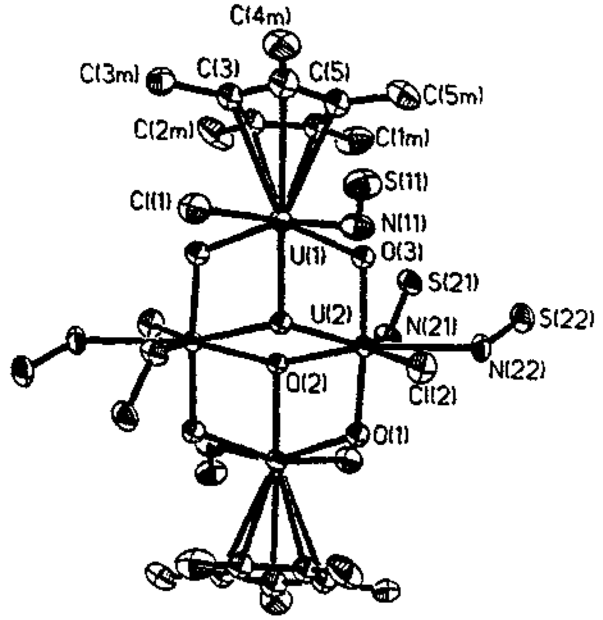

Fig. 47. Molecular structure of $[Cp(Cl)(HNSPh_2)U(\mu_3\text{-}O)(\mu_2\text{-}O)_2U(Cl)(HNSPh_2)_2]_2$ (Ph groups are removed for clarity). Selected bond distances (Å): U(1)-C(C_5Me_5) range from 2.753(15) to 2.851(13); U(1)-O(3), 2.302(12); U(1)-O(1A), 2.265(11); U(1)-O(2A), 2.192(13); U(2)-O(2), 2.358(10); U(2)-O(2A), 2.296(11); U(2)-O(1), 1.964(14); U(2)-O(3), 1.977(13); U(1)-Cl(1), 2.746(7); U(2)-Cl(2), 2.803(5); U(1)-N(11), 2.465(13); U(2)-N(21), 2.515(14); U(2)-N(22), 2.563(16).

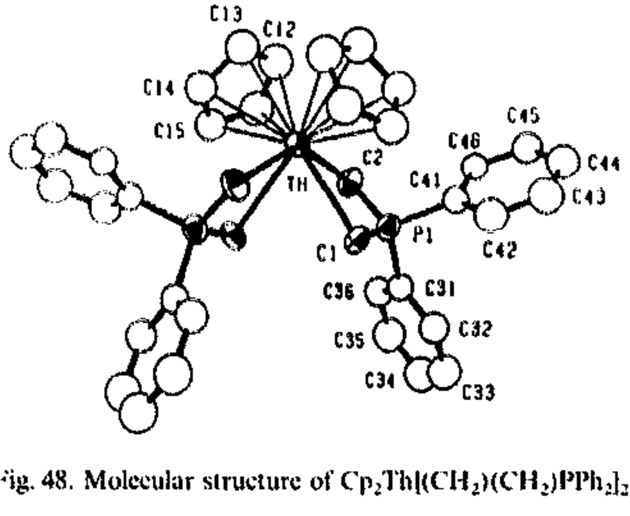

Fig. 48. Molecular structure of $Cp_2Th[(CH_2)(CH_2)PPh_2]_2$.

(Scheme 28). Obtained from Cp^*_2UMeCl and lithium anilide in the presence of teramethylethylenediamine (TMED), the complex $[Li(TMED)][Cp^*_2U(NC_6H_5)Cl]$ has been characterized by X-ray diffraction. The complex has a typical "bent metallocene" structure with an average U-CCp* distance of 2.77(2) Å and a Cp*(cent.)-U-Cp*(cent.) angle of 132.4°. The U-Cl and U-N(NC_6H_5) bond lengths are 2.690(5) and 2.051(14) Å, respectively. The complex $Cp^*_2U(N\text{-}2,4,6\text{-}tBu_3C_6H_2)$ prepared by protonation of $Cp^*_2UMe_2$ with $H_2N\text{-}2,4,6\text{-}tBu_3C_6H_2$ was also structurally characterized. The structure is presented in Fig. 49. The most interesting feature of the molecule is the very short U-N bond

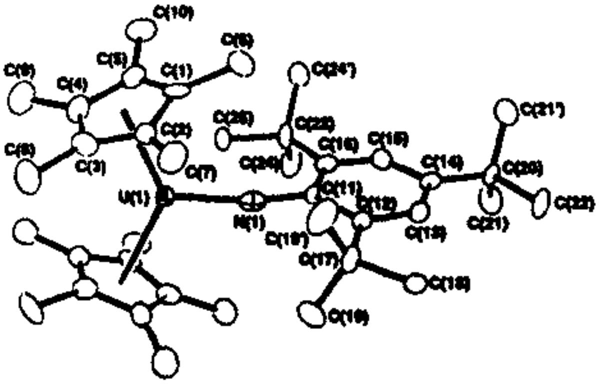

Fig. 49. Molecular structure of $Cp^*_2U(N\text{-}2,4,6\text{-}tBu_3C_6H_2)$.

length of 1.952(12) Å. The average U–C(Cp*) and U–Cp*(cent.) distances are 2.790(12) and 2.515 Å, respectively. Organometallic complexes of uranium(VI) with organoimido and oxo functional groups of the type $Cp^*_2U(=NR)(=E)$ (E=NR or O) have been prepared by two-electron oxidative atom transfer using organic azides, amine N-oxides or nitrous oxide. Another way of synthesizing these compounds is the reductive cleavage of 1,2-disubstituted hydrazines (Scheme 29).

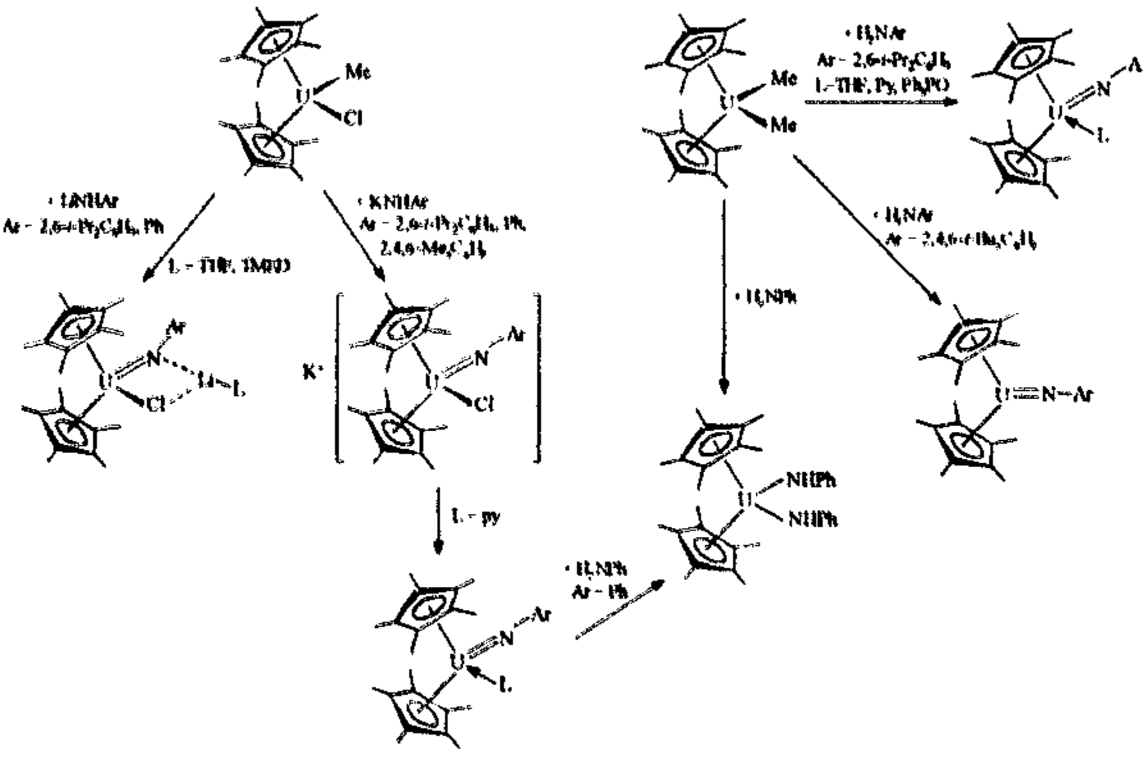

Scheme 28.

M.F. Lappert et al. [107] reported the synthesis, spectroscopic properties and crystal structures of $[ML_2Cl_2]$ [M=Th or U; L=η-$C_5H_3(SiMe_3)_2$-1,3] and $[UL_2X_2]$ (X=Br, I or BH_4). The synthetic routes are summarized in Scheme 30. According to X-ray diffraction studies the complexes $[M\{C_5H_3(SiMe_3)_2\text{-}1,3\}_2Cl_2]$

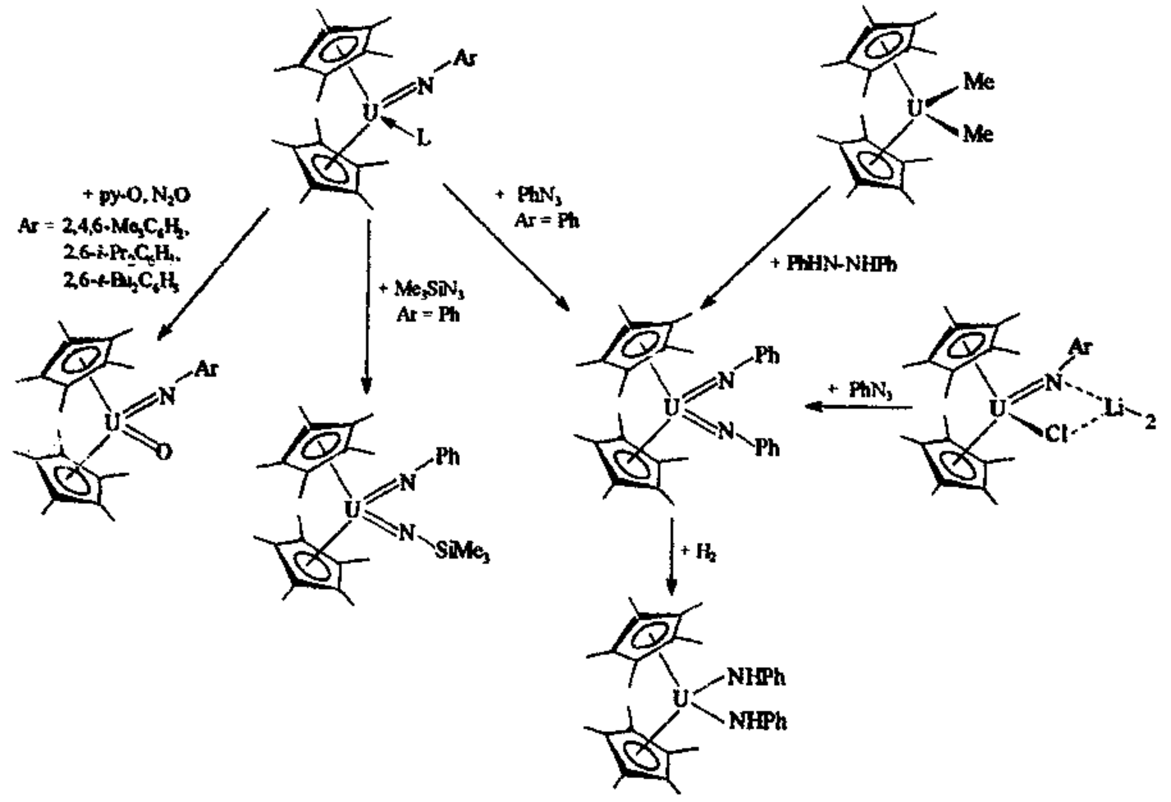

Scheme 29.

(M = U or Th) and [U{$C_5H_3(SiMe_3)_2$-1,3}$_2X_2$] (X = Br or BH_4) are monomeric, isostructural (space group C2/c) and have typical sandwich bis(cyclopentadienyl)actinoid(IV) halide structures. The iodo complex [U{$C_5H_3(SiMe_3)_2$-1,3}$_2I_2$] is also monomeric but crystallizes in the space group $P2_12_12_1$ and has non-equivalent η-$C_5H_3(SiMe_3)_2$-1,3 and iodide ligands (Fig. 50). In the complex the average U–Cp distance is 2.71(2) Å and the U–I bond lengths are 2.953(2) and 2.954(2) Å. ^1H and ^{11}B NMR investigations of

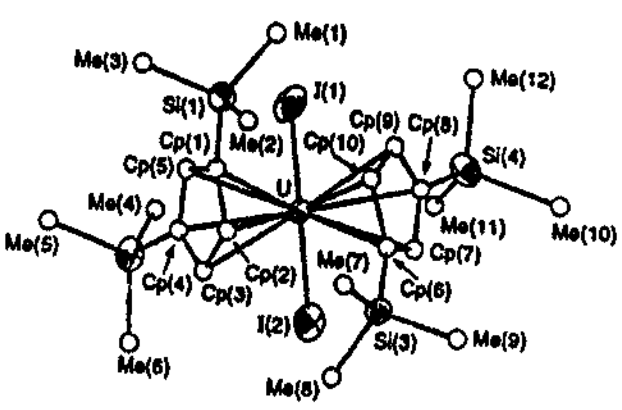

Fig. 50. Molecular structure of [U{$C_5H_3(SiMe_3)_2$-1,3}$_2I_2$].

$[\mathrm{M\{C_5H_3(SiMe_3)_2\text{-}1,3\}_2(BH_4)_2}]$ complexes revealed fluxional processes for the compounds in solution.

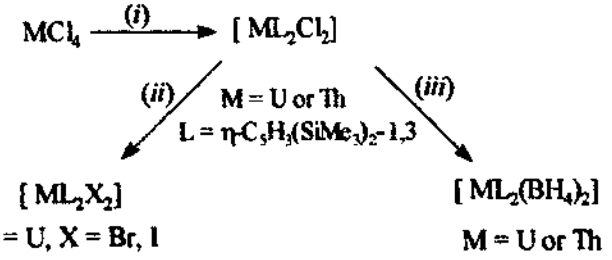

Scheme 30. (i) 2 LiL, THF (OEt$_2$ for Th), ca. 20 °C, ca. 15 h; (ii) BX$_3$ (X = Br or I), n-C$_6$H$_{14}$, ca. 20 °C, ca. 3 h; (iii) excess of NaBH$_4$, OEt$_2$–THF, ca. 20 °C, 12 h.

M.F. Lappert et al. [96] published the synthesis and characterization of seven new bis(cyclopentadienyl)thorium(IV) compounds, $[\mathrm{ThCp'''_2Cl_2(OEt_2)}]$, $[\mathrm{ThCp'''_2Cl_2}]$, $[\mathrm{ThCp^*_2Br_2(THF)}]$, $[\mathrm{ThCp^{\ddagger}_2Cl_2}]$, $[\mathrm{ThCp^{\ddagger}_2Cl_2(dmpe)}]$, $[\mathrm{ThCp^{\ddagger}_2(Cl)\{CH(SiMe_3)_2\}}]$ and $[\mathrm{ThCp^{\ddagger}_2(acac)Cl}]$ ($\mathrm{Cp'''} = \eta\text{-}\mathrm{C_5H_2(SiMe_3)_3\text{-}1,2,4}$; $\mathrm{Cp^*} = \eta\text{-}\mathrm{C_5Me_5}$; $\mathrm{Cp^{\ddagger}_2} = \eta - \mathrm{C_5H_3(SiMe_2Bu^t)_2} - 1,3$; pmdeta = $\mathrm{MeN(CH_2CH_2NMe_2)_2}$, dmpe = $\mathrm{(Me_2PCH_2)_2}$ and acacH = $\mathrm{MeCOCH_2COMe}$). The complexes $[\mathrm{ThCp'''_2Cl_2(OEt)_2}]$ and $[\mathrm{ThCp'''_2Cl_2}]$ were obtained by reaction of $\mathrm{ThCl_4}$ and $\mathrm{LiCp'''}$ in $\mathrm{Et_2O}$ followed by sublimation of the evaporated reaction mixture in vacuo. $[\mathrm{ThCp^*_2Br_2(THF)}]$ was synthesized by reaction of $[\mathrm{Th(\eta\text{-}C_5H_3(SiMe_3)_2\text{-}1,3)_2Cl_2}]$ with LiCp* and subsequent treatment of the product with $\mathrm{BBr_3}$. The organothorium bromide was characterized by X-ray diffraction. The structure has a distorted edge-capped tetrahedral geometry (Fig. 51). The thorium atom is five coordinated by two Cp*-rings, two bromides and one oxygen of the solvating THF molecule. The Th Cp*(cent.) and Th Br distances are 2.535 and 2.895(2) Å, respectively. Thorium

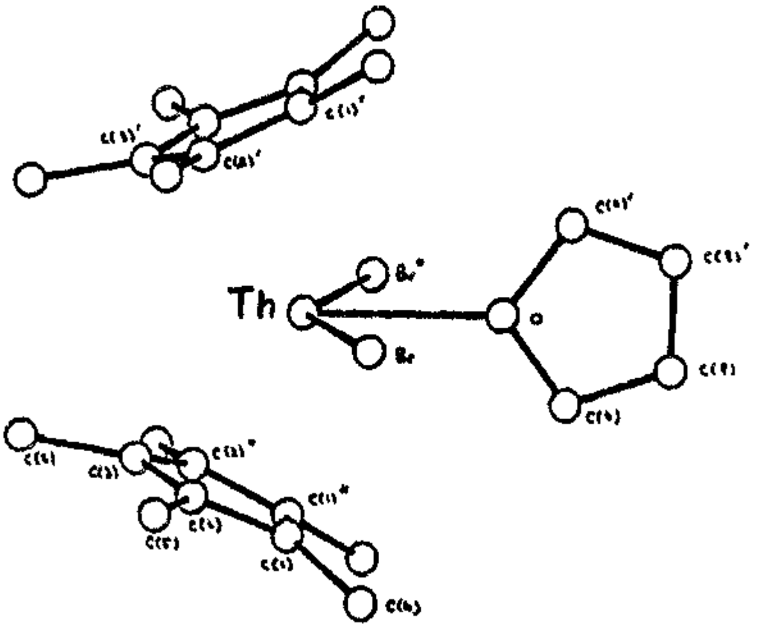

Fig. 51. Molecular structure of $[\mathrm{Cp^*_2ThBr_2(THF)}]$.

complexes with the η-$C_5H_3(SiMe_2Bu^t)_2$-1,3 ligand were prepared according to Scheme 31. The compounds [$ThCp_2^{tt}Cl_2$(dmpe)] (disordered) and [$ThCp_2^{tt}$(Cl){$CH(SiMe_3)_2$}] were studied by X-ray diffraction crystallography. In the crystal structure of [$ThCp_2^{tt}$(Cl){$CH(SiMe_3)_2$}] the thorium has a distorted tetrahedral environment formed by two Cp^{tt} ring centroids, the carbon atom of the $CH(SiMe_3)_2$ ligand and one chloride ligand. The Th–Cp^{tt}(cent.) distances are 2.53 and 2.52 Å and the angle Cp^{tt}(cent.)–Th–Cp^{tt}(cent.) is 126.7°. The Th–Cl and Th–C($CH(SiMe_3)_2$) bond lengths are 2.607(6) and 2.55(2) Å, respectively.

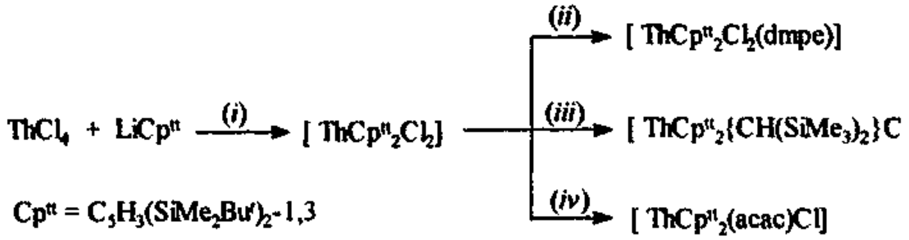

Scheme 31. (i) 2 $LiCp^{tt}$, OEt_2, 48 h, ca. 25 °C; (ii) dmpe, PhMe, 5 h, 70–80 °C; (iii) Li{$CH(SiMe_3)_2$}, OEt_2, 48 h, ca. 25 °C; (iv) Na(acac), OEt_2, 48 h, ca. 25 °C.

D. Baudry et al. [98] reported the synthesis and ^1H and ^{11}B NMR study of the bis(cyclopentadienyl)uranium borohydrides $Cp_2^*U(BH_4)_2$ ($Cp^*=C_5Me_5$; C_5Me_4H; $C_5Me_4PPh_2$; C_5H_5, $C_5H_4PPh_2$; $C_5Me_4PPh_2(BH_3)$; $C_5H_4PPh_2(BH_3)$). A correlation between the electronic density around the uranium and the chemical shifts of the nuclei was investigated.

M.S. Gill and V.S. Sagoria [99] synthesized and characterized by elemental analysis, IR, ^{19}F NMR and MS spectroscopy a bis(cyclopentadienyl) uranium(IV) complex with a fluorinated diketonate ligand, [$Cp_2U(C_4H_3SCOCHCOCF_3)_2$].

M. Ephritikhine et al. [101] prepared and characterized by X-ray diffraction the bis(cyclopentadienyl) uranium(V) complex [$Cp_2^*U(NEt_2)_2$][BPh_4]. The compound was obtained by oxidation of the neutral tetravalent precursor [$Cp_2^*U(NEt_2)_2$] by $AgBPh_4$ in THF. The crystal structure of [$Cp_2^*U(NEt_2)_2$][BPh_4] consists of discrete cation–anion pairs. The cation [$Cp_2^*U(NEt_2)_2$]$^+$ has the pseudo-tetrahedral geometry. The uranium atom is coordinated by two Cp* rings and two nitrogen atoms of the NEt_2 ligands. The average U–C distance is 2.76(2) Å and the two U–N bond lengths are 2.167(9) and 2.162(9) Å.

The same authors [102] also reported the synthesis of the cationic uranium(IV) bis(cyclopentadienyl) complexes [$Cp_2^*U(NEt_2)$(THF)][BPh_4] (R = H or Me) and [$Cp_2^*U(NMe_2)$(THF)][BPh_4] by protonolysis of the correspondent neutral amido precursors [$Cp_2^*U(NR'_2)_2$] (R′ = Me or Et) with $NHEt_3BPh_4$. The compounds have been characterized by elemental analysis and ^1H NMR spectroscopy.

N.S. Radu et al. [108] published synthesis of metaloxyketene thorium complexes via "double insertion" of carbon monoxide into thorium–silicon bonds (Scheme 32). The structure of $Cp_2^*Th(Cl)[OC(=C=O)Si(SiMe_3)_3]$ has been studied by X-ray diffraction. In the structure the ketene unit is oriented roughly in the plane bisecting the Cp* rings (Fig. 52). The Th–Cl and Th–O bond distances are 2.651(5) and 2.15(1) Å, respectively.

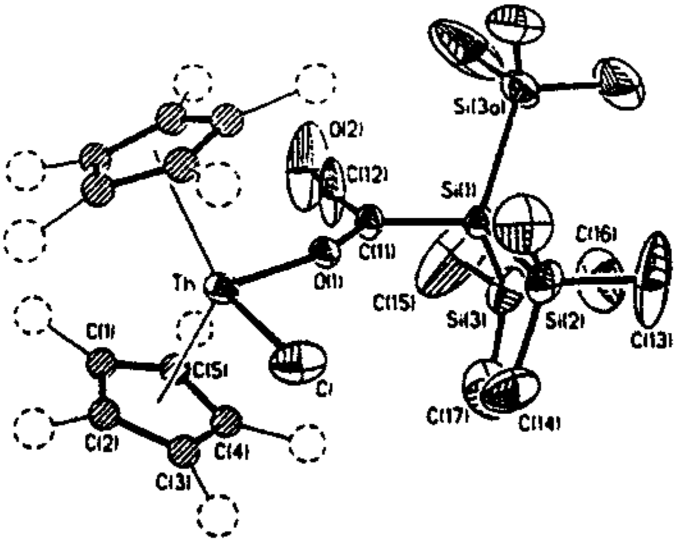

Fig. 52. Molecular structure of $Cp^*_2Th(Cl)[OC(=C=O)Si(SiMe_3)_3]$.

P. Scott and P.B. Hitchcock [109] reported the synthesis, structure and electrochemistry of the first fulvalene actinide complex $[(Me_4Fv)_2FeThCl_2]$ (Me_4Fv = 1,2,3,4-tetramethylfulvalene). The compound was obtained by reaction of dilithio[1,1′-bis(tetramethylcyclopentadienyl)ferrocene] with $ThCl_4$ in THF (Scheme 33). According to X-ray diffraction the complex consists of two tetramethylfulvalene fragments bridging the Fe and $ThCl_2$ centers (Fig. 53). The average Th–C(Cp) and Th–Cl bond distances are 2.79 and 2.63 Å, respectively. An electrochemical study revealed a quasi-reversible couple at −0.15 V vs an internal standard of ferrocene.

3.2.3. Tris(cyclopentadienyl) complexes

J. Parry et al. [110] published the synthesis and crystal structure of the uranium carbonyl adduct $(C_5Me_4H)_3U(CO)$. The compound was prepared by reaction of the uranium(III) complex $(C_5Me_4H)_3U$ with CO at ca. 1 atm at room temperature. In the structure of $(C_5Me_4H)_3U(CO)$ the carbonyl ligand is bound through the carbon atom to the uranium center (Fig. 54). The three U–Cp(cent.) distances are 2.528, 2.535 and 2.531 Å. The U–C(CO) bond length is 2.383(6) Å.

$$(C_5Me_4H)_3U + CO \rightarrow (C_5Me_4H)_3U(CO)$$

R.A. Andersen et al. [111] reported reactions of a compound containing a uranium(IV) tertiary alkyl bond. The tertiary alkyl complex $(MeC_5H_4)_3U(t\text{-}Bu)$ was prepared by reaction of $(MeC_5H_4)_3UX$ (X = Cl, MeC_5H_4) with t-BuLi in toluene. Treatment of $(MeC_5H_4)_3U(t\text{-}Bu)$ with Lewis bases (L = PMe_3, THF, t-BuCN, t-BuNC, EtNC) led to the reduced uranium(III) base derivatives $(MeC_5H_4)_3U(L)$. $(MeC_5H_4)_3U(t\text{-}Bu)$ reacted with CO under 1 atm to give the uranium(IV) acyl complex $(MeC_5H_4)_3U[C(O)\text{-}t\text{-}Bu]$. The complex $(MeC_5H_4)_3U(t\text{-}Bu)$ also reacted slowly with ethylene (210 psi) to form the ethylene monoinsertion product $(MeC_5H_4)_3U(CH_2CH_2\text{-}t\text{-}Bu)$. Treatment of various thorium

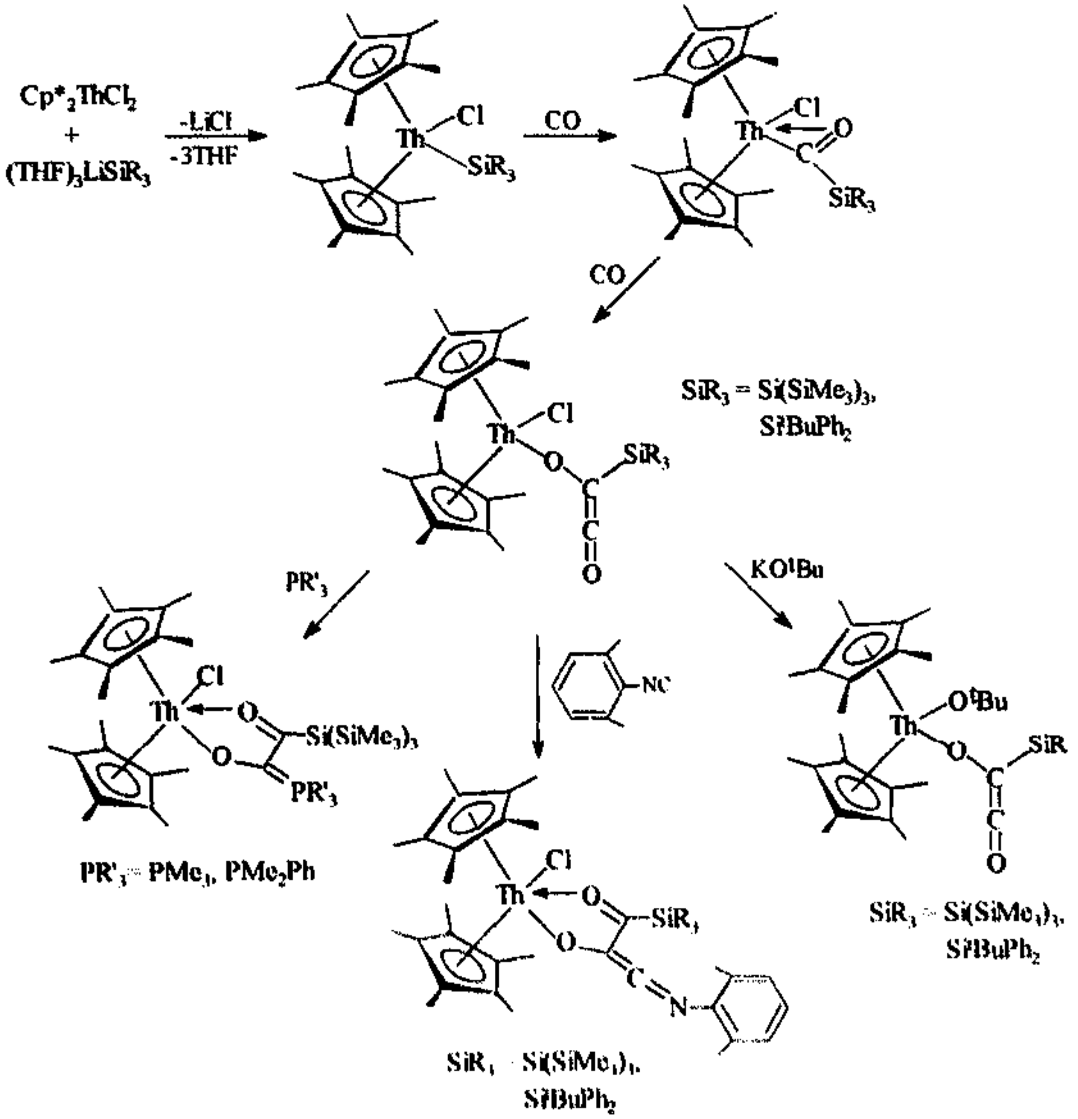

Scheme 32.

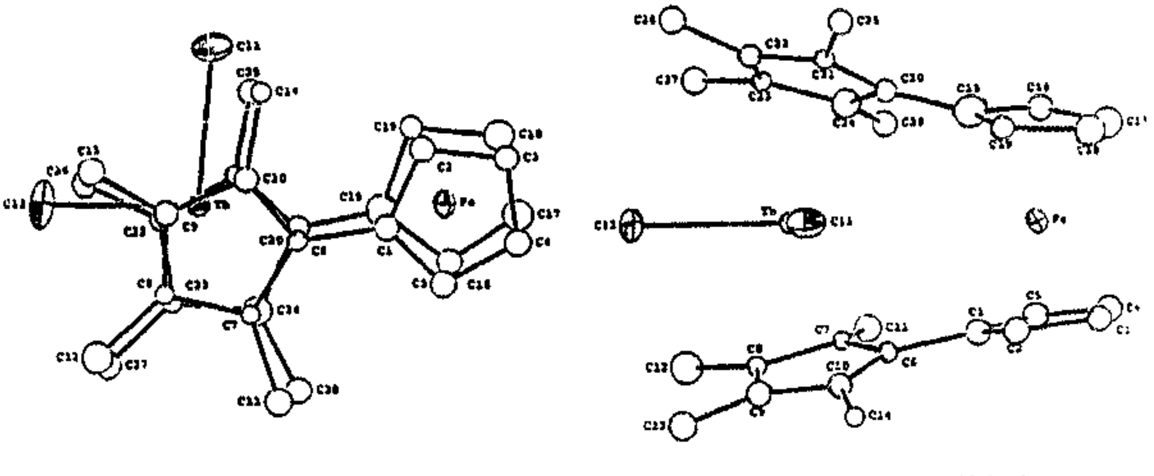

Fig. 53. Molecular structure of [(Me$_4$Fv)$_2$FeThCl$_2$] (Me$_4$Fv = 1,2,3,4-tetramethylfulvalene).

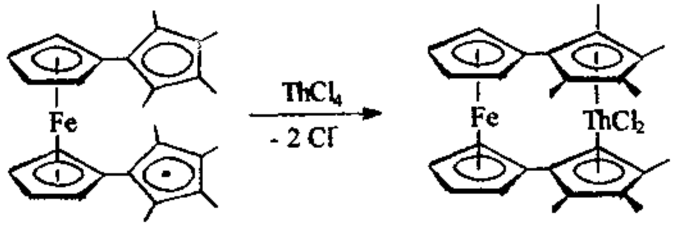

Scheme 33.

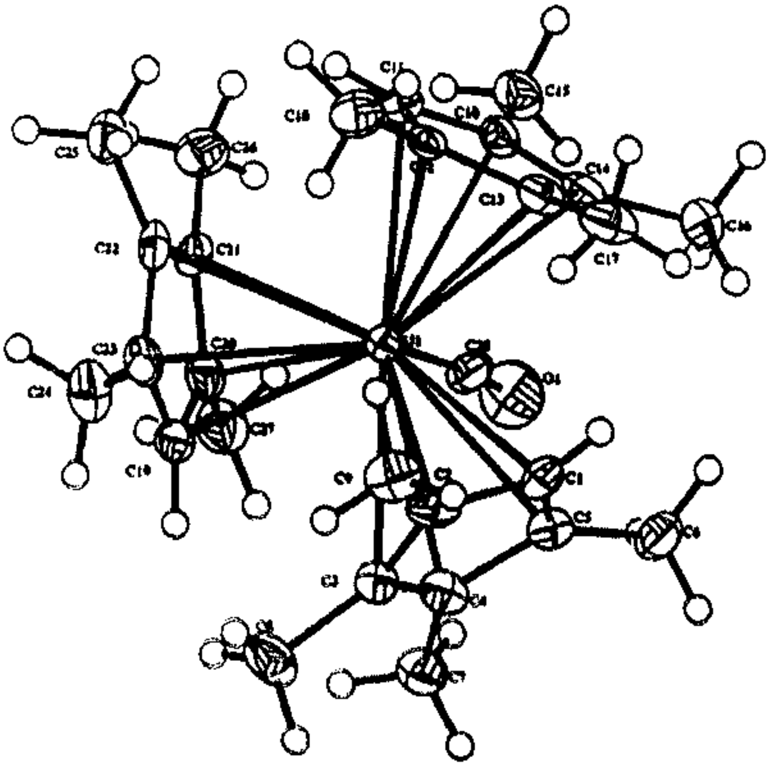

Fig. 54. Molecular structure of $(C_5Me_4H)_3U(CO)$.

complexes of the type $(MeC_5H_4)_3ThX$ (X = Cl, I, MeC_5H_4, O-2,6-$Me_2C_6H_3$) with *t*-BuLi in toluene led to intractable products only. However, the ionic complexes $[(RC_5H_4)_3Th][BPh_4]$ (R = Me_3Si, *t*-Bu) reacted with *t*-BuLi to give the thorium hydrides $(RC_5H_4)_3ThH$.

$$MeC_5H_4)_3UX + t-BuLi \xrightarrow{\text{toluene}} (MeC_5H_4)_3U(t-Bu) + LiX$$

$$X = Cl,\ MeC_5H_4$$

$$(MeC_5H_4)_3U(t-Bu) + L \xrightarrow{\text{toluene}} (MeC_5H_4)_3U(L)$$

$$L = PMe_3,\ THF,\ t-BuCN,\ t-BuNC,\ EtNC$$

$$(MeC_5H_4)_3U(t-Bu) + CO \xrightarrow{\text{toluene}} (MeC_5H_4)_3U(C(O)-t-Bu)$$

$$(\mathrm{MeC_5H_4})_3\mathrm{U}(t-\mathrm{Bu})+\mathrm{H_2C{=}CH_2}\xrightarrow{\text{toluene}}(\mathrm{MeC_5H_4})_3\mathrm{U}(\mathrm{CH_2CH_2}-t-\mathrm{Bu})$$

D. Baudry et al. [98] synthesized and characterized by ^{1}H and ^{11}B NMR a number of tris(cyclopentadienyl)uranium borohydrides Cp'_3UBH_4 ($Cp'=C_5Me_5$; C_5Me_4H; $C_5Me_4PPh_2$; C_5H_5, $C_5H_4PPh_2$; $C_5Me_4PPh_2(BH_3)$; $C_5H_4PPh_2(BH_3)$)). The authors established a correlation between the electronic density around uranium and the chemical shifts of the nuclei directly bound to the paramagnetic uranium center.

M.S. Gill and V.S. Sagoria [99] reported the synthesis of tris(cyclopentadienyl)uranium(IV) complexes with fluorinated ligands $Cp_3U(L)$ ($L=CF_3COCHCOCF_3^-$, $CH_3COCHCOCF_3^-$, $C_4H_3SCOCHCOCF_3^-$. The compounds were characterized by elemental analysis, IR, ^{19}F NMR and MS spectroscopy.

M. Ephritikhine et al. [102] prepared the cationic uranium(IV) tris(cyclopentadienyl) complex $[Cp_3U(THF)][BPh_4]$ by protonolysis of the corresponding neutral amide $[Cp_3U(NEt_2)]$ with $NHEt_3BPh_4$. The complex was characterized by elemental analysis and ^{1}H NMR spectroscopy.

W.A. King and T.J. Marks [52] measured metal–silicon bond disruption enthalpies for a series of metallocene complexes including $Cp_3USi(SiMe_3)_3$. The complex was synthesized by treatment of Cp_3UCl with $LiSi(SiMe_3)_3 \cdot 3THF$ in diethyl ether. The thermodynamic data were obtained by titration calorimetry with I_2.

$$\mathrm{Cp_3USi(SiMe_3)_3+I_2\rightarrow Cp_3UI+(Me_3Si)_3SiI}$$

The resulting $D[Cp_3U–Si(SiMe_3)_3]$ value of 37(3) kcal mol^{-1} was calculated from the equation:

$$\begin{aligned}\mathrm{D[Cp_3U-Si(SiMe_3)_3]} &= D[\mathrm{Cp_3U-I}]\\ &\quad + D[\mathrm{(SiMe_3)_3Si-I}] + \Delta H_{\mathrm{rxn}} - D[\mathrm{I-I}]\\ &\quad (\text{where } \Delta H_{\mathrm{rxn}} = -58(1)\ \mathrm{kcal\ mol^{-1}})\end{aligned}$$

3.2.4. *Mixed cyclopentadienyl-cyclooctatetraenyl and cyclooctatetraenyl complexes*

M. Ephritikhine et al. [101] prepared the cationic (cyclooctatetraenyl)uranium(V) complex $[U(\eta\text{-}C_8H_8)(NEt_2)_2(THF)][BPh_4]$ by oxidation of the neutral tetravalent precursor $[U(\eta\text{-}C_8H_8)(NEt_2)_2]$ with one equivalent of $AgBPh_4$ in THF. Treatment of $[U(\eta\text{-}C_8H_8)(NEt_2)_2]$ with $Tl(\eta\text{-}C_5H_5)$ gave the mixed neutral cyclopentadienyl-cyclooctatetraenyl uranium complex $[U(\eta\text{-}C_8H_8)(\eta\text{-}C_5H_5)(NEt_2)_2]$. The isolated compounds were characterized by elemental analyses and ^{1}H NMR spectroscopy.

The same authors [102] also reported the synthesis of the cationic uranium (IV) cyclooctatetraenyl and cyclopentadienyl-cyclooctatetraenyl complexes $[U(\eta\text{-}C_8H_8)(NEt_2)(THF)_2][BPh_4]$ and $[U(\eta\text{-}C_5H_5)(\eta\text{-}C_8H_8)(THF)_2][BPh_4]$ (R = H, Me). The compounds were obtained by protonolysis of the corresponding neutral amide precursors with $NHEt_3BPh_4$ (Scheme 34). The complex $[Cp^*U(\eta\text{-}C_8H_8)(THF)_2][BPh_4]$ was characterized by single-crystal X-ray diffraction. The structure consists of discrete cation–anion pairs. In the cation

$[Cp^*U(\eta-C_8H_8)(THF)_2]^+$ (Fig. 55) the uranium atom has a pseudo-tetrahedral coordination environment. The average U–C(Cp*) and U–C(C_8H_8) distances are 2.74(1) and 2.65(2) Å respectively, and the angle $(Cp^*)_{cent}$–U–$(C_8H_8)_{cent}$ is 139.6(5)°.

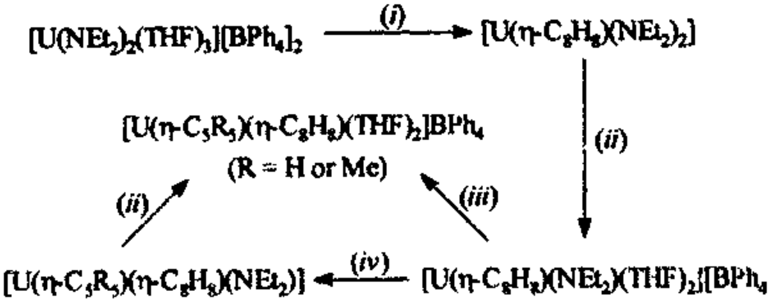

Scheme 34. (i) $K_2(C_8H_8)$; (ii) $NHEt_3BPh_4$; (iii) cyclopentadiene; (iv) $K(C_5H_5)$ or KC_5Me_5. All reactions in THF.

A. Streitwieser et al. [112] prepared and investigated by ^1H NMR 1,1′-dimesityluranocene (Fig. 56). The compound was synthesized by reaction of UCl_4 with the potassium salt of the mesityl-cyclooctatetraene dianion in THF. The ^1H NMR

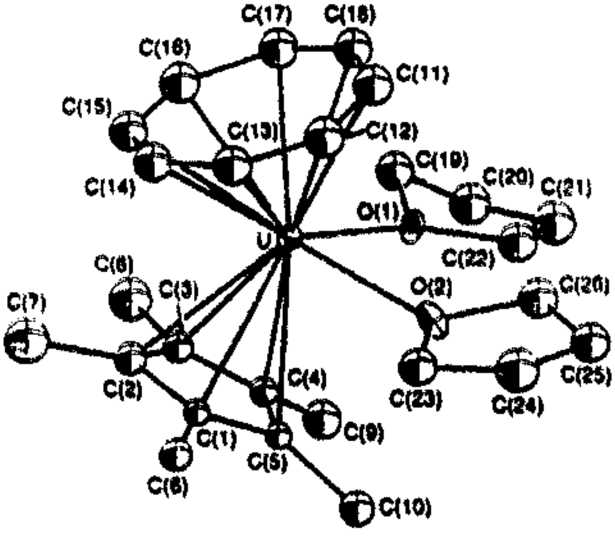

Fig. 55. Structure of $[Cp^*U(\eta-C_8H_8)(THF)_2]^+$ cation.

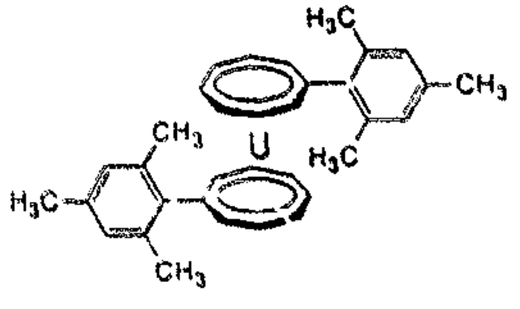

Fig. 56. Structure formula of 1,1′-dimesityluranocene.

spectrum revealed that the mesityl groups are in a locked position with *exo*- and *endo*-*ortho*-methyl groups. The two mesityl rings were found to be held close to each other, presumably by van der Waals attraction.

M. Dolg et al. [68] calculated large-scale state-average multi-configuration self-consistent field, configuration interaction, averaged coupled-pair functional and spin–orbit configuration interaction calculations for thorocene, $Th(C_8H_8)_2$. It was found that thorocene has a $^1A_{1g}(A_{1g})$ ground state and single-determinant wavefunction may be pictured as a Th(IV) compound with $5f^0\pi_{e2u}^4$ configuration. The calculated Th–C_8H_8(ring) distance of 2.03 Å was in good agreement with the experimental value of 2.00 Å.

3.3. Organoactinide catalysis

M.S. Eisen et al. [113] reported the organoactinide-catalyzed oligomerization of terminal acetylenes. Reaction of $Cp^*_2AcMe_2$ ($Cp^* = C_5Me_5$; Ac = U, Th) with excess of *tert*-butylacetylene led mainly to the head-to-tail dimer 2,4-di-*tert*-butyl-1-butene-3-yne and to traces of the head-to-head dimer (*E*)-1,4-di-*tert*-butyl-1-butene-3-yne (Scheme 35). The analogous reaction with excess of $HC{\equiv}CSiMe_3$ yielded small amounts (<5%) of the head-to-tail dimer 2,4-bis(trimethylsilyl)-1-butene-3-yne and large amounts (90–95%) of the head-to-tail-to-head trimer (*E*)-1,4,6-tris(trimethylsilyl)-1,3-hexadiene-5-yne (Scheme 35). The plausible reaction mechanism was discussed.

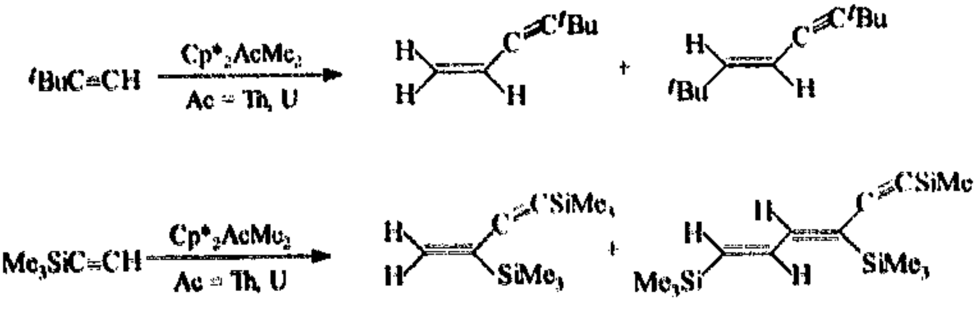

Scheme 35.

Acknowledgements

We thank the Alexander von Humboldt Foundation for providing a fellowship to Yu.K. Gun'ko.

References

[1] H. Schumann, J.A. Meese-Marktscheffel, L. Esser, Synthesis, structure, and reactivity of organometallic π-complexes of the rare earths in the oxidation state Ln^{3+} with aromatic ligands, Chem. Rev. 95 (1995) 865.

[2] W.J. Evans, Beyond bis(pentamethylcyclopentadienyl) coordination environments: An approach to alternative ancillary ligand sets in organometallic lanthanide chemistry, New J. Chem. 19 (1995) 525–533.

[3] F.T. Edelmann, Rare earth cyclooctatetraenyl complexes. Organolanthanide chemistry in three oxidation states, New J. Chem. 19 (1995) 535–550.

[4] J.R. van den Hende, P.B. Hitchcock, S.A. Holmes, M.F. Lappert, S. Tian, Synthesis and characterization of ytterbium(II) alkyls, J. Chem. Soc., Dalton Trans. 23 (1995) 3933–3939.

[5] W.J. Evans, J.L. Shreeve, R.N.R. Broomhall-Dillard, J.W. Ziller, Isolation and structure of a homoleptic yttrium trimethylsilylmethyl complex, J. Organomet. Chem. 501 (1995) 7–11.

[6] M. Westerhausen, M. Hartmann, A. Pfitzner, W. Schwarz, Bis(trimethylsilyl)amide und – methanide des Yttriums – Molekülstrukturen von Tris(diethylether-O)lithium-(μ- chloro)tris[bis(trimethylsilyl)methyl]yttriat, solvensfreiem Yttrium-tris[bis(trimethylsilyl)amid] sowie dem bis(benzonitril)-komplex, Z. Anorg. Allg. Chem. 621 (1995) 837–850.

[7] L. Lee, D.J. Berg, G.W. Bushnell, Synthesis, X-ray crystal structure, and thermal stability of Y[DAC][$CH_2(SiMe_3)$] (DAC = deprotonated 4,13-Diaza-18-crown-6), Organometallics 14 (1995) 8–10.

[8] M.C. Holthausen, C. Heinemann, H.H. Cornehl, W. Koch, H. Schwarz, The performance of density-functional/Hartree–Fock hybrid methods: cationic transition-metal methyl complexes MCH_3^+ (M = Sc–Cu, La, Hf–Au), J. Chem. Phys. 102 (1995) 4931–4941.

[9] W. Kretschmer, K.-H. Thiele, Beiträge zur Organolanthanidchemie. III Darstellung und Eigenschaften von 1,4-Diaryl-1,3-butadien-komplexen der Lanthanide, Z. Anorg. Allg. Chem. 621 (1995) 1304–1310.

[10] P. Biagini, G. Lugli, L. Abis, R. Millini, Alkylation of lanthanide(η^6-arene)-tetrahalogenoaluminates: Synthesis and catalytic activity of Ln(η^6-arene)(AlX_3R)$_3$ derivatives. Molecular structure of Nd(η^6-C_6H_5Me)($AlCl_3Me$)$_3$, New J. Chem. 19 (1995) 713–722.

[11] K.B. Shelimov, D.E. Clemmer, M.F. Jarrold, Structures and isomerization of LaC_n^+ clusters, J. Phys. Chem. 99 (1995) 11 376–11 386.

[12] K.B. Shelimov, D.E. Clemmer, M.F. Jarrold, Drift tube studies of metallofullerenes, Proc. Electrochem. Soc. 95-10 (1995) 1437–47, Chem. Abstr. 124: 161311.

[13] K.B. Shelimov, M.F. Jarrold, Networked and endohedral $La_2C_n^+$ ($n = 28$–100) metallofullerenes, J. Am. Chem. Soc. 117 (1995) 6404–6405.

[14] M. Liu, J.M. Cowley, Encapsulation of metal carbides in carbon nanotubes and nanoparticles, Proc.-Electrochem. Soc. 95-10 (1995) 621–635

[15] L. Mingoqui, J.M. Cowley, Encapsulation of lanthanum carbide in carbon nanotubes and carbon nanoparticles, Carbon 33 (1995) 225–232.

[16] H. Funasaka, K. Sugiyama, K. Yamamoto, T. Takahashi, Synthesis of lanthanum compounds encapsulated within carbon nanoparticles, Chem. Phys. Lett. 236 (3) (1995) 277–284.

[17] M. Ata, A.J. Hudson, K. Yamaura, K. Kurihara, Carbon nanotubes filled with gadolinium and hafnium carbides, Jpn. J. Appl. Phys. 34 (1995) 4207–4212.

[18] S.J. Swamy, H. Schumann, Synthesis and characterization of 9-pentamethylcyclopentadienyl-9-lanthanoidfluorenes, Indian J. Chem. 34A (1995) 396–397.

[19] M.N. Bochkarev, A.V. Protchenko, L.N. Zakharov, G.K. Fukin, Y.T. Struchkov, Reactions of cyclopentadienyl-naphthalene complexes of lutetium with C- and N-unsaturated compounds: molecular and crystal structure of [CpLu(DME)]$_2$[1,1-μ-4,4-μ-(Ph)C–(Ph)C=C(Ph)–C(Ph)], J. Organomet. Chem. 501 (1995) 123–128.

[20] W. Kretschmer, K.-H. Thiele, Beiträge zur Organolanthanidchemie. II. Cyclopentadienyllanthanid-1,3-butadien-komplexe – Darstellung, Eigenschaften und Reaktionen, Z. Anorg. Allg. Chem. 621 (1995) 1093–1097.

[21] X. Zhou, H. Ma, Z. Wu, X. You, Z. Xu, X. Huang, Synthesis and structure of a new organolanthanide oxide complex, $(CH_3C_5H_4)_5Yb_4(\mu\text{-}Cl)_6(\mu_3\text{-}Cl)(\mu_4\text{-}O)(THF)_3$, J. Organomet. Chem. 503 (1995) 11–13.

[22] M.-R. Spirlet, J. Goffart, Dicyclopentadienyl complexes of ytterbium(III). The crystal structure of [Yb(η^5-$C_5H_4SiMe_3$)$_2$(μ-Cl)]$_2$, J. Organomet. Chem. 493 (1995) 149–151.

[23] X. Zhou, H. Ma, G. Wei, Z. Jin, Z. Wu, Z. Xu, X. You, Thermolytic reactivity of Cp_2HoCl and X-ray structure of the thermolysis product $[(C_5H_3CH{=}CHCH_2C{=}CHC_5H_4)_2Ho_2Cl_2]_\infty$, Chin. Sci. Bull. 40 (1995) 552–556.

[24] H. Schumann, M. Glanz, H. Hemling, F.E. Hahn, Metallorganische Verbindungen der Lanthanoide, 93. Tetramethylcyclopentadienyl-Komplexe ausgewählter 4f-Elemente, Z. Anorg. Allg. Chem. 621 (1995) 341–345.

[25] H. Schumann, E.C.E. Rosenthal, G. Kociok-Koehn, G.A. Molander, J. Winterfeld, Organometallic compounds of the lanthanides. XCVII. Synthesis and crystal structures of monomeric bis(ethyltetramethylcyclopentadienyl) amide and alkyl derivatives of the lanthanides, J. Organomet. Chem. 496 (1995) 233–240.

[26] H. Schumann, M. Glanz, H. Hemling, Organometallic compound of the lanthanides, 94. Bis(ethyltetramethylcyclopentadienyl) complexes of samarium(II) and ytterbium(II), New J. Chem. 19 (1995) 491–494.

[27] M.G. Silva-Valenzuela, L.B. Zinner, A. Domingos, N. Marques, A. Pires de Matos, Synthesis and characterization of a tetramethylurea adduct of a biscyclopentadienyl ytterbium(II) complex: X-ray crystal structure of $YbCp_2 \cdot 2TMU$, J. Alloys Compd. 225 (1995) 331–333.

[28] D.J. Schwartz, R.A. Andersen, Solution-state interactions of bis(pentamethylcyclopentadienyl)ytterbium, Cp^*_2Yb, with trialkylphosphines and R_3PX complexes ($X = O$, NR', CHR''), Organometallics 14 (1995) 4308–4318.

[29] D.J. Schwartz, G.E. Ball, R.A. Andersen, Interactions of *cis*-P_2PtX_2 complexes ($X = H$, CH_3) with bis(pentamethylcyclopentadienyl)ytterbium, J. Am. Chem. Soc. 117 (1995) 6027–6040.

[30] K.-H. Thiele, R. Seifert, Zur Bildung von Vinylverbindungen des Lanthans und Lutetiums, Z. Anorg. Allg. Chem. 621 (1995) 2089–2092.

[31] A. Scholz, K.-H. Thiele, J. Scholz, R. Weimann, Synthese und Charakterisierung von $Cp^*_2M(DAD)$-Komplexen ($M = Y$ oder La) Molekülstruktur von $Cp^*_2Y\{N(C_6H_4\text{-}4\text{-}Me){=}C(Ph)C(Ph){=}N(C_6H_4\text{-}4\text{-}Me)\}$, J. Organomet. Chem. 501 (1995) 195–200.

[32] K. Jacob, M. Schäfer, A. Steiner, G.M. Sheldrick, F.T. Edelmann, Neuartige Koordination eines Cyclopentadienylrings im heterotrimetallischen Organoyttrium-Komplex $Li[Cp_2Y(FcN)_2]$ (fcn = 2-dimethylaminomethylferrocenyl), J. Organomet. Chem. 487 (1995) C18–C20.

[33] F. Shen, J. Hu, M. Xie, S. Wang, X. Huang, Synthesis and structural investigation of lanthanide organometallics involving cyclopentadienyl and 2-naphthoyltrifluoroacetonato chelate ligands, J. Organomet. Chem. 485 (1995) C6–C9.

[34] G. Lin, W.-T. Wong, Synthesis and crystal structure of $[(\eta^5:\eta^1\text{-}C_5H_4PPh_2)Tl]_\infty$ and the divalent ytterbium derivative $[(\eta^5\text{-}C_5H_4PPh_2)_2Yb(DME)]$, J. Organomet. Chem. 495 (1995) 203–208.

[35] G. Lin, W.-T. Wong, Preparation and structural characterization of a functionalized trigonal organoerbium cluster with two bridging hydroxyl groups and a μ_3-oxo group, Polyhedron 14 (1995) 3167–3169.

[36] J.S. Xia, G.C. Wei, Z.S. Jin, W.Q. Chen, W.C. Xue, New synthetic route to di-η^5-cyclopentadienylytterbiumditetrahydrofuranate and its crystal structure. Report, ISTIC TR-95190; Order No. PB95-245528GAR, 8 pp. Avail. NTIS From: Gov. Rep. Announce. Index (U.S.) 1995, 95(20), Abstr. No. 20-00,724, 1995. Chem. Abstr. 124:146351.

[37] K. Takaki, T. Kusodo, S. Uebori, Y. Makioka, Y. Taniguchi, Y. Fujiwara, A facile generation of organosamarium η^3-allyl complexes by reductive cleavage of allylic ethers with $(C_5Me_5)_2Sm(THF)_n$, Tetrahedron Lett. 36 (1995) 1505–1508.

[38] Y. Makioka, K. Koyama, T. Nishiyama, K. Takaki, Generation of allenic samarium complexes from propargylic ethers and $(C_5Me_5)_2Sm(THF)_2$, and their electrophilic trapping, Tetrahedron Lett. 36 (1995) 6283–6286.

[39] W.J. Evans, M.A. Ansari, J.W. Ziller, Organosamarium tetrathiometalate chemistry: synthesis and structure of the mixed-metal complexes $\{[(C_5Me_5)_2Sm]_2Mo(\mu\text{-}S)_4\}$ and $[(C_5Me_5)_2Sm(\mu\text{-}S)_2WS_2]$, Organometallics 14 (1995) 3–4.

[40] W.J. Evans, K.J. Forrestal, J.W. Ziller, Synthesis and structure of a thermally stable, nonclassical, 7-norbornadienyl carbocation obtained from $(C_5Me_5)_3Sm$ and CO, J. Am. Chem. Soc. 117 (1995) 12635–12636.

[41] B.-J. Deelman, M. Booij, A. Meetsma, J.H. Teuben, H. Kooijman, A.L. Spek, Activation of ethers and sulfides by organolanthanide hydrides. Molecular structures of $(Cp_2^*Y)_2(\mu\text{-}OCH_2CH_2O)(THF)_2$ and $(Cp_2^*Ce)_2(\mu\text{-}O)(THF)_2$, Organometallics 14 (1995) 2306–2317.

[42] B.-J. Deelman, F. Wierda, A. Meetsma, J.H. Teuben, Reaction of $(Cp_2^*LnH)_2$ (Ln = Y, La) and $Cp_2^*Y(2\text{-}C_6H_4CH_2NMe_2)$ with esters and amides and molecular structure of $[Cp_2^*Y(\mu\text{-}OCMe{=}CHC(OEt)O)]_2$, Appl. Organomet. Chem. 9 (1995) 483–490.

[43] Y.K. Gun'ko, P.B. Hitchcock, M.F. Lappert, Activation of a C–O bond by reaction of a tris(cyclopentadienyl)lanthanide complex with an alkali metal in dimethoxyethane (DME); crystal structures of $[Nd\{\eta\text{-}C_5H_3(SiMe_3)_2\text{-}1,3\}_2(\mu\text{-}OMe)_2Li(DME)]$ and $[\{Ce(\eta\text{-}C_5H_3{}^tBu_2\text{-}1,3)_2(\mu\text{-}OMe)\}_2]$, J. Organomet. Chem. 499 (1995) 213–219.

[44] W.J. Evans, M.A. Ansari, S.I. Khan, Formation of a cyclopentadienyl arene coordination complex of potassium in the presence of THF and aryloxide ligands: synthesis and structure of $\{K[(\mu\text{-}C_5H_5)_2Nd(\mu\text{-}O\text{–}C_6H_3Me_2\text{-}2,6)_2]\}_n$, Organometallics 14 (1995) 558–560.

[45] Y.H. Lin, D.S. Zeng, Q. Shen, Binuclear lanthanide complexes containing sodium. Syntheses and crystal structure of $(C_5Me_5)_2Nd(\mu\text{-}Cl)_2Na(DME)_2$ and $(C_5Me_5)_2Nd(\mu\text{-}OCH_3)_2Na(DME)_2$. Report, ISTIC-TR-95195; Order No. PB95-245320GAR, 8 pp. Avail. NTIS From: Gov. Rep. Announce. Index (U.S.) 1995, 95(19), Abstr. No. 19-00,706, 1995. Chem. Abstr.: 124:146349.

[46] Z.-Z. Wu, Z.-E. Huang, R.-F. Cai, Synthesis, characterization and study of the thermal stability of dimeric bis(cyclopentadienyl)lanthanide furylmethoxide complexes, Synth. React. Inorg. Met.-Org. Chem. 25 (1995) 1401–1416.

[47] Z.-Z. Wu, Z.-E. Huang, R.-F. Cai, Z. Hu, X.-Z. You, X.-Y. Huang, Synthesis and characterization of dinuclear organolanthanide alkoxides, X-ray crystal structures of $[(C_5H_5)_2Yb(\mu\text{-}OCH_2CH_2CH_2CH_2CH_3)]_2$ and $[(C_5H_5)_2Yb(\mu\text{-}OCH_2CH_2CH(Me)_2)]_2$, Polyhedron 15 (1995) 13–22.

[48] Z.-Z. Wu, D.-M. Fan, Z.-E. Huang, R.-F. Cai, Synthesis and characterization of binuclear biscyclopentadienyl lanthanide acetoximate derivatives; X-ray crystal structures of $[Cp_2Gd(\mu,\eta^2\text{-}ONCMe_2)]_2$, Polyhedron 15 (1995) 127–133.

[49] G.B. Deacon, G.D. Fallon, B.M. Gatehouse, A. Rabinovich, B.W. Skelton, A.H. White, Organolanthanoids XIX. The X-ray crystal structures of di[μ-(acetato O,O: O')bis(diphenylphosphino-η^5-cyclopentadienyl)ytterbium(III)] and di[μ-(acetato O,O: O')bis(η^5-cyclopentadienyl)ytterbium(III)] – unexpected examples of formal nine coordination in lanthanoid organometallics, J. Organomet. Chem. 501 (1995) 23–30.

[50] P. Poremba, M. Noltemeyer, H.-G. Schmidt, F.T. Edelmann, Monomere Bis(η^5-cyclopentadienyl)lanthanoid(III) Komplexe mit raumerfüllenden Alkoxid- and Thiolatliganden: Molekülstruktur von $(C_5H_5)_2Yb(THF)[SC_6H_2(CF_3)_3\text{-}2,4,6]$, J. Organomet. Chem. 501 (1995) 315–319.

[51] S.A. Vinogradov, A.E. Mistrukov, I.P. Beletskaya, New organolanthanide complexes containing a σ-bonded 1,3-dithiane. Crystal structures of $[M(C_5H_4Bu^t)_2(C_4H_7S_2\text{-}1,3)]\cdot LiCl\cdot 2thf$ (M = Lu or Y; thf = tetrahydrofuran), J. Chem. Soc., Dalton Trans. (1995) 2679–2687.

[52] W.A. King, T.J. Marks, Metal-silicon bonding energetics in organo-group 4 and o organo-f-element complexes. Implications for bonding and reactivity, Inorg. Chim. Acta 229 (1995) 343–354.

[53] T.V. Timofeeva, J.-H. Lii, N.L. Allinger, Molecular mechanics explanation of the metallocene bent sandwich structure, J. Am. Chem. Soc. 117 (1995) 7452–7459.

[54] W. de Oliveira, R. Bazito, P.M. Gatti, An alternative route for preparing tricyclopentadienyl lanthanides $[LnCp_3]$, J. Braz. Chem. Soc. 6 (1995) 243–244.

[55] P.S. Tanner, D.J. Burkey, T.P. Hanusa, Cyclopentadienyl ring metathesis with bis(pentamethylcyclopentadienyl)calcium as a route to mixed ring organolanthanide complexes; the crystal structure of $(C_5Me_5)_2Nd(C_5H_5)$, Polyhedron 14 (1995) 331–333.

[56] D.C. Chadwick, R.A. Andersen, A general synthesis and crystal structure of $[(Me_3C)_2C_5H_3)_3]Ce$, J. Organomet. Chem. 501 (1995) 271–276.

[57] W.-K. Wong, J. Guan, Q. Chen, L. Zhang, Y. Lin, W.-T. Wong, Synthesis, s solution dynamics and X-ray crystal structures of neodymium-ylide complexes,$[(C_5H_4R)_3NdCH_2P(Me)Ph_2]$ (R = H, Bu^t), Polyhedron 14 (1995) 277–283.

[58] M. Shimizu, H. Fujisawa, T. Shiosaki, MOCVD of ferroelectric PLZT thin films and their properties, Microelectron. Eng. 29 (1995) 173–176.

[59] W.J. Evans, J.L. Shreeve, J.W. Ziller, Synthesis and structure of inverse cyclooctatetraenyl sandwich complexes of europium(II): $[(C_5Me_5)(THF)_2Eu]_2(\mu\text{-}C_8H_8)$ and $[(THF)_3K(\mu\text{-}C_8H_8)]_2Eu$, Polyhedron 14 (1995) 2945–2951.

[60] H. Schumann, M. Glanz, J. Winterfeld, H. Hemling, N. Kuhn, H. Bohnen, D. Bläser, R. Boese, Metallorganische Verbindungen der Lanthanoide XCVI. Ylidartige Olefinkoordination in Komplexen dreiwertiger 4f-Elemente, J. Organomet. Chem. 493 (1995) C14–18.

[61] J. Jin, X. Zhuang, Z. Jin, W. Chen, Syntheses and crystal structures of $(C_8H_8)Nd(C_5H_9C_5H_4)(THF)_2$ and $[(C_8H_8)Gd(C_5H_9C_5H_4)(THF)][(C_8H_8)Gd(C_5H_9C_5H_4)(THF)_2]$, J. Organomet. Chem. 490 (1995) C8–C13.

[62] W.J. Evans, T.S. Gummersheimer, J.W. Ziller, The reactivity of samarium(II) in a bis(indenyl) coordination environment, Appl. Organomet. Chem. 9 (1995) 437–447.

[63] Z. Ye, S. Wang, D. Kong, X. Huang, The formation and molecular structure of $[Na(THF)_6][(\eta^5\text{-}C_9H_7)_3Pr(\mu\text{-}Cl)Pr(\eta^5\text{-}C_9H_7)_3]$, J. Organomet. Chem. 491 (1995) 57–60.

[64] S. Wang, D. Kong, Z. Ye, X. Huang, Synthesis and X-ray structural investigation of triindenyl tetrahydrofuranato praseodymium, J. Organomet. Chem. 496 (1995) 37–41.

[65] H. Schumann, E.C.E. Rosenthal, J. Winterfeld, G. Kociok-Köhn, Metallorganische Verbindungen der Lanthanoide XCVIII. Synthese und Strukturaufklärung von Dichloro(-2,5-di-*tert*-butylpyrrolyl)bis(tetrahydrofuran)ytterbium(III), J. Organomet. Chem. 495 (1995) C12–C14.

[66] H.-J. Gosink, F. Nief, L. Ricard, F. Mathey, Phospholylsamarium(III) complexes, Inorg. Chem. 34 (1995) 1306–1307.

[67] H. Schumann, J. Winterfeld, H. Hemling, F.E. Hahn, P. Reich, K.-W. Brzezinka, F.T. Edelmann, U. Kilimann, M. Schäfer, R. Herbst-Irmer, (Cyclooctatetraenyl)[-bis(trimethylsilyl)benzamidinato]-und -[diphenylbis(trimethylsilylimido)phosphinato]-Komplexe der Seltenen Erden; röntgenstrukturanalyse von $(C_8H_8)Tm[PhC(NSiMe_3)_2](THF)$, $(C_8H_8)Lu[4\text{-}MeOC_6H_4C(NSiMe_3)_2](THF)$ und $(C_8H_8)Nd[Ph_2P(NSiMe_3)_2](THF)$, Chem. Ber. 128 (1995) 395–404.

[68] M. Dolg, P. Fulde, H. Stoll, H. Preuss, A. Chang, R.M. Pitzer, Formally tetravalent cerium and thorium compounds: a configuration interaction study of cerocene $Ce(C_8H_8)_2$ and thorocene $Th(C_8H_8)_2$ using energy-adjusted quasirelativistic ab initio pseudopotentials, Chem. Phys. 195 (1995) 71–82.

[69] R.M. Giuliano, F.J. Villani, Jr., Stereoselectivity of addition of organometallic reagents to pentodialdo-1,4-furanoses: synthesis of *L*-axenose and *D*-evermicose from a common intermediate, J. Org. Chem. 60 (1995) 202–211.

[70] J.W. Timberlake, D. Pan, J. Murray, B.S. Jursic, T. Chen, *Ortho* methyl group effects in cumyl systems, J. Org. Chem. 60 (1995) 5295–5298.

[71] J. Betz, M. Heuschmann, A new alpha-selective synthetic equivalent for the crotyl anion in additions to imines, Tetrahedron Lett. 36 (1995) 4043–4046.

[72] G. Ulibarri, W. Nadler, T. Skrydstrup, H. Audrain, A. Chiaroni, C. Riche, D.S. Grierson, Construction of the bicyclic core structure of the enediyne antibiotic esperamicin-A_1 in either enantiomeric form from (−)-quinic acid, J. Org. Chem. 60 (1995) 2753–2761.

[73] P.M.J. Jung, A. Burger, J.-F. Biellmann, Rapid and efficient stereocontrolled synthesis of C-3′-ethynyl ribo- and xylonucleosides by organocerium additions to 3′-ketonucleosides, Tetrahedron Lett. 36 (1995) 1031–1034.

[74] M. Kunishima, S. Tanaka, K. Kono, K. Hioki, S. Tani, SmI_2-mediated coupling reactions between iodoalkynes and ketones or aldehydes to give propargyl alcohols, Tetrahedron Lett. 36 (1995) 3707–3710.

[75] E. Ihara, M. Taguchi, H. Yasuda, Syntheses of monodispersed methyl methacrylate oligomers via organolanthanide complexes and introduction of hydroxyl groups into the oligomer, Appl. Organomet. Chem. 9 (1995) 427–429.

[76] X. Yang, A.M. Seyam, T.J. Marks, Rare earth homogeneous catalysts for the ring-opening polymerization and copolymerization of strained-ring olefins, U.S. US 5422406 A 950606, 7 pp. Cont.-in-part of U.S. 5,300,598.

[77] P.-F. Fu, T.J. Marks, Silanes as chain transfer agents in metallocene-mediated olefin polymerization. Facile in Situ catalytic synthesis of silyl-terminated polyolefins, J. Am. Chem. Soc. 117 (1995) 10747–10748.

[78] M.A. Giardello, Y. Yamamoto, L. Brard, T.J. Marks, Stereocontrol in the polymerization of methyl methacrylate mediated by chiral organolanthanide metallocenes, J. Am. Chem. Soc. 117 (1995) 3276–3277.

[79] W.J. Evans, D.M. DeCoster, J. Greaves, Field desorption mass spectrometry studies of the samarium-catalyzed polymerization of ethylene under hydrogen, Macromolecules 28 (1995) 7929–7936.

[80] E. Ihara, M. Morimoto, H. Yasuda, Living polymerizations and copolymerizations of alkyl acrylates by the unique catalysis of rare earth metal complexes, Macromolecules 28 (1995) 7886–7892.

[81] E. Ihara, M. Morimoto, H. Yasuda, Living polymerizations of alkyl acrylates by the unique catalytic action of rare earth metal complexes, Proc. Jpn. Acad., Ser. B 71B (1995) 126–131.

[82] B.M. Novak, L.S. Boffa, Polymerization using bimetallic, bis-lanthanoid initiators, PCT Int. Appl. WO 9521873 A1 950817, 16 pp.

[83] H. Yasuda, E. Ihara, Preparation of block copolymer of an olefin and an ethylenically unsaturated monomer or lactone. Eur. Pat. Appl. EP 634429 A1 950118, 9 pp.

[84] F. Xu, L.L. Zhang, Y.M. Yao, Y.C. Ding, Z.M. Bai, Q. Shen, Selective dimerization of butanal to butyl butyrate catalyzed by lanthanocene/*n*-BuLi systems, Chin. Chem. Lett. 6 (1995) 617–620.

[85] B.-J. Deelman, E.A. Bijpost, J.H. Teuben, Organolanthanide-catalyzed oligomerization of 2-cycloalken-1-ones, J. Chem. Soc., Chem. Commun. (1995) 1741-1742.

[86] T. Imori, V. Lu, H. Cai, T. Don Tilley, Metal-catalyzed dehydropolymerisation of secondary stannanes to high molecular weight polystannanes, J. Am. Chem. Soc. 117 (1995) 9931–9940.

[87] P.-F. Fu, L. Brard, Y. Li, T.J. Marks, Regioselection and enantioselection in organolanthanide-catalyzed olefin hydrosilylation. A kinetic and mechanistic study, J. Am. Chem. Soc. 117 (1995) 7157–7168.

[88] G.A. Molander, W.H. Retsch, Selective hydrosilylation of alkynes catalyzed by an organoyttrium complex, Organometallics 14 (1995) 4570–4575.

[89] G.A. Molander, P.J. Nicols, Organoyttrium-catalyzed sequential cyclization/silylation reactions of 1,5-dienes and 1,6-dienes, J. Am. Chem. Soc. 117 (1995) 4415–4416.

[90] E.A. Bijpost, R. Duchateau, J.H. Teuben, Early transition metal catalyzed-hydroboration of alkenes, J. Mol. Cat. A: Chemical 95 (1995) 121–128.

[91] N.S. Radu, T. Don Tilley, Autocatalytic mechanism for σ-bond metathesis reactions of $(\eta^5\text{-C}_5\text{Me}_5)_2\text{SmCH}(\text{SiMe}_3)_2$ with silicon–hydrogen bonds, J. Am. Chem. Soc. 117 (1995) 5863–5864.

[92] M. Takeno, S. Kikuchi, K.-I. Morita, Y. Nishiyama, Y. Ishii, A new coupling reaction of vinyl esters with aldehydes catalyzed by organosamarium compounds, J. Org. Chem. 60 (1995) 4974–4975.

[93] D. Baudry, A. Dormond, A. Hafid, Synthesis and reactivity of alkynyl-(silylamido)uranium complexes, J. Organomet. Chem. 494 (1995) C22–C23.

[94] M. Silva, N. Marques, A. Pires de Matos, Synthesis and reactivity of hydrotris(pyrazolyl)borate σ-hydrocarbyl uranium(IV) complexes, J. Organomet. Chem. 493 (1995) 129–132.

[95] T. Arligue, M. Lance, M. Nierlich, J. Vigner, M. Ephritikhine, Synthesis and crystal structure of $[\text{K}(\text{C}_{12}\text{H}_{24}\text{O}_6)][\text{U}(\eta\text{-C}_7\text{H}_7)_2]$. The first cycloheptatrienyl sandwich compound, J. Chem. Soc., Chem. Comm. (1995) 184–184.

[96] M.A. Edelman, P.B. Hitchcock, J. Hu, M.F. Lappert, Organoactinide chemistry. Part 2. The chemistry of some novel cyclopentadienylthorium complexes, New J. Chem. 19 (1995) 481–489.

[97] D.M. Barnhart, R.J. Butcher, D.L. Clark, J.C. Gordon, J.G. Watkin, B.D. Zwick, An unprecedented cyclic structure for a monocyclopentadienyl metal complex: preparation and X-ray crystal structure of $[(\eta\text{-C}_5\text{H}_5)\text{Th}_2(\text{O-}i\text{-Pr})_7]_\infty$, New J. Chem. 19 (1995) 503–508.

[98] D. Baudry, A. Dormond, O. Lesprit, RMN ^{1}H et ^{11}B des complexes borohydrure mono-, bis- et triscyclopentadienyluranium. Relation entre deplacement chimique et densite electronique autour de l'uranium, Bull. Soc. Chim. Fr. 132 (1995) 183–187.

[99] M.S. Gill, V.S. Sagoria, Cyclopentadienyl uranium(IV) β-diketonates and alkoxides, Indian J. Chem., Sect A: Inorg., Bio-inorg., Phys., Theor., Anal. Chem. 34A (1995) 997–999.

[100] D.L. Clark, J.C. Gordon, J.C. Huffman, J.G. Watkin, B.D. Zwick, Preparation of mono-pentamethylcyclopentadienyl uranium(IV) sulfido clusters through oxidation of $(\eta\text{-}C_5Me_5)UI_2(THF)_3$. X-ray structural characterization of $(\eta\text{-}C_5Me_5)_3U_3(\mu_3\text{-}I)(\mu_3\text{-}S)(\mu_2\text{-}I)_3I_3$, New J. Chem. 19 (1995) 495–502.

[101] C. Boisson, J.-C. Berthet, M. Lance, M. Nierlich, J. Vigner, M. Ephritikhine, Synthesis of organouranium(V) compounds by oxidation of neutral tetravalent precursors. Crystal structures of $[U(\eta\text{-}C_5Me_5)(NMe_2)_3(OC_4H_8)][BPh_4]$ and $[U(\eta\text{-}C_5Me_5)_2(NEt_2)_2][BPh_4]$, the first cationic uranium(V) complexes, J. Chem. Soc., Chem. Commun. (1995) 543–544.

[102] J.-C. Berthet, C. Boisson, M. Lance, J. Vigner, M. Nierlich, M. Ephritikhine, Synthesis of cationic uranium compounds by protonolysis of amide precursors: cyclopentadienyl and cyclooctatetraene complexes, J. Chem. Soc., Dalton Trans. (1995) 3027–3033.

[103] P. Scott, P.B. Hitchcock, Exploring the auxiliary co-ordination sphere of tripodal amino(triamido) actinide complexes, J. Chem. Soc., Dalton Trans. (1995) 603–609.

[104] R.E. Cramer, K.A.N.S. Ariyaratne, J.W. Gilje, Uranium-sulfilimine chemistry. The preparation of $Cp^*_2UCl_2(HNSPh_2)$ and its hydrolysis with $HNSPh_2 \cdot H_2O$, Z. Anorg. Allg. Chem. 621 (1995) 1856–1864.

[105] R.E. Cramer, J. Hitt, T. Chung, J.W. Gilje, Contrasting the $Cp_3MCl/Li(CH_2)(CH_2)PPh_2$ ($M = U$, Th) systems. Synthesis and structure of $Cp_2Th[(CH_2)(CH_2)PPh_2]_2$, New J. Chem. 19 (1995) 509–514.

[106] D.S.J. Arney, C.J. Burns, Synthesis and properties of high-valent organouranium complexes containing terminal organoimido and oxo functional groups. A new class of organo-f-element complexes, J. Am. Chem. Soc. 117 (1995) 9448–9460.

[107] P.C. Blake, M.F. Lappert, R.G. Taylor, J.L. Atwood, W.E. Hunter, H. Zhang, Organometallic chemistry of the actinides. Part 1. Synthesis, spectroscopic properties and crystal structures of $[ML_2Cl_2]$ [$M = Th$ or U; $L = \eta\text{-}C_5H_3(SiMe_3)_2\text{-}1,3$] and $[UL_2X_2]$ ($X = Br$, I or BH_4), J. Chem. Soc., Dalton Trans. (1995) 3335–3341.

[108] N.S. Radu, M.P. Engeler, C.P. Gerlach, T. Don Tilley, A.L. Rheingold, Isolation of the first metalloxy ketene complexes via "double insertion" of carbon monoxide into thorium–silicon bonds, J. Am. Chem. Soc. 117 (1995) 3621–3622.

[109] P. Scott, P.B. Hitchcock, Synthesis, structure and electrochemistry of the first fulvalene derivative of an actinide, J. Organomet. Chem. 497 (1995) C1–C3.

[110] J. Parry, E. Carmona, S. Coles, M. Hursthouse, Synthesis and single crystal X-ray diffraction study on the first isolable carbonyl complex of an actinide, $(C_5Me_4H)_3U(CO)$, J. Am. Chem. Soc. 117 (1995) 2649–2650.

[111] M. Weydert, J.G. Brennan, R.A. Andersen, R.G. Bergman, Reactions of a uranium(IV) tertiary alkyl bond: facile ligand-assisted reduction and insertion of ethylene and carbon monoxide, Organometallics 14 (1995) 3942–3951.

[112] A. Streitwieser, M.H. Lyttle, H.-K. Wang, T. Boussie, A. Weinländer, J.P. Solar, 1,1'-Dimesityluranocene and its unusual dynamic NMR phenomena, J. Organomet. Chem. 501 (1995) 245–249.

[113] T. Straub, A. Haskel, M.S. Eisen, Organoactinide-catalyzed oligomerization of terminal acetylenes, J. Am. Chem. Soc. 117 (1995) 6364–6365.